



5-1999

## **Numerical investigation of error properties of Green's Function Discretization**

Sany Izan Ihsan

Follow this and additional works at: [https://trace.tennessee.edu/utk\\_gradthes](https://trace.tennessee.edu/utk_gradthes)

---

### **Recommended Citation**

Ihsan, Sany Izan, "Numerical investigation of error properties of Green's Function Discretization. " Master's Thesis, University of Tennessee, 1999.  
[https://trace.tennessee.edu/utk\\_gradthes/9868](https://trace.tennessee.edu/utk_gradthes/9868)

This Thesis is brought to you for free and open access by the Graduate School at TRACE: Tennessee Research and Creative Exchange. It has been accepted for inclusion in Masters Theses by an authorized administrator of TRACE: Tennessee Research and Creative Exchange. For more information, please contact [trace@utk.edu](mailto:trace@utk.edu).

To the Graduate Council:

I am submitting herewith a thesis written by Sany Izan Ihsan entitled "Numerical investigation of error properties of Green's Function Discretization." I have examined the final electronic copy of this thesis for form and content and recommend that it be accepted in partial fulfillment of the requirements for the degree of Master of Science, with a major in Aerospace Engineering.

John E. Caruthers, Major Professor

We have read this thesis and recommend its acceptance:

R. C. Reddy

Accepted for the Council:

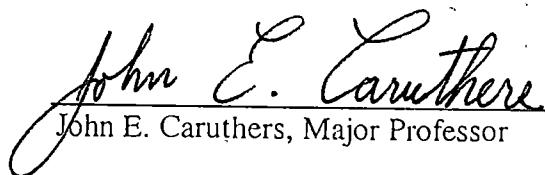
Carolyn R. Hodges

Vice Provost and Dean of the Graduate School

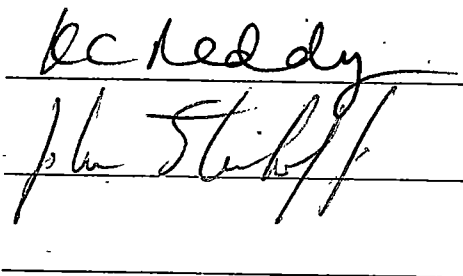
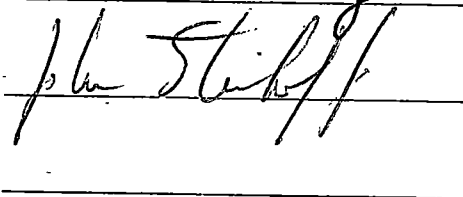
(Original signatures are on file with official student records.)

To the Graduate Council:

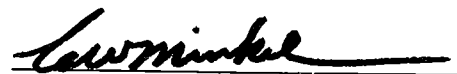
I am submitting herewith a thesis written by Sany I. Ihsan entitled "Numerical Investigation of Error Properties of Green's Function Discretization". I have examined the final copy of this thesis for form and content and recommend that it be accepted in partial fulfillment of the requirements for the degree of Master of Science, with a major in Aerospace Engineering.

  
John E. Caruthers, Major Professor

We have read this thesis and  
recommend its acceptance:

Accepted for the Council:

  
Associate Vice Chancellor  
and Dean of the Graduate School

**NUMERICAL INVESTIGATION OF  
ERROR PROPERTIES OF  
GREEN'S FUNCTION DISCRETIZATION**

A Thesis

Presented for the

Master of Science

Degree

The University of Tennessee, Knoxville

Sany I. Ihsan

May 1999

## **DEDICATION**

This thesis is dedicated to  
my beloved mother Aisyah Abdullah, for her prayer and motivation,  
to my beloved wife Suriza Ahmad Zabidi, and my children Muhammad and Zubair,  
for their continuous support and patience, and lastly to the God for  
His blessing and inspiration.

## ACKNOWLEDGMENTS

I would like to thank to my major professor,  
Dr. John E. Caruthers,  
for his support, patience and encouragement.

## ABSTRACT

Error Property of a highly accurate method for discretization solutions of the Helmholtz equation, called the Green's Function Discretization (GFD) is studied. Numerical results indicate that 6<sup>th</sup> order of accuracy is obtained using this method in interpolating any acoustic source. Various combinations of interpolating functions are examined, and are shown to maintain the order of accuracy. The accuracy of the discretization for skewed lattice stencils is also examined by numerical example and yields satisfactory results. Preliminary study on a 3-D problem using this method shown the same order of accuracy.

# TABLE OF CONTENTS

CHAPTER 1. INTRODUCTION .....	1
1.1. Overview .....	1
1.2. Background and purpose .....	1
CHAPTER 2. THEORETICAL BASIS AND METHOD.....	6
2.1 Introduction .....	6
2.2 Review of the Green's Function Discretization (GFD) .....	6
2.3 Minimum Error Property of the GFD .....	8
2.4 Discretization of the field .....	10
2.5 Appropriate Green's function .....	13
CHAPTER 3. NUMERICAL STUDY AND RESULTS .....	15
3.1 Introduction .....	15
3.1.1 The standard case .....	16
3.1.2 Types of plots .....	18
3.2 Effect of using additional function(s) .....	20
3.2.1 Figures reference codes .....	21
3.2.2 Effect on Average Error .....	22
3.2.3 Effect on interpolating a plane wave .....	24
3.2.4 Effect on interpolating a monopole radiator .....	28
3.2.5 Effect on interpolating an evanescent wave .....	36
3.3 Influence coefficient study .....	42
3.3.1 Figures reference codes .....	44
3.4 Evanescent Wave study.....	47
3.4.1 Figures reference codes .....	48
3.5 Multiple monopole set study .....	52
3.5.1 Figures reference codes .....	54
3.6 Irregular stencil grid study .....	62
3.6.1 Figures reference codes .....	64
3.7 Preliminary study on 3-D interpolation using GFD method .....	79
3.7.1 Figures reference codes .....	81
CHAPTER 4. CONCLUSIONS .....	84
CHAPTER 5. RECOMMENDATIONS FOR FURTHER WORK .....	86
LIST OF REFERENCES .....	87
APPENDICES .....	90
APPENDIX 1. Derivation of the Second Order Finite Difference Scheme .....	91



APPENDIX 2. Plots of interpolation error for function at various angle .....	93
APPENDIX 3. Tables of influence coefficient for various interpolating functions .....	95
VITA .....	107

# LIST OF FIGURES

FIGURE	PAGE
2.2.1. Green's Function Discretization .....	7
2.4.1. Discretization of the field .....	11
3.1.1.1. The standard case: 20 plane waves approaching the stencil from uniformly distributed angles .....	16
3.1.1.2. The standard stencil configuration .....	17
3.2.2.1. Average Error vs. $k$ for various interpolation functions .....	23
3.2.3.1. Interpolating a plane wave .....	24
3.2.3.2. Magnitude Error vs. $k$ for various functions in interpolating a plane wave approaching at $15^\circ$ angle from the right (semi-log plot) .....	26
3.2.3.3. Magnitude Error vs. $k$ for various functions in interpolating a plane wave approaching at $15^\circ$ angle from the right (log-log plot) .....	27
3.2.4.1. Interpolating a monopole .....	28
3.2.4.2. Magnitude Error vs. $k$ for various functions in interpolating a monopole at radius $r/\delta = 10$ , at $15^\circ$ angle from the right (semi-log plot) .....	31
3.2.4.3. Magnitude Error vs. $k$ for various functions in interpolating a monopole at radius $r/\delta = 10$ , at $15^\circ$ angle from the right (log-log plot) .....	32
3.2.4.4. Magnitude Error vs. $k$ for various functions in interpolating a monopole at radius $r/\delta = 20$ , at $15^\circ$ angle from the right (semi-log plot) .....	33
3.2.4.5. Magnitude Error vs. $k$ for various functions in interpolating a monopole at radius $r/\delta = 20$ , at $15^\circ$ angle from the right (log-log plot) .....	34

3.2.4.6	Magnitude Error vs. $k$ for various functions in interpolating a monopole with $\lambda$ fixed at 40 (semi-log plot) .....	35
3.2.4.7	Magnitude Error vs. $k$ for various functions in interpolating a monopole with $\lambda$ fixed at 40 (log-log plot) .....	35
3.2.5.1	Magnitude Error vs. $k$ for various functions in interpolating an evanescent waves at phase Mach number = 0.5 (semi-log plot) .....	37
3.2.5.2	Magnitude Error vs. $k$ for various functions in interpolating an evanescent waves at phase Mach number = 0.5 (log-log plot) .....	38
3.2.5.3	Magnitude Error vs. $k$ for various functions in interpolating an evanescent waves at phase Mach number = 0.25 (semi-log plot) .....	39
3.2.5.4	Magnitude Error vs. $k$ for various functions in interpolating an evanescent waves at phase Mach number = 0.25 (log-log plot) .....	40
3.2.5.5	Magnitude Error vs. $k$ for comparing the values for the 2 different interpolation evanescent waves, at phase Mach number 0.5 and 0.25 (semi-log plot) .....	41
3.3.1	$a_n$ vs. $k$ plot for various functions .....	45
3.4.1	Average Error vs. $k$ for various interpolating functions with evanescent wave(s) added .....	49
3.4.2	Magnitude Error vs. $k$ for various functions with evanescent wave(s) added, in interpolating an evanescent waves at phase Mach number = 0.5 (semi-log plot) .....	50
3.4.3	Magnitude Error vs. $k$ for various functions with evanescent wave(s) added, in interpolating an evanescent waves at phase Mach number = 0.5 (log-log plot) .....	50
3.4.4	Magnitude Error vs. $k$ for various functions with evanescent wave(s) added, in interpolating an evanescent waves at phase Mach number = 0.25 (semi-log plot) .....	51
3.4.5	Magnitude Error vs. $k$ for various functions with evanescent wave(s) added, in interpolating an evanescent waves at phase Mach number = 0.25 (log-log plot) .....	51
3.5.1	$a_n$ vs. $k$ plot for functions with additional set(s) of monopoles .....	55

3.5.2	Average Error vs. $k$ for functions with additional set(s) of monopoles .....	56
3.5.3	Magnitude Error vs. $k$ for functions with additional set(s) of monopoles, in interpolating a plane wave approaching at $15^\circ$ angle from the right (semi-log plot) .....	57
3.5.4	Magnitude Error vs. $k$ for functions with additional set(s) of monopoles, in interpolating a plane wave approaching at $15^\circ$ angle from the right (log-log plot) .....	57
3.5.5	Magnitude Error vs. $k$ for functions with additional set(s) of monopoles, in interpolating a monopole a radius $r/\delta = 10$ , at $15^\circ$ angle from the right (semi-log plot) .....	58
3.5.6	Magnitude Error vs. $k$ for functions with additional set(s) of monopoles, in interpolating a monopole a radius $r/\delta = 10$ , at $15^\circ$ angle from the right (log-log plot) .....	58
3.5.7	Magnitude Error vs. $k$ for functions with additional set(s) of monopoles, in interpolating a monopole a radius $r/\delta = 20$ , at $15^\circ$ angle from the right (semi-log plot) .....	59
3.5.8	Magnitude Error vs. $k$ for functions with additional set(s) of monopoles, in interpolating a monopole a radius $r/\delta = 20$ , at $15^\circ$ angle from the right (log-log plot) .....	59
3.5.9	Magnitude Error vs. $k$ for functions with additional set(s) of monopoles, in interpolating an evanescent waves at phase Mach number = 0.5 (semi-log plot) .....	60
3.5.10	Magnitude Error vs. $k$ for functions with additional set(s) of monopoles, in interpolating an evanescent waves at phase Mach number = 0.5 (log-log plot) .....	60
3.5.11	Magnitude Error vs. $k$ for functions with additional set(s) of monopoles, in interpolating an evanescent waves at phase Mach number = 0.25 (semi-log plot) .....	61
3.5.12	Magnitude Error vs. $k$ for functions with additional set(s) of monopoles, in interpolating an evanescent waves at phase Mach number = 0.25 (log-log plot) .....	61
3.6.1	$45^\circ$ skewed stencil grid configuration .....	63
3.6.2	$a_n$ vs. $k$ plots for functions with skewed stencil grid of case 1 .....	66

3.6.3	$a_n$ vs. $k$ plots for functions with skewed stencil grid of case 2 .....	67
3.6.4	Average Error vs. $k$ for functions with skewed stencil grid of case 1 .....	68
3.6.5	Average Error vs. $k$ for functions with skewed stencil grid of case 2 .....	68
3.6.6	Magnitude Error vs. $k$ for functions with skewed stencil grid of case 1, in interpolating a plane wave approaching at $15^\circ$ angle from the right (semi-log plot) .....	69
3.6.7	Magnitude Error vs. $k$ for functions with skewed stencil grid of case 2, in interpolating a plane wave approaching at $15^\circ$ angle from the right (semi-log plot) .....	69
3.6.8	Magnitude Error vs. $k$ for functions with skewed stencil grid of case 1, in interpolating a plane wave approaching at $15^\circ$ angle from the right (log-log plot) .....	70
3.6.9	Magnitude Error vs. $k$ for functions with skewed stencil grid of case 2, in interpolating a plane wave approaching at $15^\circ$ angle from the right (log-log plot) .....	70
3.6.10	Magnitude Error vs. $k$ for functions with skewed stencil grid of case 1, in interpolating a monopole at radius $r/\delta = 10$ , at $15^\circ$ angle from the right (semi-log plot) .....	71
3.6.11	Magnitude Error vs. $k$ for functions with skewed stencil grid of case 2, in interpolating a monopole at radius $r/\delta = 10$ , at $15^\circ$ angle from the right (semi-log plot) .....	71
3.6.12	Magnitude Error vs. $k$ for functions with skewed stencil grid of case 1, in interpolating a monopole at radius $r/\delta = 10$ , at $15^\circ$ angle from the right (log-log plot) .....	72
3.6.13	Magnitude Error vs. $k$ for functions with skewed stencil grid of case 2, in interpolating a monopole at radius $r/\delta = 10$ , at $15^\circ$ angle from the right (log-log plot) .....	72
3.6.14	Magnitude Error vs. $k$ for functions with skewed stencil grid of case 1, in interpolating a monopole at radius $r/\delta = 20$ , at $15^\circ$ angle from the right (semi-log plot) .....	73
3.6.15	Magnitude Error vs. $k$ for functions with skewed stencil grid of case 2, in interpolating a monopole at radius $r/\delta = 20$ , at $15^\circ$ angle from the right (semi-log plot) .....	73

3.6.16	Magnitude Error vs. $k$ for functions with skewed stencil grid of case 1, in interpolating a monopole at radius $r/\delta = 20$ , at $15^\circ$ angle from the right (log-log plot) .....	74
3.6.17	Magnitude Error vs. $k$ for functions with skewed stencil grid of case 2, in interpolating a monopole at radius $r/\delta = 20$ , at $15^\circ$ angle from the right (log-log plot) .....	74
3.6.18	Magnitude Error vs. $k$ for functions with skewed stencil grid of case 1, in interpolating an evanescent waves at phase Mach number = 0.5 (semi-log plot) .....	75
3.6.19	Magnitude Error vs. $k$ for functions with skewed stencil grid of case 2, in interpolating an evanescent waves at phase Mach number = 0.5 (semi-log plot) .....	75
3.6.20	Magnitude Error vs. $k$ for functions with skewed stencil grid of case 1, in interpolating an evanescent waves at phase Mach number = 0.5 (log-log plot) .....	76
3.6.21	Magnitude Error vs. $k$ for functions with skewed stencil grid of case 2, in interpolating an evanescent waves at phase Mach number = 0.5 (log-log plot) .....	76
3.6.22	Magnitude Error vs. $k$ for functions with skewed stencil grid of case 1, in interpolating an evanescent waves at phase Mach number = 0.25 (semi-log plot) .....	77
3.6.23	Magnitude Error vs. $k$ for functions with skewed stencil grid of case 2, in interpolating an evanescent waves at phase Mach number = 0.25 (semi-log plot) .....	77
3.6.24	Magnitude Error vs. $k$ for functions with skewed stencil grid of case 1, in interpolating an evanescent waves at phase Mach number = 0.25 (log-log plot) .....	78
3.6.25	Magnitude Error vs. $k$ for functions with skewed stencil grid of case 2, in interpolating an evanescent waves at phase Mach number = 0.25 (log-log plot) .....	78
3.7.1	3-D stencil grid configuration .....	79
3.7.2	$a_n$ vs. $k$ plot for 3-D functions .....	82

3.7.3	Average Error vs. $k$ for 3-D functions .....	82
3.7.4	Magnitude Error vs. $k$ for 3-D functions, in interpolating a plane wave approaching at $\theta = 15^\circ$ and $\phi = 15^\circ$ angles (semi-log plot) .....	83
3.7.5	Magnitude Error vs. $k$ for 3-D functions, in interpolating a plane wave approaching at $\theta = 15^\circ$ and $\phi = 15^\circ$ angles (log-log plot) .....	83
A2.1	Magnitude error in interpolating a plane wave at various angle .....	94

# LIST OF TABLES

TABLE		PAGE
A3.1	Table of $a_1$ .....	95
A3.2	Table of $a_2$ .....	101



## NOMENCLATURE

$\mathbf{a}$	Denotes a vector or a matrix
$a$	Denotes a scalar
$a_i$	Denotes $i^{\text{th}}$ component of vector $\mathbf{a}$
$a_{ij}$	Denotes $i^{\text{th}}$ row and $j^{\text{th}}$ column of matrix $\mathbf{a}$
$a_{ij}^+$	Denotes $i^{\text{th}}$ row and $j^{\text{th}}$ column of pseudo-inverse matrix $\mathbf{a}$
$c$	Speed of sound
$G$	Green's function
$H^{(2)}$	Hankel function of second kind
$i$	$\sqrt{-1}$
$J_0$	Zeroth order Bessel function of first kind
$k$	Reduced frequency, $\left(\frac{\omega\delta}{c}\right)$
$\delta$	Length parameter
$M$	Phase Mach number
$T$	Period
$Y_0$	Zeroth order Bessel function of second kind
$\lambda$	Wavelength
$\phi$	Acoustic potential
$\omega$	Angular frequency = $\frac{2\pi}{T}$
$\gamma$	Source strength

# LIST OF ABBREVIATIONS

Computational Fluid Dynamics .....	CFD
Finite Difference .....	FD
Green's Function Discretization .....	GFD
Singular Value Decomposition .....	SVD

# CHAPTER 1

## INTRODUCTION

### 1.1 Overview

This thesis analyzes numerically, error properties of a unique discretization method introduced by Dr. J. E. Caruthers et. al. [1], namely the Green's Function Discretization (GFD). The GFD method has been proven to produce accurate solutions to the Helmholtz equation. Recently, theoretical analysis has shown the error produced by this method is minimized.

This thesis begins with some general background on acoustics issues and further discussions on the existing numerical methods. Chapter 2 is intended to explain the theoretical idea behind the GFD method and its minimum error property. Methodology used in this study is also explained. Numerical results of the analysis are then presented. Thesis concludes with some suggestions for further work.

### 1.2 Background and purpose

Acoustics is a branch of science, which deals with the phenomena of sound. Its objective is to develop understanding on how sound propagates through a medium and how it interacts with boundaries. By understanding this behavior, people hope to improve human life in general; to reduce unpleasant sound/noise such as noise from jet engines and machinery, or to improve the sound quality/performance such as for musical

instruments. Sound is also recently being applied for other purposes such as for medical treatment and for structural engineering just to name a few. In short, modern acoustics is playing a significant role and is the subject of many diverse applications in our daily life.

In Computational Mechanics, the study of fluid dynamics, namely Computational Fluid Dynamics (CFD) has been developed for over 20 year, and has made impressive progress to become a reliable design tool [9]. Over the years, many schemes have been introduced in this area such as the Finite Element Method (FEM), Finite Boundary Method (FBM), and Finite Difference Method (FDM) to name a few. These methods have been very successful for the class of problems for which they were intended. It is generally agreed that a desirable quality of CFD schemes is ranked by the order of (Taylor Series) truncation. Therefore, it is expected that a Fourth-order scheme is in some sense, better than a Second-order scheme and so on [7].

In Computational Aeroacoustics (CAA) however, there is still much need for knowledge and understanding of numerical method. Due to its distinctive behavior and property, many schemes from CFD cannot be directly applied to acoustics problems. However, there have been attempts to modify the existing CFD schemes in order to take into account the differences. Current methods that exist include the Boundary Element Method (BEM), Finite Element and Spectral Methods, Finite Difference, including Central Differencing and Implicit Finite Difference (IFD), and Ordinary Differential Equation (ODE) methods. Unfortunately, there are still many potential difficulties which arise in applying the CFD methods even with some modifications to satisfy acoustic behavior. This includes the need to include the far field into the calculation, which is used to allow the waves in the solution to dissipate, ensuring that errors due to discretized

boundary conditions are not reflecting back into the solution. Extended computation into the far field would require prohibitively huge computer storage and CPU times.

Caruthers [1] had attempted to overcome the problems by incorporating some of the basic physical understanding of how waves propagate. It first started when he and Raviprakash [13] formulated a radiation boundary condition, which allows acoustic energy to flow out of a near field boundary without any reflections. This results in a major advantage over the other methods since the far field calculation, which in general causes the system of equations to be large and therefore unrealistic to solve, can be excluded from the general computation.

Caruthers then further extended this idea to introduce a general field discretization method. This method, called the Green's Function Discretization (GFD) had been proven, both theoretically [1] and numerically [2], to produce more accurate solutions than other methods in determining the acoustic potential. This method utilizes well known free space Green's functions for a constant coefficient equation, to obtain a field point discretization. In general, this discretization can be thought of as simply relating the value of the unknown at each discrete point of the domain of interest, to the values at a selected set of neighboring points. This method was shown to accurately discretize the Helmholtz equation for frequencies approaching the resonant frequency of the local computational stencil.

Another significant advantage of this method is that it requires only 2 to 3 discretizing points per wave in order to accurately obtain the wave solutions. This is a major improvement since for the existing standard Finite Difference and Finite Element Methods for example, to obtain an acceptable accuracy, a minimum number of 10 of

points per wave is needed [13]. Since the number of arithmetic operations required for direct solution of the final linear algebraic system resulting from discretization is proportional to the 4<sup>th</sup> power of the number for 2-D problems and the 7<sup>th</sup> power for 3-D, this improvement is an enormous gain in computational efficiency [8].

Recently, during a seminar on this topic presented by Dr. Caruthers, a suggestion was raised by Dr. John Steinhoff to further explore the minimum error property of this method. That is, to further investigate if it has any advantage over the other methods, and if possible to further improve the method. Further theoretical analysis surprisingly shows that the error norm produced in this method is a minimum, i.e. the GFD method is the most accurate method possible. This is actually due to the fact that:

*"The minimum norm condition applied to the Green's function expansion also implies that the interpolating error norm over the set of expansion functions is also minimum." [3, pg. 3]*

Previous numerical results, obtained by this method to interpolate plane wave functions have indicated that an order of accuracy of 6 is obtained for a uniform square  $3 \times 3$  lattice [3].

This result was considered deficient, however, in the sense that it was obtained only for plane wave test functions. Since plane waves were used in the interpolating function, it might not be surprising that it would accurately interpolate plane waves. Would this high order property persist for interpolating non-plane wave solutions of the Helmholtz equation, such as evanescent wave or monopole solutions? Can the method be improved by adding monopole or evanescent wave functions to the interpolating function of plane waves? The new theoretical result referred to above concerning the minimum

error norm property suggested that some improvements might be obtained by enlarging the space of the interpolating functions.

This thesis presents a compilation of numerical results examining the error produced by GFD in discretizing a broader class of solutions to the Helmholtz equation. It also examines the effects of expanding the interpolating function space on improving the interpolation accuracy. The studies were conducted over a wide frequency range from zero to beyond  $\frac{\omega\delta}{c} = \frac{\pi}{\sqrt{2}}$  where the method ceases to yield accurate results.

# CHAPTER 2

## THEORETICAL BASIS AND METHOD

### 2.1 Introduction

This chapter begins with a general review of the Green's Function Discretization to give some general ideas of the method. It then proceeds with a discussion on an analytical proof of the minimum error property of the discretization. This is the main idea behind this thesis.

This chapter ends with a detailed description on the methodology, of how this numerical study is conducted.

### 2.2 Review of the Green's Function Discretization (GFD)

Full discussion in this method of discretization is given in reference [1], [6] and [8]. For the sake of completeness, parts are reproduced here.

We seek to solve the Helmholtz equation in potential form  $\nabla^2\phi + k^2\phi = 0$ . Harmonic time dependence is assumed. Given a region  $\mathbf{V}$  as shown in figure 2.2.1, there exists within the region, a cluster of  $M$  points  $\mathbf{r}_i$ ,  $i = 1, 2, \dots, M$ , surrounding a neighboring point,  $\mathbf{r}_0$ . This is later referred to as a stencil of points for  $\mathbf{r}_0$ . Then the acoustic potential,  $\phi$  at point  $\mathbf{r}_0$  may be given as a linear combination of the values of the surrounding  $M$  points. Then,



$$\phi(\mathbf{r}_i) = \sum_{j=1}^N \gamma_j \chi_j(\mathbf{r}_i) \quad ; i = 1, 2, \dots, M \quad (2.2.1)$$

where the set of  $N$  functions  $\chi_j(\mathbf{r}_i)$  are all solutions of a linear equation,  $L\{\chi\} = 0$ , valid within the region and  $\gamma$  is the source strength of each function.

Rewritten in matrix notation,

$$\varphi^T = \gamma^T \chi \quad (2.2.2)$$

where  $\varphi^T$  and  $\gamma^T$  are  $1 \times M$  and  $1 \times N$  respectively and  $\chi$  is an  $N \times M$  matrix.

For the case with  $N > M$ , there exists an infinite set of solutions,  $\gamma$  to equation (2.2.2) all producing  $\varphi$ 's which satisfy the Helmholtz equation exactly and match the  $M$  given values at  $\mathbf{r}_i$ . Minimum  $L^2$  norm solution is then sought.

Letting

$$\gamma^T = \alpha^T \chi^H \quad (2.2.3)$$

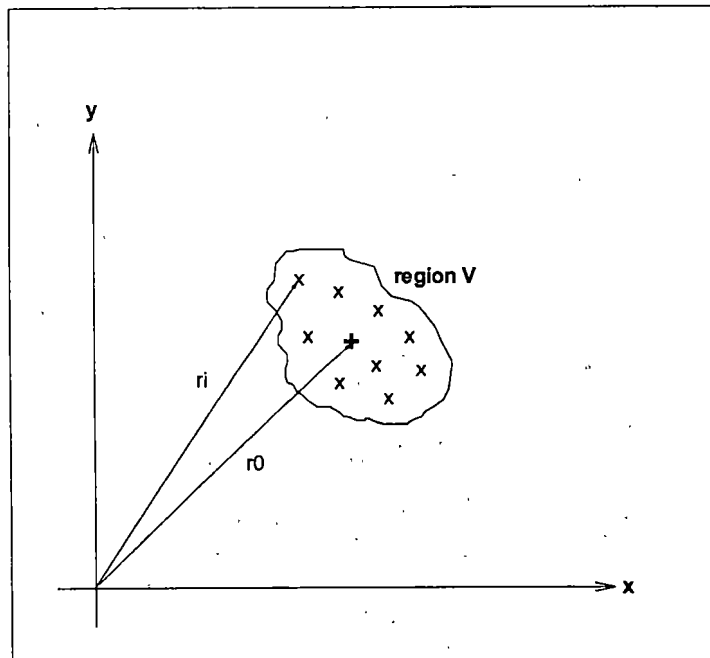


Figure 2.2.1: Green's Function Discretization.

where  $\chi^H$  is the complex conjugate transpose (Hermitian) of  $\chi$ . Then,

$$\varphi^T = \alpha^T \chi^H \chi \quad (2.2.4)$$

$$\alpha^T = \varphi^T [\chi^H \chi]^{-1} \quad (2.2.5)$$

Therefore,

$$\gamma^T = \varphi^T [\chi^H \chi]^{-1} \chi^H \quad (2.2.6)$$

Now, the acoustic potential of interest,  $\phi(\mathbf{r}_0)$  can be written as,

$$\phi(\mathbf{r}_0) = \sum_{j=1}^N \gamma_j \chi_j(\mathbf{r}_0) \quad (2.2.7)$$

or rewritten in matrix form,

$$\phi(\mathbf{r}_0) = \gamma^T \chi_0 = \varphi^T [\chi^H \chi]^{-1} \chi^H \chi_0 \quad (2.2.8)$$

This is the discretized form sought. To emphasize the finite difference form of the result, let

$$\mathbf{a} = [\chi^H \chi]^{-1} \chi^H \chi_0 \quad (2.2.9)$$

so that,

$$\phi(\mathbf{r}_0) = \varphi^T \mathbf{a} \quad (2.2.10)$$

### 2.3 Minimum Error Property of the GFD

This section is to show that the discretization of the GFD method yields optimal solution, in the sense that the  $L^2$  error norm obtained is minimized. Discussion of this topic is presented in reference [6] and reproduced here for completeness.

For a single stencil, the desired linear discretized form about  $\mathbf{r}_0$  is given by,

$$\phi(\mathbf{r}_0) = \varphi^T \mathbf{a} \quad (2.3.1)$$

or,

$$\Phi = \sum_{i=1}^M a^i \phi(\mathbf{r}_i) \quad (2.3.2)$$

where  $\Phi$  is the interpolated value for  $\phi$  at  $\mathbf{r}_0$ . Applying equation (2.3.2) to each function of a given set,  $\chi_j(\mathbf{r}_i); j = 1, 2, \dots, N$ , the interpolated values are now given by,

$$\Psi_j = \sum_{i=1}^M \chi_j(\mathbf{r}_i) a^i \quad (2.3.3)$$

The error is given by,

$$E_j = \Psi_j - \chi_j(\mathbf{r}_0) \quad (2.3.4)$$

In matrix form,

$$\Psi = \chi \mathbf{a} \quad (2.3.5)$$

$$E = \chi \mathbf{a} - \chi_0 \quad (2.3.6)$$

Since complex numbers are involved, the least  $L^2$  error norm is given by,

$$\|E\|^2 = E^H E = [\chi \mathbf{a} - \chi_0]^H [\chi \mathbf{a} - \chi_0] \quad (2.3.7)$$

$$= [\mathbf{a}^H \chi^H - \chi_0^H] [\chi \mathbf{a} - \chi_0]$$

$$= \mathbf{a}^H \chi^H \chi \mathbf{a} - \mathbf{a}^H \chi^H \chi_0 - \chi_0^H \chi \mathbf{a} + \chi_0^H \chi_0$$

The derivative of  $\|E\|^2$  with respect to the components of  $\mathbf{a}$  yields,

$$\frac{\partial}{\partial a^i} \|E\|^2 = \left[ \mathbf{a}^H \chi^H - \chi_0^H \right] \chi_i \quad (2.3.8)$$

where  $\frac{\partial}{\partial a^i}$  indicate the derivation of the  $i^{\text{th}}$  component of  $\mathbf{a}$ .

Using equation (2.3.8) and substitute  $\mathbf{a}^H$  obtained from the GFD procedure gives,

$$\begin{aligned}
[\mathbf{a}^H \boldsymbol{\chi}^H - \chi_0^H] \boldsymbol{\chi} &= [\chi_0^H \boldsymbol{\chi} [\boldsymbol{\chi}^H \boldsymbol{\chi}]^{-1} \boldsymbol{\chi}^H - \chi_0^H] \boldsymbol{\chi} \\
&= \chi_0^H \boldsymbol{\chi} [[\boldsymbol{\chi}^H \boldsymbol{\chi}]^{-1} \boldsymbol{\chi}^H \boldsymbol{\chi}] - \chi_0^H \boldsymbol{\chi} \\
&= \chi_0^H \boldsymbol{\chi} - \chi_0^H \boldsymbol{\chi} = 0
\end{aligned} \tag{2.3.9}$$

which yields the minimum error norm as claimed.

By substituting for  $\mathbf{a}$  in equation (2.3.7), the corresponding minimum error norm is obtained as

$$\begin{aligned}
\|\mathbf{E}\|_{\min}^2 &= \chi_0^H \boldsymbol{\chi} [\boldsymbol{\chi}^H \boldsymbol{\chi}]^{-1} \boldsymbol{\chi}^H \chi_0 - \chi_0^H \boldsymbol{\chi} [\boldsymbol{\chi}^H \boldsymbol{\chi}]^{-1} \boldsymbol{\chi}^H \chi_0 \\
&\quad - \chi_0^H \boldsymbol{\chi} [\boldsymbol{\chi}^H \boldsymbol{\chi}]^{-1} \boldsymbol{\chi}^H \chi_0 + \chi_0^H \chi_0 \\
&= \chi_0^H (I - \boldsymbol{\chi} [\boldsymbol{\chi}^H \boldsymbol{\chi}]^{-1} \boldsymbol{\chi}^H) \chi_0 \neq 0 \quad (\text{for } N > M)
\end{aligned} \tag{2.3.10}$$

## 2.4 Discretization of the field

Following the discussion above, we seek to show numerically the error produced by this method. Before going any further, a grid of nodes must first be established. The grid does not have to be uniform, however having a uniform grid could simplify the solution computation and is known to exhibit the best error properties. This is because, since the grid lattice is uniform, the influence coefficient, denoted as  $\mathbf{a}$  is the same throughout the field domain. Hence, one calculation of  $\mathbf{a}$  is sufficient for the whole field. Throughout this study, uniform Cartesian and skew-Cartesian grids are used.

A stencil of points is now defined. As mentioned in section 2.2, in general, a stencil consists of a cluster of  $M$  neighboring points,  $\mathbf{r}_i$ ,  $i = 1, 2, \dots, M$ , surrounding a point,  $\mathbf{r}_0$ . This point is denoted by a filled circle in figure 2.4.1, where the solution is to be

sought. This node will be referred to as the computed node from now on.  $M$  can be any number of neighboring points to the computed node. As shown in references [2] and [8], as  $M$  is increased, a solution that is more accurate is obtained. However, increasing  $M$  may also increase the computing time due to larger band matrix structure. In this study, a 9-point stencil is used, where a linear combination of 8 local nodes is taken as an approximation to the computed node. These points are shown as empty circles in figure 2.4.2. Note that the local nodes need to surround the computed node at any location. Therefore, the stencil can not be centered on the boundary of the field. This would lead to a radiation boundary condition with an unknown source location. This condition is discussed in detail in reference [11] and is not intended to be covered in this study.

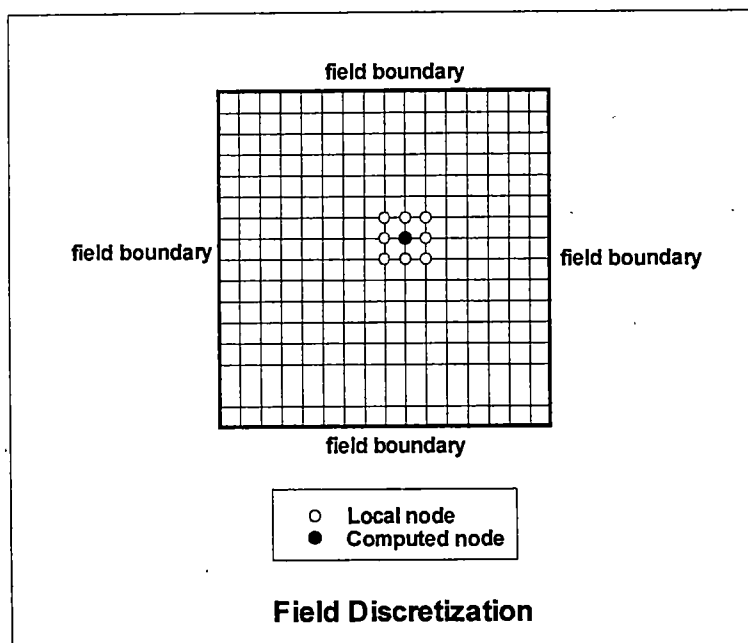


Figure 2.4.1: Discretization of the field.

A set of  $N$  interpolating functions is used. This can be any function that is solution of a linear equation,  $L\{\chi\} = 0$ . As shall be shown in chapter 3, the functions used in this

study are either a set of plane waves, monopoles, evanescent waves, or a combination of any of them. As for the monopole interpolating function, the function has to be placed outside the field domain of interest, to avoid singularity problem.

Throughout this study, the number of interpolating functions,  $N$  is maintained to be larger than the number of points on the stencil,  $M$ . This is to ensure the existence of under-constrained condition in the system of equations. Besides improving its ability to more accurately interpolate any incoming wave (by having more interpolating functions), this condition causes the system to have an infinite number of solutions to the equations. Thus, the minimum  $L^2$  error norm is chosen to restrict the solutions.

Now, let the influence of the first interpolating function,  $\chi_1$ , on the second local node,  $\phi(r_2)$  be  $\chi_{12}$ . Therefore,  $\chi_{ji}$  would be interpreted as the influence of the  $j^{\text{th}}$  interpolating function,  $\chi_j$  on the  $i^{\text{th}}$  local node,  $\phi(r_i)$ . The matrix form of this function is defined as  $\chi$ .

Similarly, let define the influence of the first interpolating function,  $\chi_1$ , on the computed node  $\phi(r_0)$  as  $\chi_1(r_0)$  and in general form,  $\chi_j(r_0)$ . Let these be components of the vector,  $\chi_0$ .

The Influence coefficient vector,  $\mathbf{a}$  can then be computed using equation 2.2.9, that is:

$$\mathbf{a} = [\chi^H \chi]^{-1} \chi^H \chi_0 \quad (2.2.9)$$

To obtain the  $L^2$  error norm solution to the approximation, Singular Value Decomposition (SVD) from the LINPACK FORTRAN codes is used [12] to find the

inverse matrix of  $[\chi^H \chi]$ . SVD separates the matrix into two orthogonal matrices, namely  $Q_1$  and  $Q_2$ , and a diagonal matrix  $\Sigma$ :

$$[[\chi]^H \chi] = Q_1 \Sigma Q_2^T$$

The pseudo-inverse of the matrix can then be defined as

$$[[\chi]^H \chi]^{-1} = [[\chi]^H \chi]^+ = Q_2 \Sigma^+ Q_1^T$$

This pseudo-inverse matrix will be used as the inverse of the matrix. More information on SVD and the pseudo-inverse is discussed in [5].

Then, any sound source approaching the field domain can be interpolated using equation 2.3.3:

$$\Psi_j = \sum_{i=1}^M \chi_j(\mathbf{r}_i) \alpha^i \quad (2.3.3)$$

## 2.5 Appropriate Green's Function

Similar Green's functions used by French [2] are repeated here. For the Helmholtz equation in potential form  $\nabla^2 \phi + k^2 \phi = 0$ , a wave's amplitude and phase values over a distance from the wave's source can be described by free space Green's functions satisfying the following equation [2]:

$$\nabla^2 \mathbf{G} + k^2 \mathbf{G} = -\delta(\mathbf{r} - \mathbf{r}_0)$$

and the outgoing wave condition (Sommerfeld condition). Harmonic time dependence is assumed and therefore factored out. There are three different types of interpolating functions used, namely plane wave, monopole (free space Green's functions), and evanescent wave functions. They are given as follows:

**Plane wave:**

$$\chi = e^{-ik\hat{n}\cdot r} \quad \text{where } \hat{n} = \langle n_x \hat{i} + n_y \hat{j} \rangle \quad \text{for 2-D}$$

$$\hat{n} = \langle n_x \hat{i} + n_y \hat{j} + n_z \hat{k} \rangle \quad \text{for 3-D}$$

**Evanescent wave:**

$$\chi = e^{-ik\hat{n}\cdot r} \quad \text{where } n_x \text{ is real and larger than 1} \quad \text{for 2-D}$$

$n_y$  is imaginary

**Monopole:**

$$\chi = -\frac{i}{4} H_0^{(2)}(kr) = J_0(kr) - iY_0(kr) \quad \text{for 2-D}$$

$$\chi = \frac{e^{-ikr}}{4\pi r} \quad \text{for 3-D}$$



# CHAPTER 3

## NUMERICAL STUDY AND RESULTS

### 3.1 Introduction

As shown in section 2, the error in interpolating a given arbitrary large set of functions is theoretically optimized. The slope  $\frac{d(\ln \text{error})}{d(\ln \delta)}$  gives the order of the method. This is further discussed in section 3.1.2. It is of interest to know how the accuracy and order vary with different interpolating and test functions.

This chapter is intended to present the numerical results and analysis on the error properties in using the GFD method with various interpolating and test functions. The standard case is first defined so that comparison between various functions can be made. Since satisfactory work was previously done using a set of plane waves as interpolation functions, this set is adopted as the standard interpolating function.

In the earlier sections of this chapter, comparison of the error in using various interpolating functions, namely plane wave, monopole radiator, evanescent wave and combinations of them are made. The 2<sup>nd</sup> order Finite Difference (FD) method is also included for comparison of the error as well as the order of accuracy, with the existing method. Next, the behavior of the influence coefficient is studied.

An analysis on an irregular stencil is then shown. This analysis is to show how the accuracy of the solution will be affected in using irregular, skewed stencils.

The chapter ends with a preliminary study in applying this method in 3-D. This study is done recently and added to the thesis to show if there is any difference in the accuracy and error in 3-D as compared to 2-D.

### 3.1.1 The standard case

In order to make comparisons of the various interpolation functions; a standard case has to be established. Figure 3.1.1.1 shows the standard function, where a set of 20 plane waves, uniformly distributed around the circle approaching the stencil are used as the interpolating functions. French [2] has shown that as the number of (hypothetical) sources (used as the interpolating functions) is increased, the accuracy improves significantly until about 15 sources. Beyond 15, the accuracy is not significantly affected.

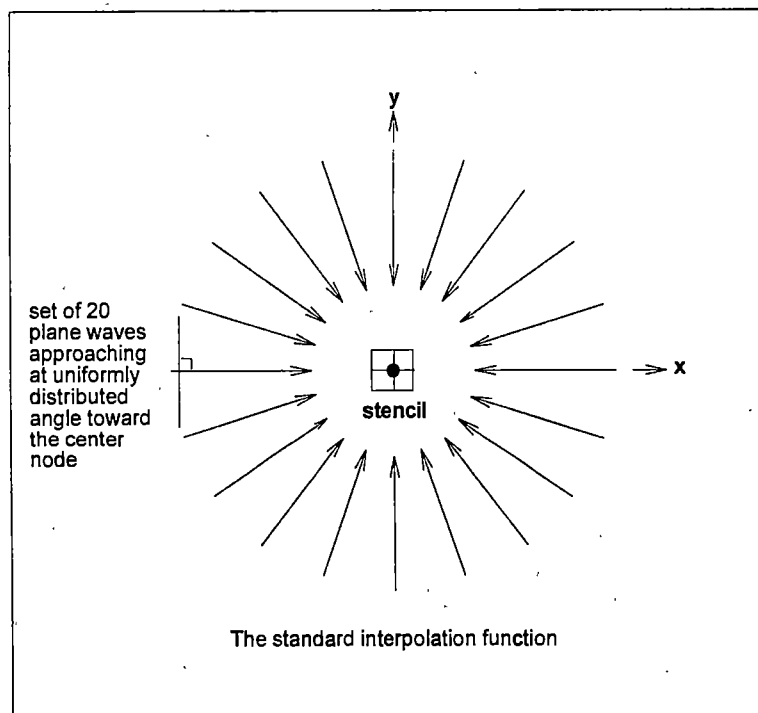


Figure 3.1.1.1: The standard case: 20 plane waves approaching the stencil from uniformly distributed angles.

Other standard parameters include:

- Square stencil grid as shown in figure 3.1.1.2.
- Computed node is the grid's center node shown in figure 3.1.1.2 as a filled circle (●).
- 8 other neighboring nodes located around the computed node. A weighted combination of these nodes is used as an approximation to the computed node. These nodes are shown in figure 3.1.1.2 as empty circles (○).
- Normalized stencil spacing, delta ( $\delta$ ) = 1 as shown in figure 3.1.1.2.
- All positions are nondimensionalized by  $\delta$ .
- The influence coefficients are denoted by the  $a$ 's.

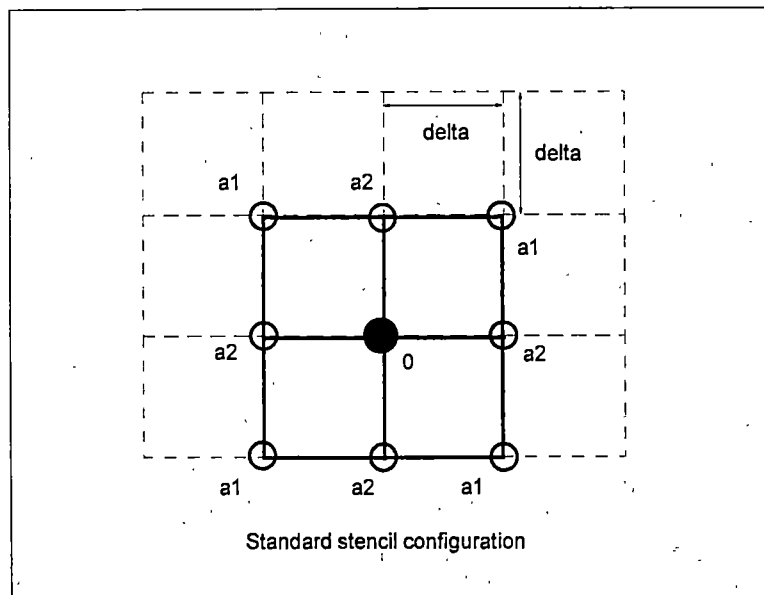


Figure 3.1.1.2: The standard stencil configuration. The computed node is located in the center of the stencil and surrounded by 8 neighboring nodes.

### 3.1.2 Types of plots

There are 3 different types of plots used throughout this thesis:

1. Average error vs. reduced frequency,  $k$ .
2. Magnitude error vs.  $k$ .
3. Influence coefficient,  $a_n$  vs.  $k$ .

In determining the accuracy of the method, the exact solution for some test functions are compared with the computed solution using equation 2.3.4. The acoustic potential has exact analytical solutions for plane waves, monopoles and evanescent waves, and these exact solutions are used as the test functions to compute the exact values for the 8 neighboring nodes shown in figure 3.1.1.2. The computed node in the figure is the only node whose acoustic potential is to be determined, using equation 2.3.3.

The errors used are average square relative error (average error) and relative magnitude errors (magnitude error) produced in interpolating functions and test functions respectively. The magnitude error is defined as follows:

$$\varphi = a + ib$$

$$\text{magnitude\_error} = \frac{\sqrt{[\varphi_{\text{exact}} - \varphi_{\text{computed}}]^* [\varphi_{\text{exact}} - \varphi_{\text{computed}}]}}{|\varphi_{\text{exact}}|} \geq 0$$

The relative average error is defined as:

$$\text{average\_error} = \frac{\sum_{i=1}^N \left( [\phi_{i(\text{exact})} - \phi_{i(\text{computed})}]^* [\phi_{i(\text{exact})} - \phi_{i(\text{computed})}] \right) / |\phi_{i(\text{exact})}|}{N} \geq 0$$

where  $N$  is the number of waves in the interpolation function. Since the computed node is located at the center of coordinate, the exact values of both plane wave and evanescent

wave functions are automatically normalized. Monopole is normalized by dividing all the components in matrix  $\chi$  corresponding to each component vector  $\chi_0$ .

The magnitude and average error plots' scaling are linear for the x-axis and logarithmic for the y-axis. For magnitude error, a log-log plot is also shown. Using this plot, the order of accuracy of the solution can be computed as follows:

$$\text{Error}, E \approx (\Delta x)^n$$

$$\log(E) = \log(\Delta x)^n + \text{const.}$$

$$\log(E) = n \log(\Delta x) + \text{const.}$$

$$n = \frac{d[\log(E)]}{d[\log(\Delta x)]}$$

where  $n$  is the order of magnitude of accuracy of the solution. In this study, reduced frequency,  $k$  is used as the independent variable. It is defined as  $k = \frac{\omega \delta}{c}$ , where  $\omega$  is an angular frequency,  $\delta$  is the stencil length, and  $c$  is the speed of sound. Then

$$n = \frac{d[\log(E)]}{d[\log(\Delta x)]} = \frac{d[\log(E)]}{d[\log(k)]}$$

Since the order of accuracy for second order operators, say  $m$  is always 2 order lower than the order of the function,  $m = n - 2$ . Interpolating monopole functions at small radius introduces a second variable,  $R/\delta$  where  $R$  is the distance of the monopole from the center node. This is discussed further in section 3.2.4. The  $a_n$  vs.  $k$  plot is a linear plot. This is to show how the influence coefficient behaves for various interpolation function sets as a function of the reduced frequency,  $k$ . Results are obtained for  $0.0005 \leq k \leq 3$  in increments of 0.01. Computation is done with double precision.

### 3.2 Effect of using additional function(s)

This section examines how the accuracy is affected as different types of acoustic potential functions are added to the standard set as the interpolating functions for the Green's Function Discretization. Four different combinations are used to compare with the standard case:

- Using a set of 20 monopoles uniformly distributed at radius,  $r/\delta = 5$  around the center node.
- Using a set of 20 monopoles uniformly distributed at radius,  $r/\delta = 10$  around the center node.
- Using a combination of a set of 20 plane waves uniformly distributed in direction around the center node and a set of 20 monopoles uniformly distributed at radius,  $r/\delta = 5$  around the center node.
- Using a combination of a set of 20 plane waves uniformly distributed in direction around the center node and a set of 20 monopoles uniformly distributed at radius,  $r/\delta = 10$  around the center node.

Four different tests are run on these cases. The first test is simply to compare the average error on interpolating the function set itself. This is the set over which the average interpolating error has been minimized by the GFD procedure. The rest of the tests deal with interpolating acoustic potential solution not contained in the interpolating function set, namely a plane wave (at a direction not included in the set), a monopole and an evanescent wave. The plane wave interpolating function case may be extrapolated to the limit of an infinite number of plane waves as shown by Caruthers et. al. [3]. In

addition, in order to compare with an existing FD scheme, a 9-point 2<sup>nd</sup> order FD scheme is introduced. Discretization of this scheme is shown in Appendix 1.

### 3.2.1 Figures reference codes

In each figure in section 3.2, a short form of data name is used to indicate the various interpolating functions and test functions used. Below are the codes for each data name.

There are generally two types of plots in this section, namely average error plot and magnitude error plot. They are indicated as:

er-(i.f.)	Average error in interpolating its function set.
er2-(t.f.)-(i.f.)	Magnitude error in interpolating a test function different than any of the interpolating functions.

where (i.f.) is the interpolating function set, and (t.f.) is the test function for that particular test.

The interpolating functions are indicated as:

xx-xxx-20pw	20 plane waves (the Standard case).
xx-xxx-20mor5	20 monopoles at radius 5.
xx-xxx-20mor10	20 monopoles at radius 10.
xx-xxx-20pw20mor5	20 plane waves and 20 monopoles at radius 5.
xx-xxx-20pw20mor10	20 plane waves and 20 monopoles at radius 10.
xx-xxx-infpw	Infinite number of plane waves.
xx-xxx-fd2nd	The 2 <sup>nd</sup> order FD.

### 3.2.2 Effect on Average Error

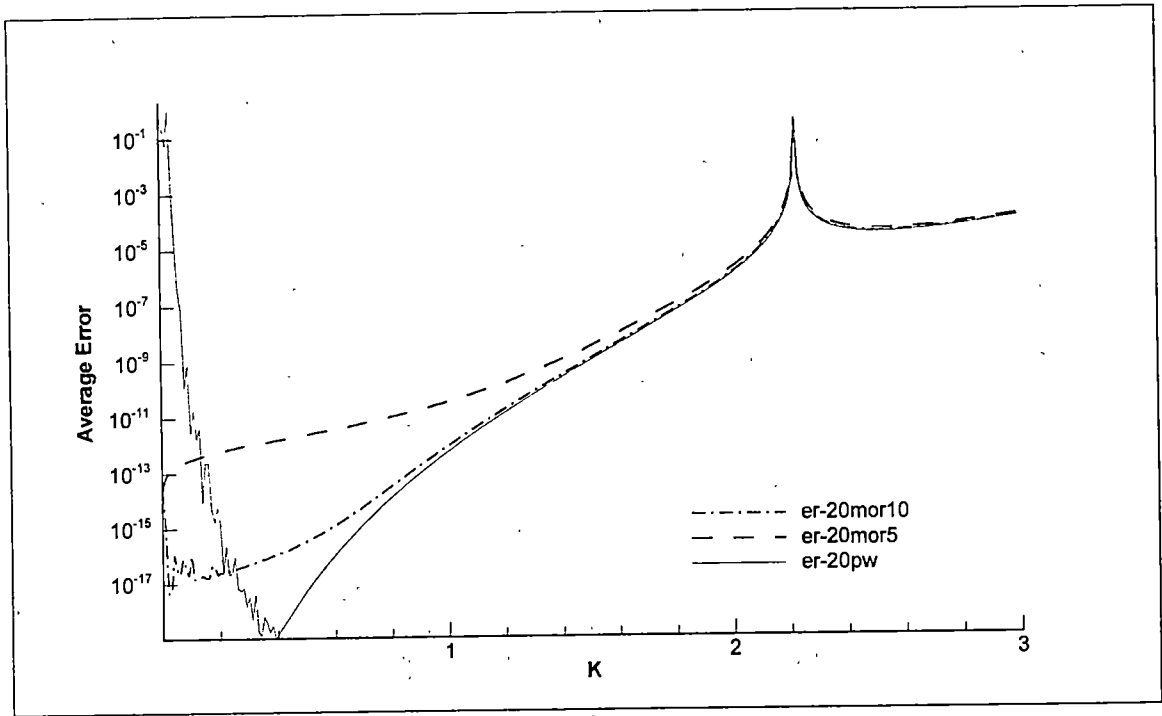
This sub-section examines the effect of using different combination of functions on the average error.

Figure 3.2.2.1a shows that by using 20 monopoles at  $r/\delta = 5$ , the average error decays smoothly as the reduced frequency,  $k$  approaches zero. However, the error (at  $k$  approaching zero) is higher than for the standard case. The apparent discontinuity occurs at about  $k = 2.221$ . This is closed to the value of  $\pi/\sqrt{2}$ , which matches the so-called Nyquist limit. This limit is discussed in detail in reference [2]. It is therefore expected that, for any 2-D GFD problem with uniform square stencil, this sharp discontinuity should appear at exactly the same value of  $k$ .

As the radius of the monopoles is increased to  $r/\delta = 10$  (figure 3.2.2.1a), the average error starts to show the same behavior as the standard case; smaller error at small  $k$ , and as  $k$  approaches zero, the smoothness of the curve tends to diminish. This is expected since, as monopole gets farther from the point of interest/listening point (center node in this case), the wave starts to behave similar to a plane wave.

In figure 3.2.2.1b, combining plane waves with monopoles shows that the monopoles' characteristic dominates the functions. For the case with monopoles at  $r/\delta = 5$ , the error is slightly lower than the previous case (20 monopoles,  $r/\delta = 5$  without plane waves) at small  $k$ . Similar trends are observed in the case with monopoles at  $r/\delta = 10$ .





a)

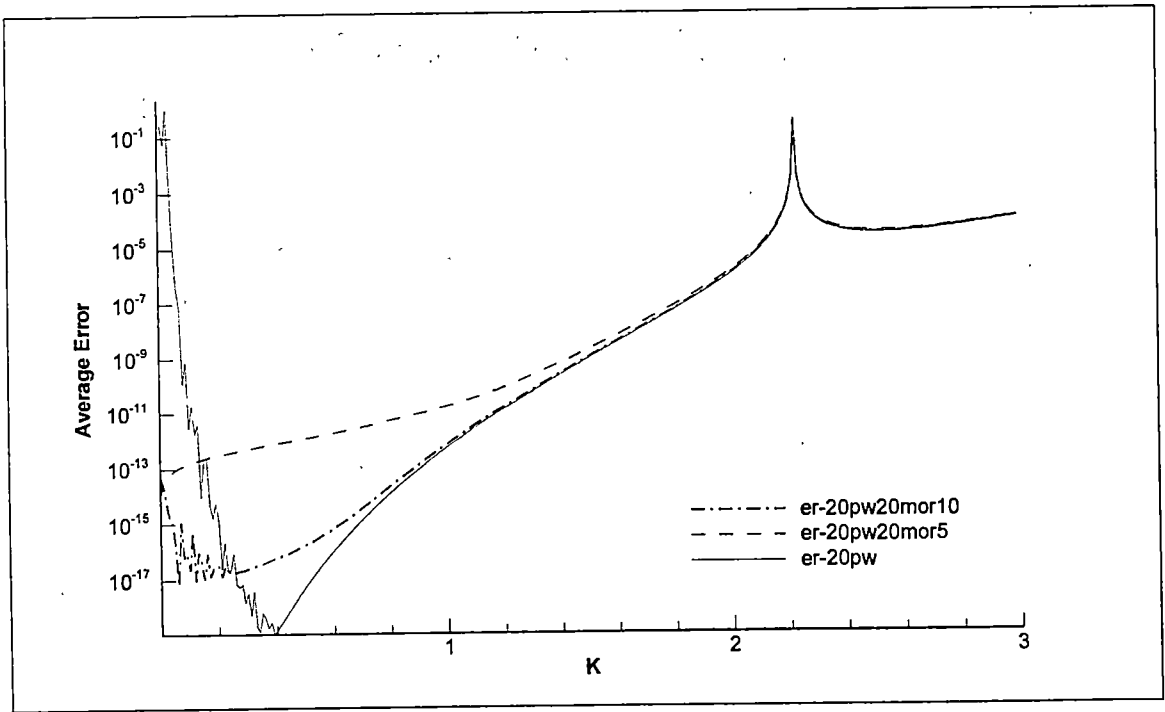


Figure 3.2.2.1: Average Error vs.  $k$  for various interpolating functions.

### 3.2.3 Effect on interpolating a plane wave

In this sub-section, the effect of interpolating a plane wave, different from any of the interpolating functions is examined. A plane wave coming at  $15^\circ$  angle is used as the wave to be interpolated by the functions (see figure 3.2.3.1 below). The same sets of functions used in the previous section are used and in addition, an infinite plane wave of GFD method and the  $2^{\text{nd}}$  order of FD Scheme are added for comparison.

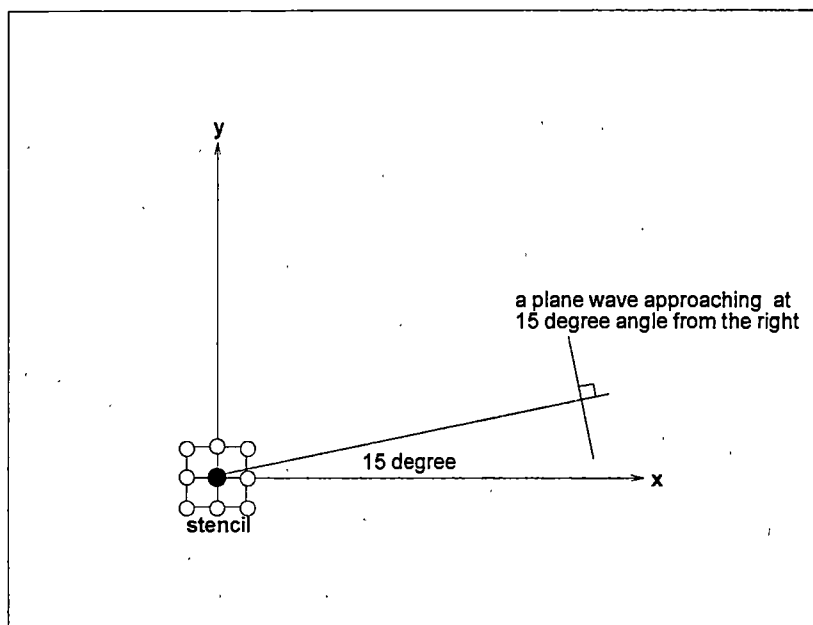
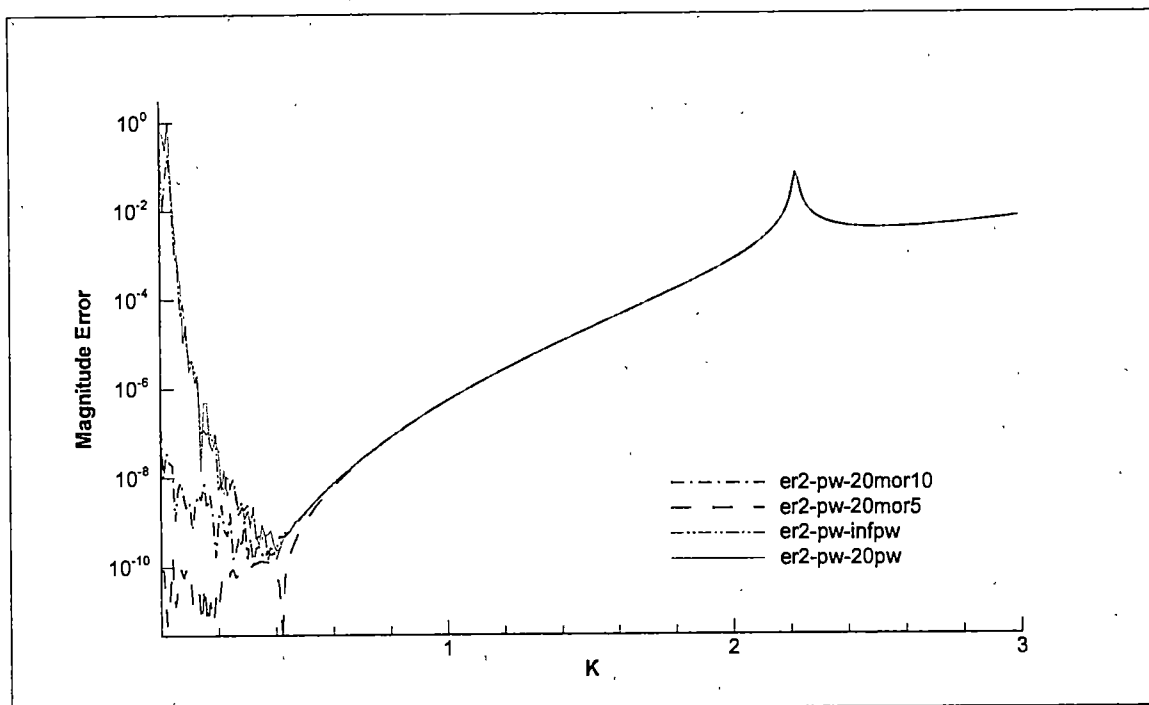


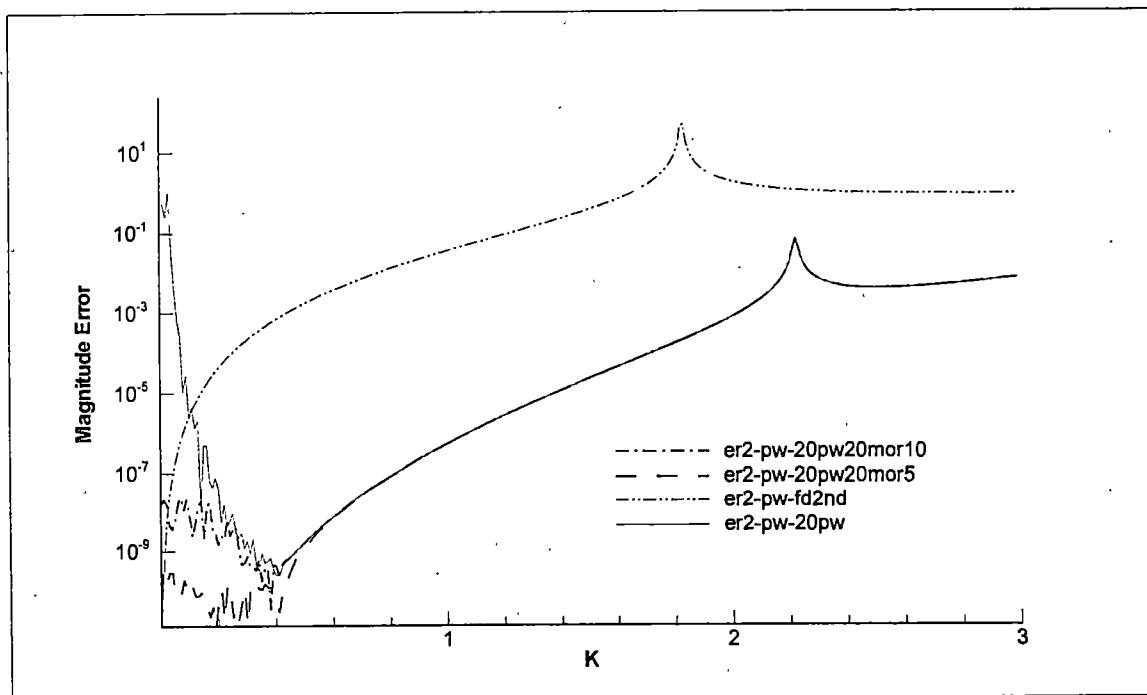
Figure 3.2.3.1: Interpolating a plane wave.

Figures 3.2.3.2 show that for the reduced frequency of around 0.6 and above, the magnitude error is remarkably the same for all functions of GFD scheme. The 20 plane waves result is shown to be very much similar to the infinite plane waves. This means, no significant changes in the magnitude error as the number of plane waves is increased. This is in agreement with the conclusion that French [2] has made in his thesis. As expected, the  $2^{\text{nd}}$  order FD scheme shows a much larger error in the interpolation.

Figures 3.2.3.3 show the same plot with a log-log scale in the x and y axes. The slope of the straight line is used to find out the order of accuracy of the method. The slope is found to be 8 for all the GFD method functions, and 4 for the 2<sup>nd</sup> order FD scheme. Therefore, as expected, the indicated order of accuracy is 6 and 2 for the GFD method and FD scheme respectively.

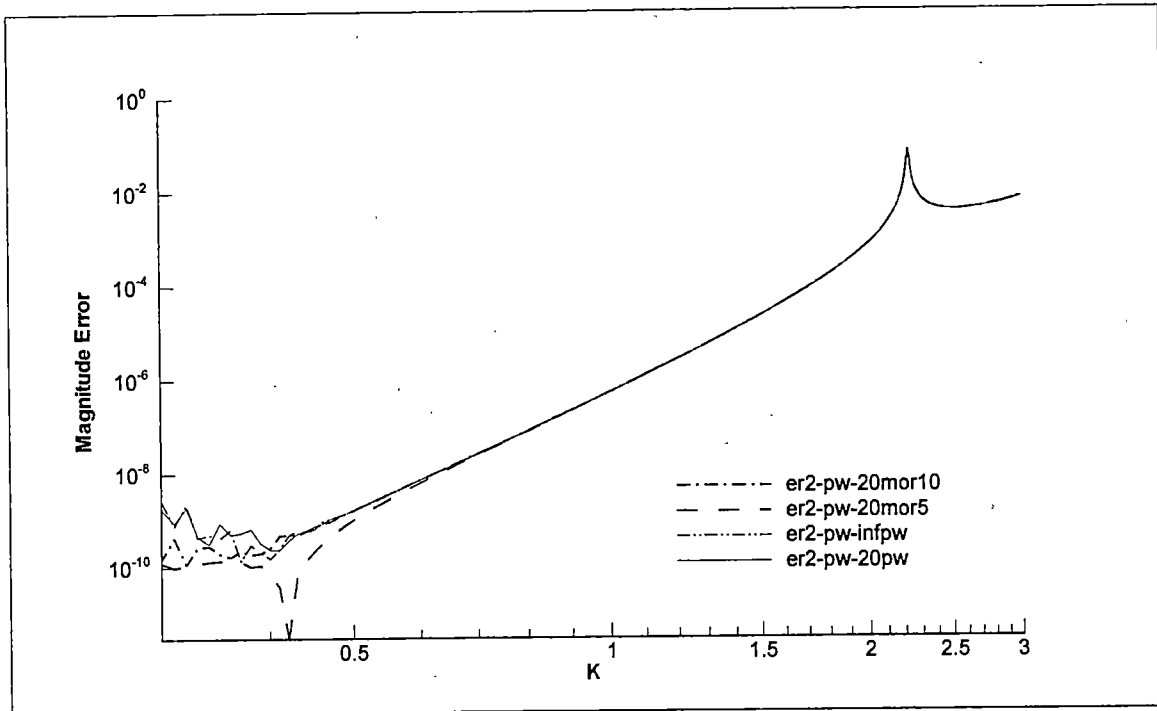


a)

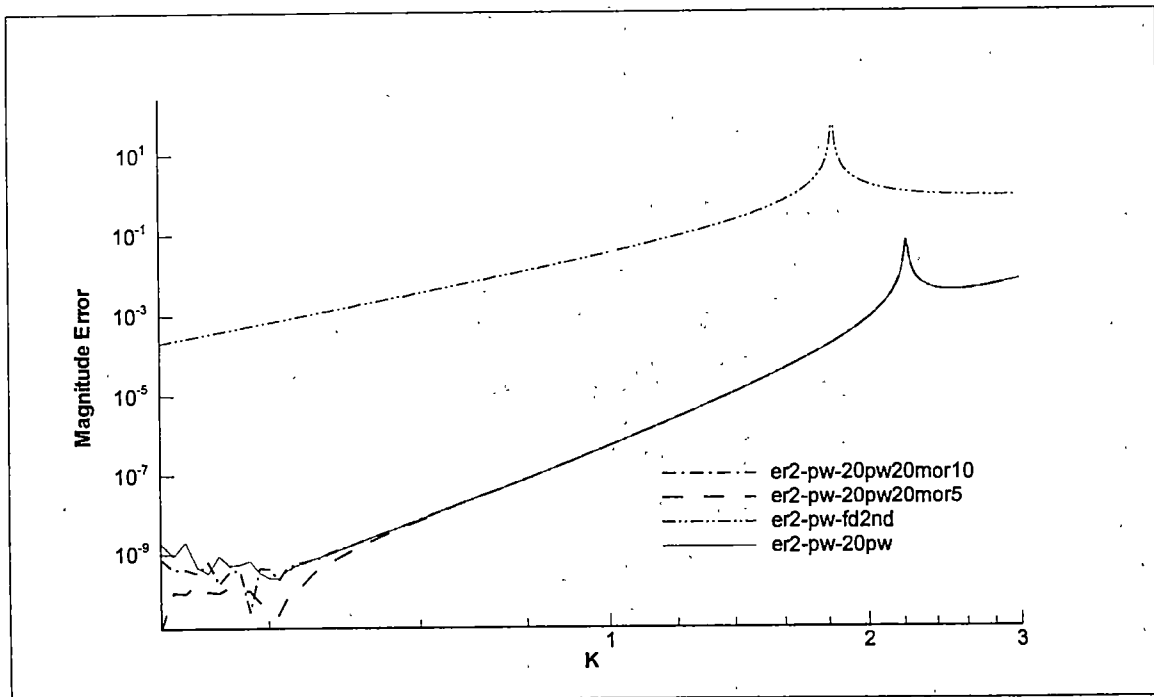


b)

Figure 3.2.3.2: Magnitude Error vs.  $k$  for various functions in interpolating a plane wave approaching at  $15^\circ$  angle from the right (semi-log plot).



a)



b)

Figure 3.2.3.3: Magnitude Error vs.  $k$  for various functions in interpolating a plane wave approaching at  $15^\circ$  angle from the right (log-log plot).

### 3.2.4 Effect on interpolating a monopole radiator

Another type of sound source that GFD method must be able to handle is a monopole. In this sub-section, two cases of monopole test functions interpolations are used; one is interpolating a monopole at radius,  $R/\delta = 10$ , and another one with radius,  $R/\delta = 20$ . Both monopoles are at the angle of  $15^\circ$  from the x axis. This is shown in figure 3.2.4.1.

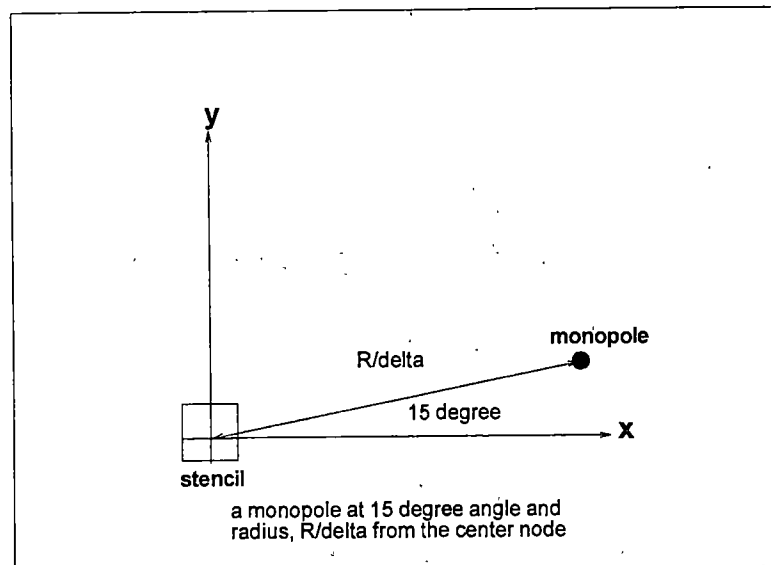


Figure 3.2.4.1: Interpolating a monopole.

As can be seen from figure 3.2.4.1 above, monopole radiator is a point sound source. The wave front surface produced by this source is like a ring, centered at the point and radiating out. The wave decays as it moves away from the point. As the wave travels further away from its source, the curvature shape of the ring starts to be reduced and the wave front starts to be seen as a straight line, similar to plane wave. In other words, as monopole gets farther from the computed node, in our case, characteristics similar to one

of the plane wave is expected to show up. The use of the monopole as a test function tests the accuracy of the method for waves with curved wave fronts.

Figures 3.2.4.2 are shown for the magnitude error of all interpolating functions used, which are the same functions from the previous section. All GFD functions agree with the standard case (20 plane wave) for large values of the reduced frequency,  $k$ . In interpolating a monopole of  $R/\delta = 10$  (figure 3.2.4.2), it is noted that the error reduction tends to become smaller as  $k$  gets small. It is then expected that the slope and therefore the order of accuracy drops significantly. This is shown in figure 3.2.4.3, where the straight lines only appear at a small range of  $k$  between 0.6 and 2 (which was computed to have a slope of 8). For  $k$  below 0.6, the slope drops to around 2.

This is thought to be in disagreement with the analytical analysis done by Caruthers [3]. Further thought on this issue brings out some possible explanation. In interpolating the monopole, the reduced frequency,  $k$  is not the only relevant variable. There is another variable,  $R/\delta$  where  $R$  is the radius of the monopole test function and  $\delta$  is the normalized stencil length. A preliminary study is done on this thought. Instead of using only the reduced frequencies as the variable, the  $R/\delta$  is also used and vary. Defining a constant variable, say  $\lambda$  as follows:

$$\lambda = \left\{ \left( \frac{\omega\delta}{c} \right) \left( \frac{r}{\delta} \right) \right\}$$

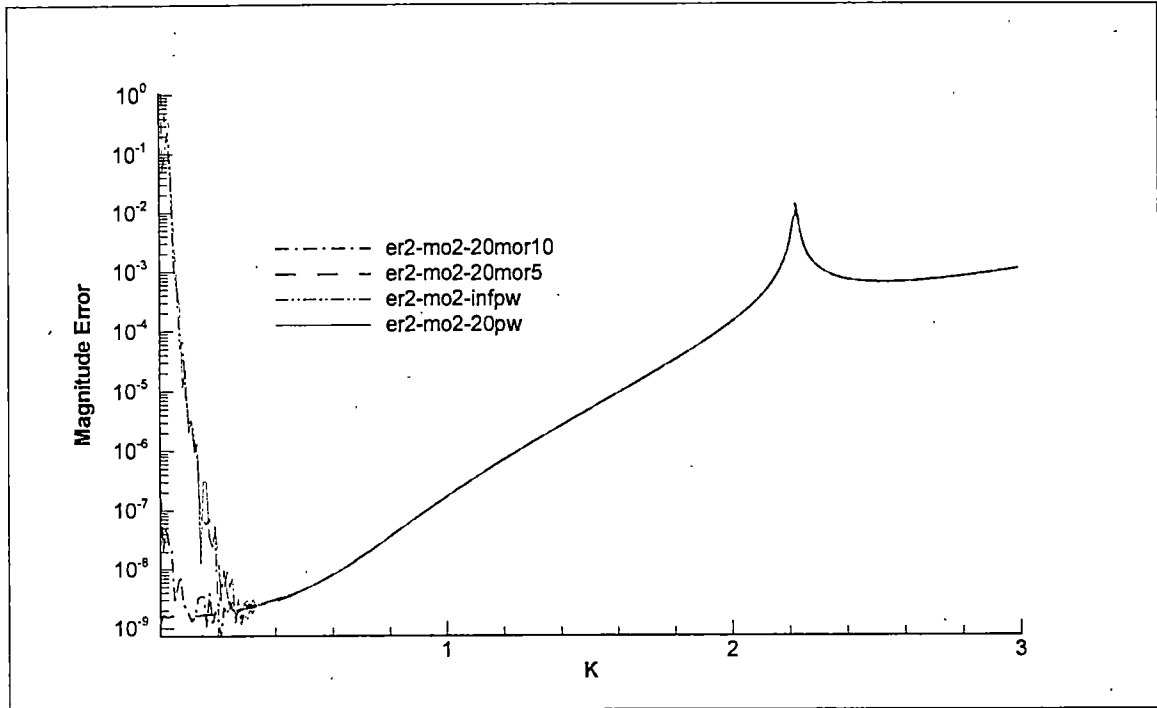
where

$$k = \left( \frac{\omega\delta}{c} \right)$$

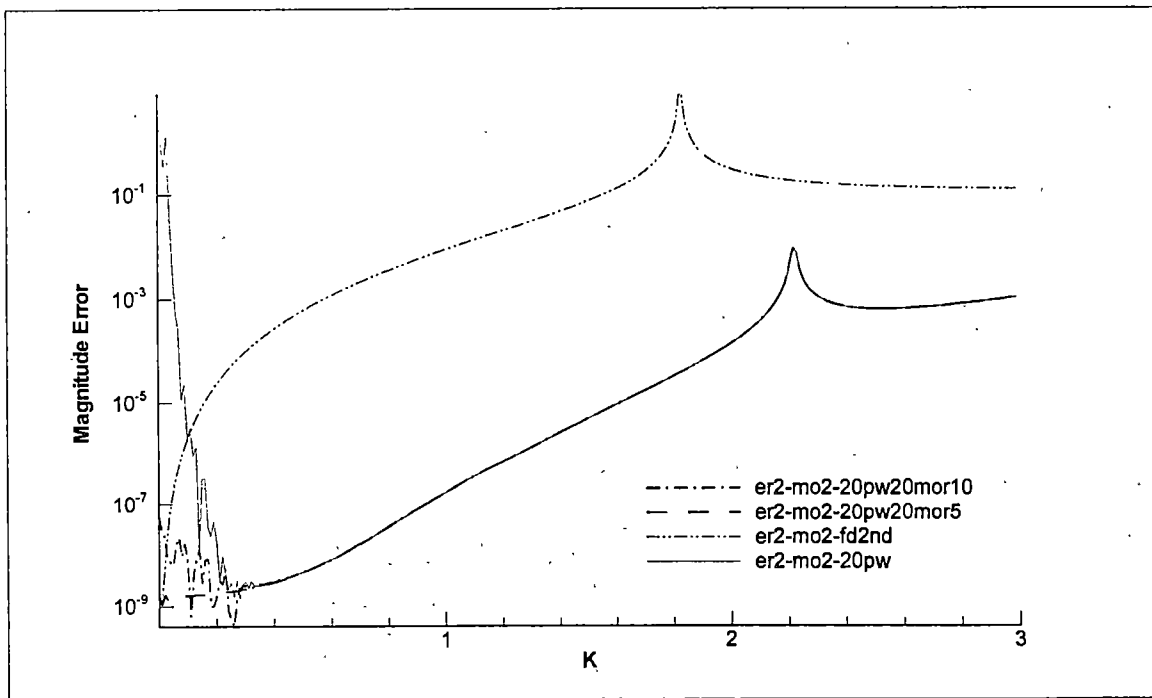
By keeping the variable,  $\lambda$  constant at any time, the test cases are rerun from  $k = 0$  to 3. Note that, as the reduced frequency increases, the distance of the monopole to be interpolated decreases, to maintain the value of  $\lambda$  constant. A case of  $\lambda = 40$  is plotted in figure 3.2.4.6 for the standard function and the two monopole sets. The error reduces more as  $k$  gets smaller, as compared to the previous result. The slopes also show a good straight lines produced. The slope of the lines (figure 3.2.4.7) all showed the accuracy maintained to 6<sup>th</sup>. Further study on this issue is beyond the scope of this thesis.

For monopole at  $R/\delta = 20$ , the phenomena (of reduced slope) seems to disappear. This agrees with the argument that as monopole gets farther from the computed node, it tends to behave like a plane wave. The order of accuracy is also maintained at 6 for this larger radius monopole. This slope plot is shown in figure 3.2.4.4.



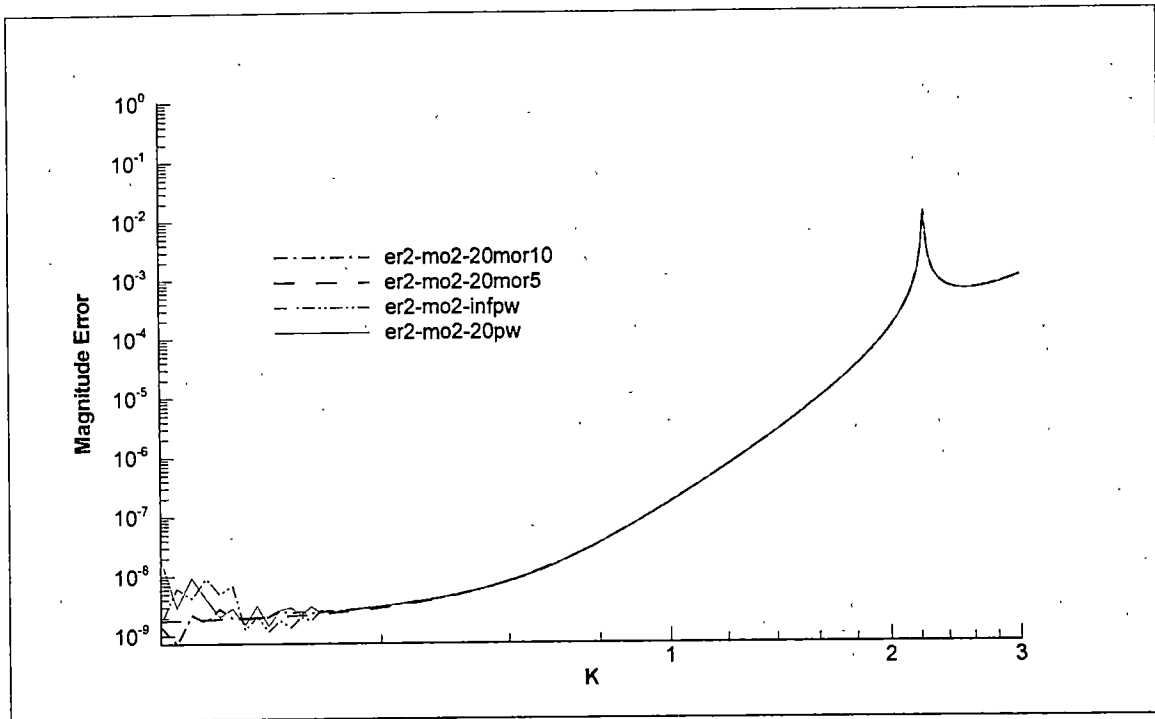


a)

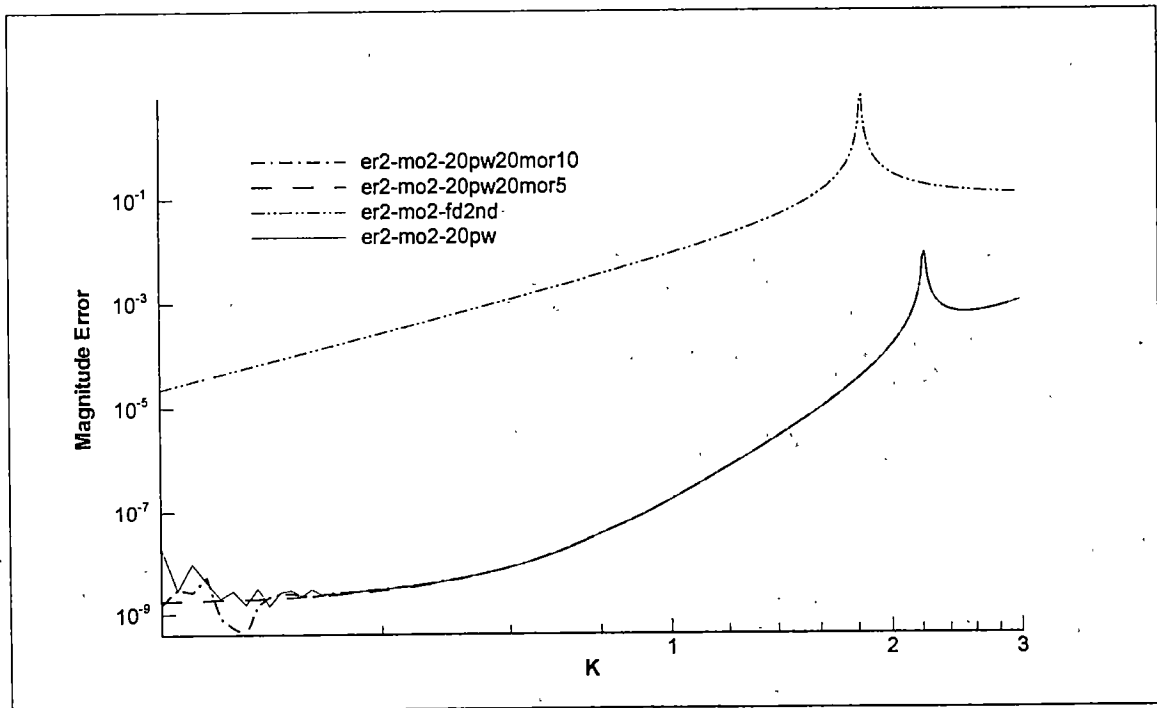


b)

Figure 3.2.4.2: Magnitude Error vs.  $k$  for various functions in interpolating a monopole at radius  $R/\delta = 10$ , at  $15^\circ$  angle from the right (semi-log plot).

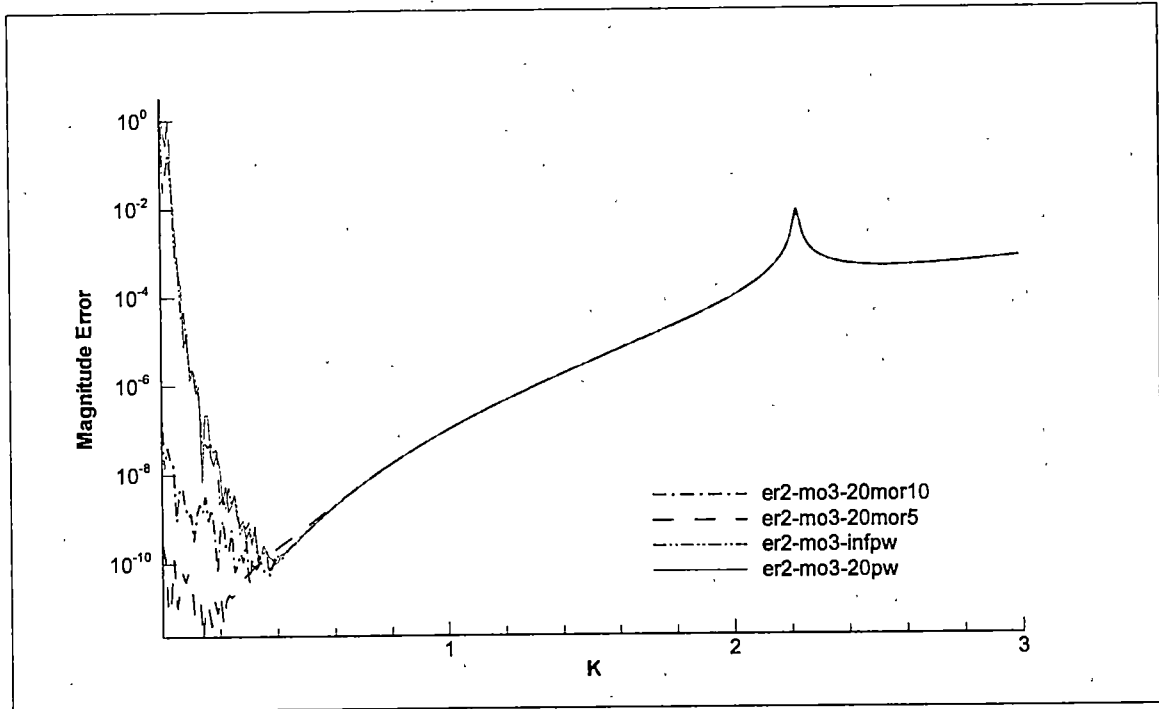


a)

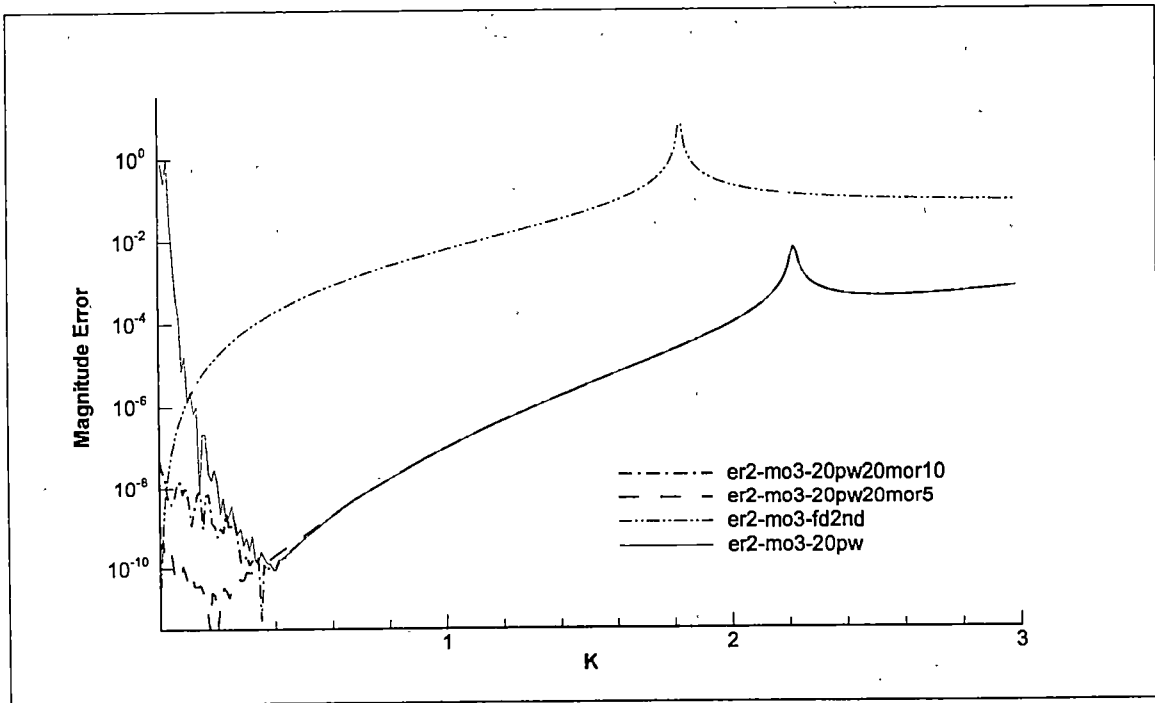


b)

Figure 3.2.4.3: Magnitude Error vs.  $k$  for various functions in interpolating a monopole at radius  $R/\delta = 10$ , at  $15^\circ$  angle from the right (log-log plot).

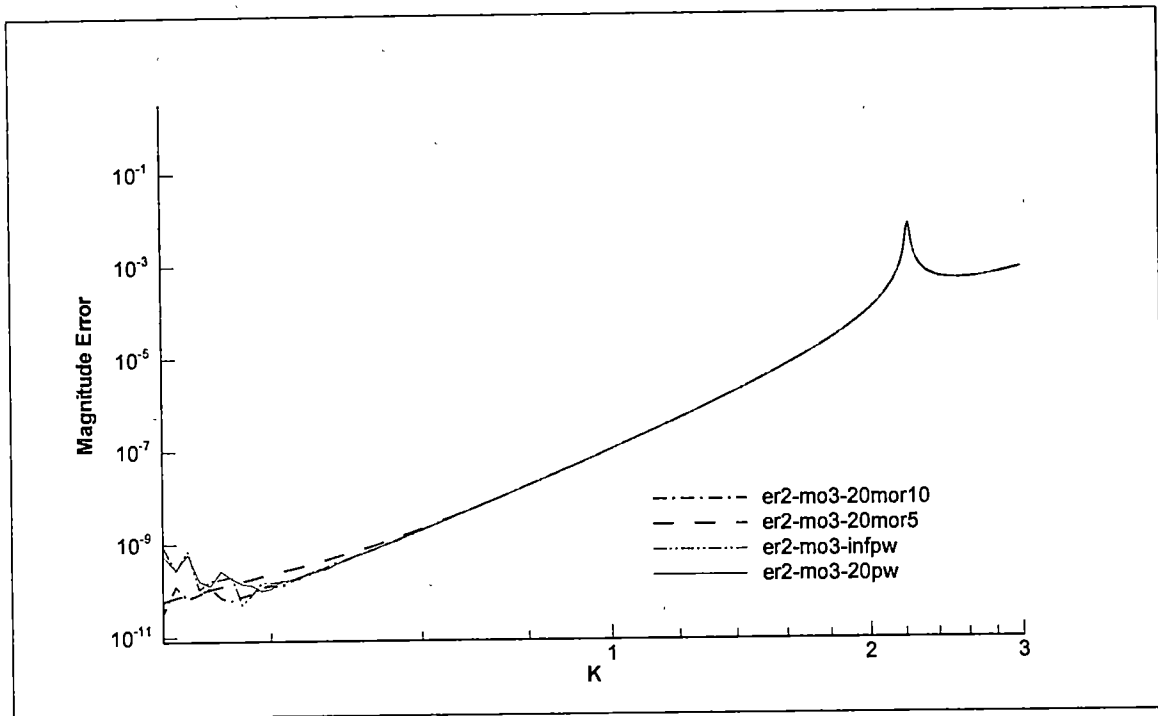


a)

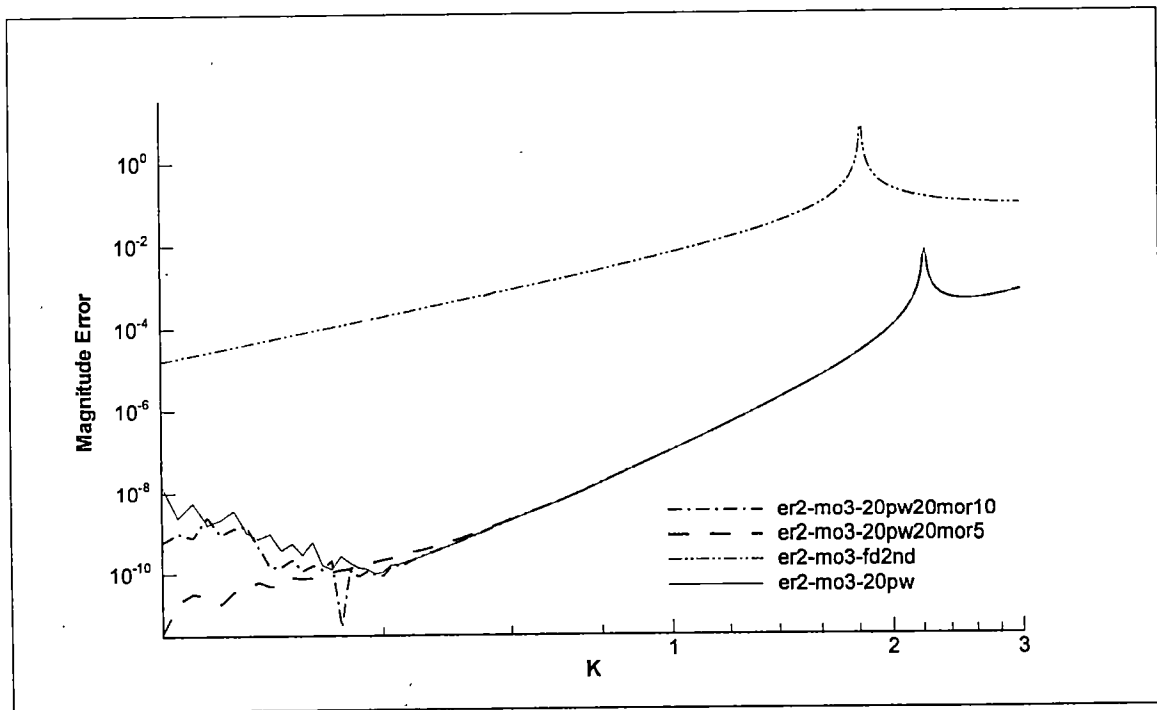


b)

Figure 3.2.4.4: Magnitude Error vs.  $k$  for various functions in interpolating a monopole at radius  $R/\delta = 20$ , at  $15^\circ$  angle from the right (semi-log plot).



a)



b)

Figure 3.2.4.5: Magnitude Error vs.  $k$  for various functions in interpolating a monopole at radius  $R/\delta = 20$ , at  $15^\circ$  angle from the right (log-log plot).

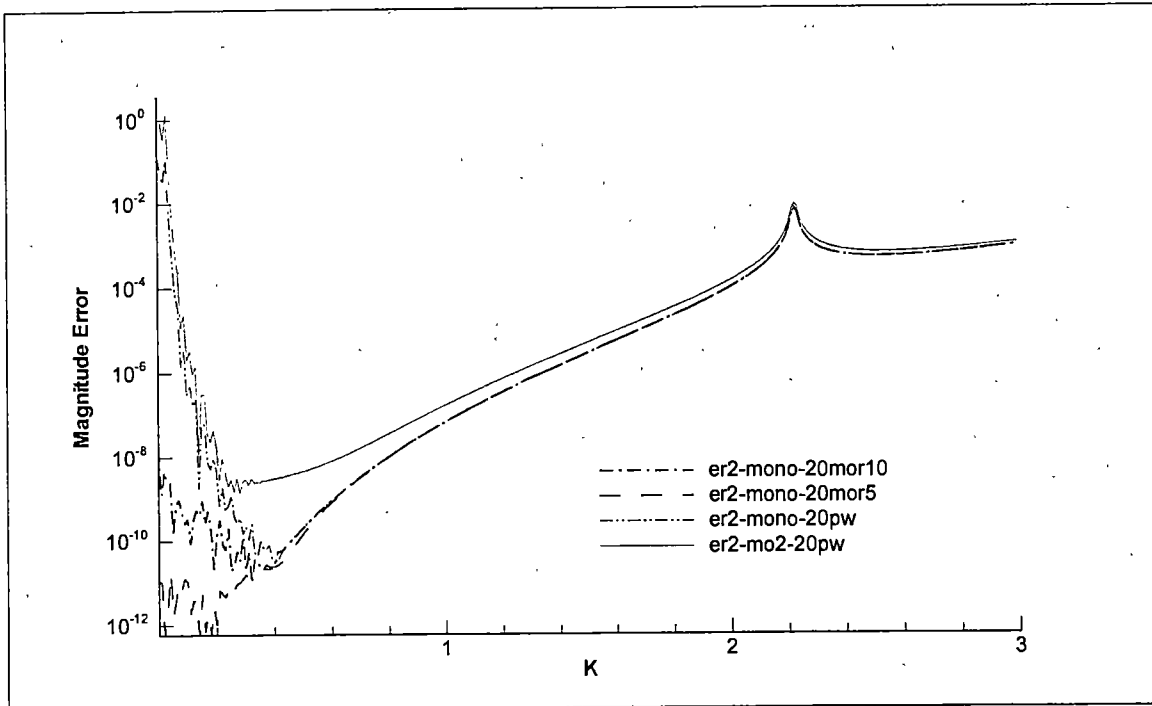


Figure 3.2.4.6: Magnitude Error vs.  $k$  for various functions in interpolating a monopole with  $\lambda$  fixed at 40 (semi-log plot).

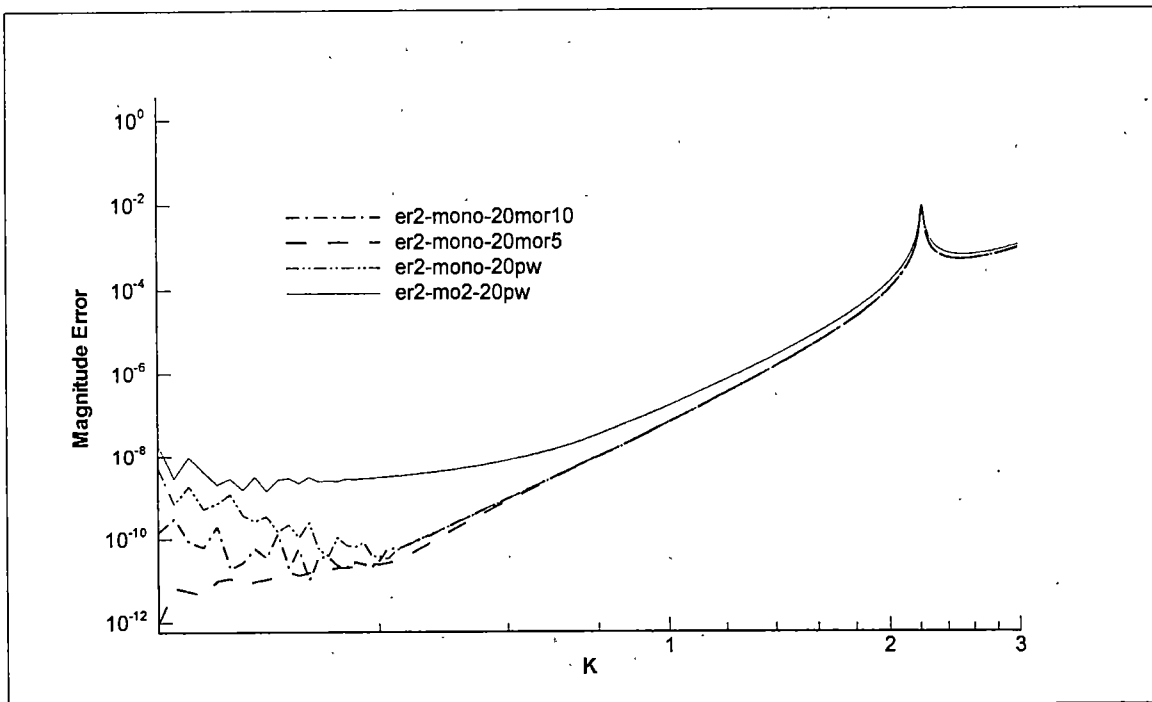


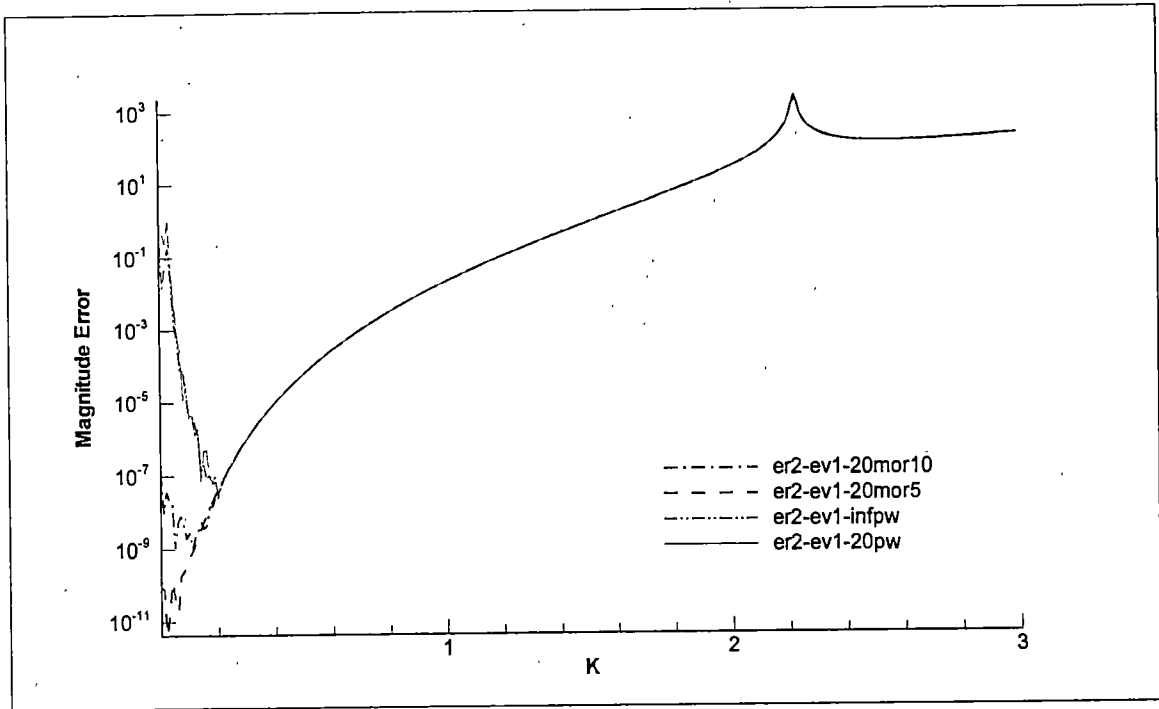
Figure 3.2.4.7: Magnitude Error vs.  $k$  for various functions in interpolating a monopole with  $\lambda$  fixed at 40 (log-log plot).

### 3.2.5 Effect on interpolating an evanescent wave

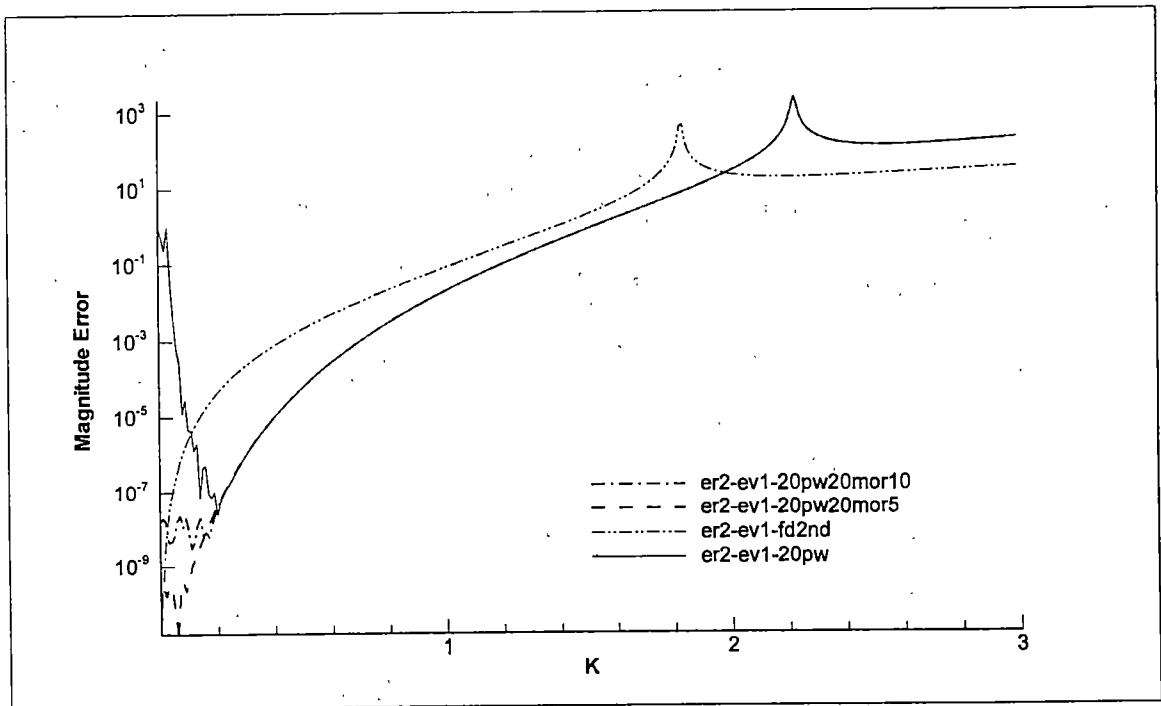
Another type of sound disturbance is an evanescent wave. An evanescent wave is similar to a plane wave along one axis, but decays exponentially along the other. In this section, evanescent waves with phase Mach number of 0.5 and 0.25 respectively, are used as the test functions. General characteristics of phase Mach number are that as the Mach number decreases, the evanescent wave decays more rapidly, and the wavelength gets shorter.

Comparing the magnitude error of all functions of GFD method show that they all behave similar to the standard case for most range of the reduced frequencies. This is true for both phase Mach numbers as shown in figures 3.2.5.1 and 3.2.5.3. For low reduced frequencies, the difference of the error value is expected as before. The slope of the errors, in figures 3.2.5.2 and 3.2.5.4 is again computed to be 8 and hence, the order of accuracy is maintained at 6<sup>th</sup>.

In figure 3.2.5.5, both evanescent wave's interpolations are compared. It shows that the error decreases significantly as the phase Mach number is increased. If the phase Mach number is supersonic ( $M > 1$ ), the evanescent wave becomes a plane wave, explaining why the evanescent errors seem to converge toward the errors of the plane wave as the phase Mach number increases [2].

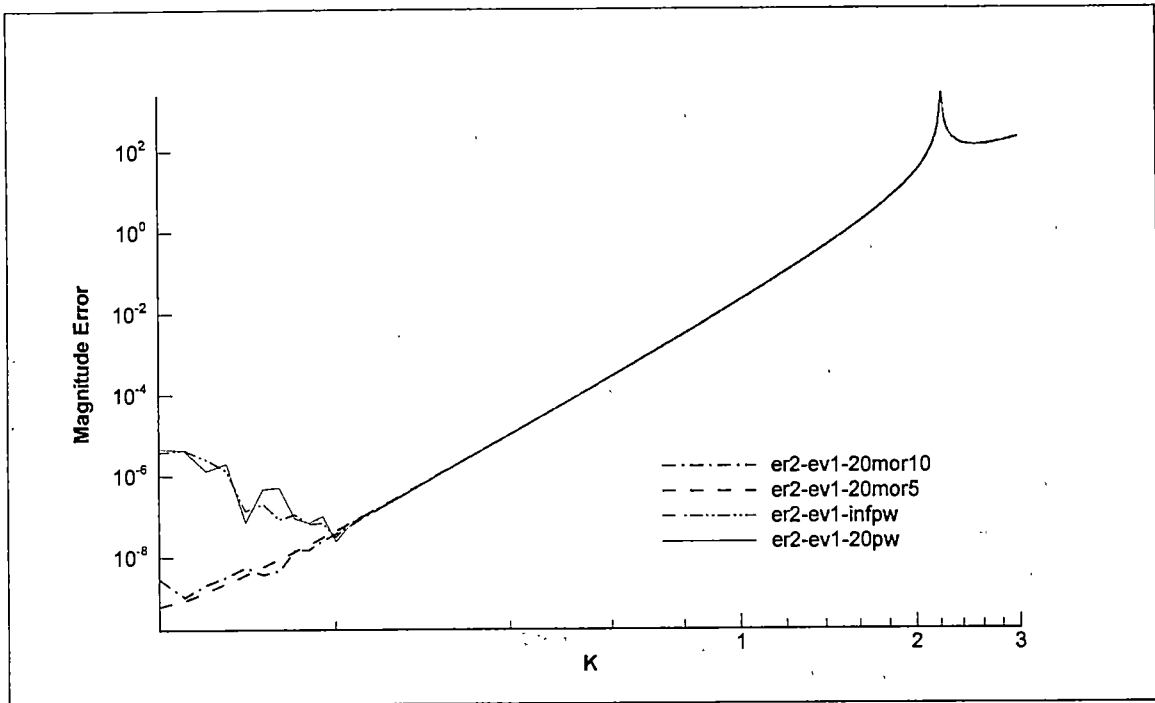


a)

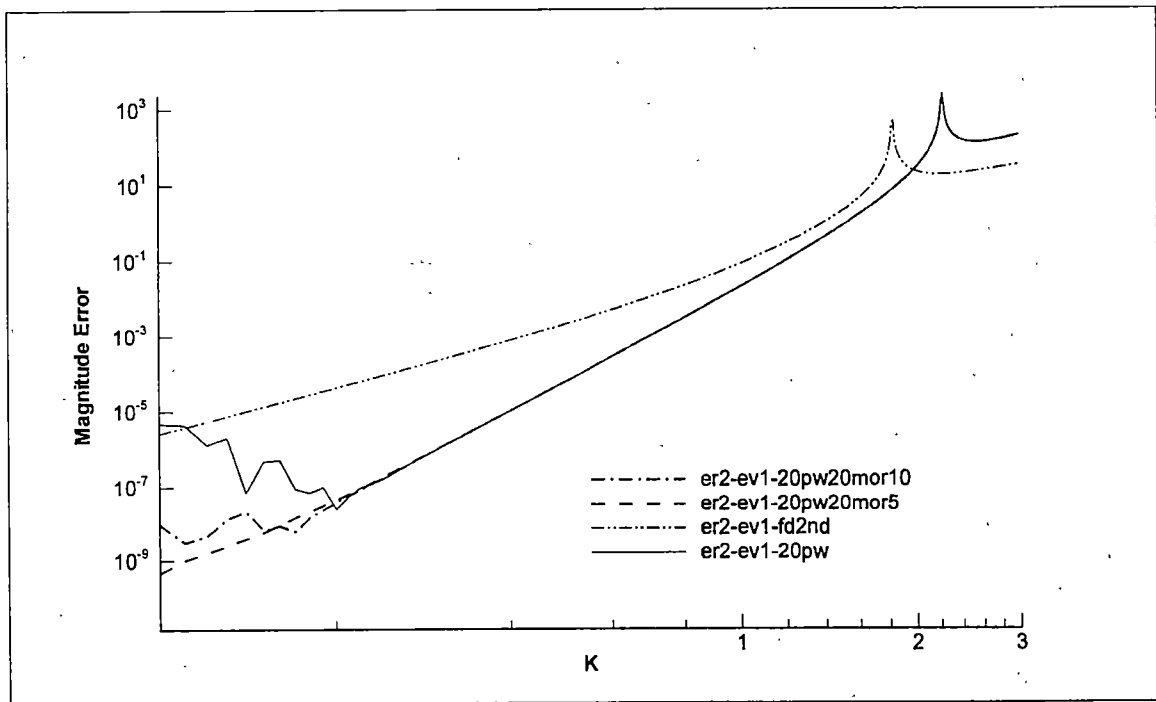


b)

Figure 3.2.5.1: Magnitude Error vs.  $k$  for various functions in interpolating an evanescent waves at phase Mach number = 0.5 (semi-log plot).



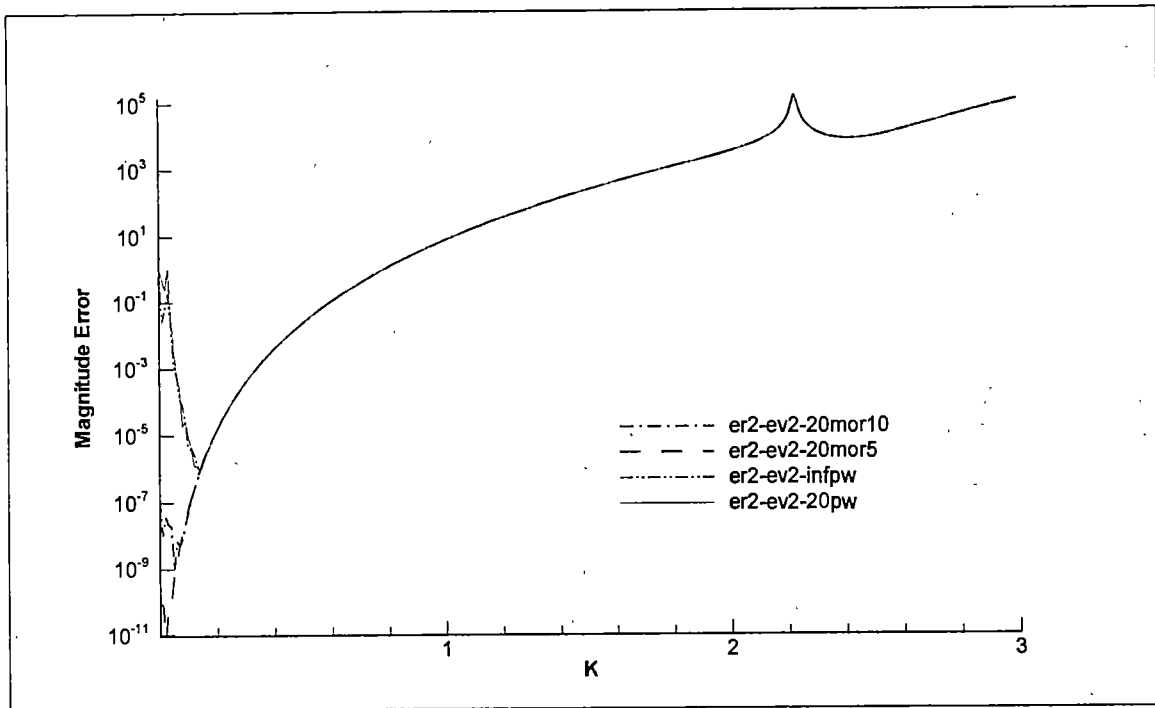
a)



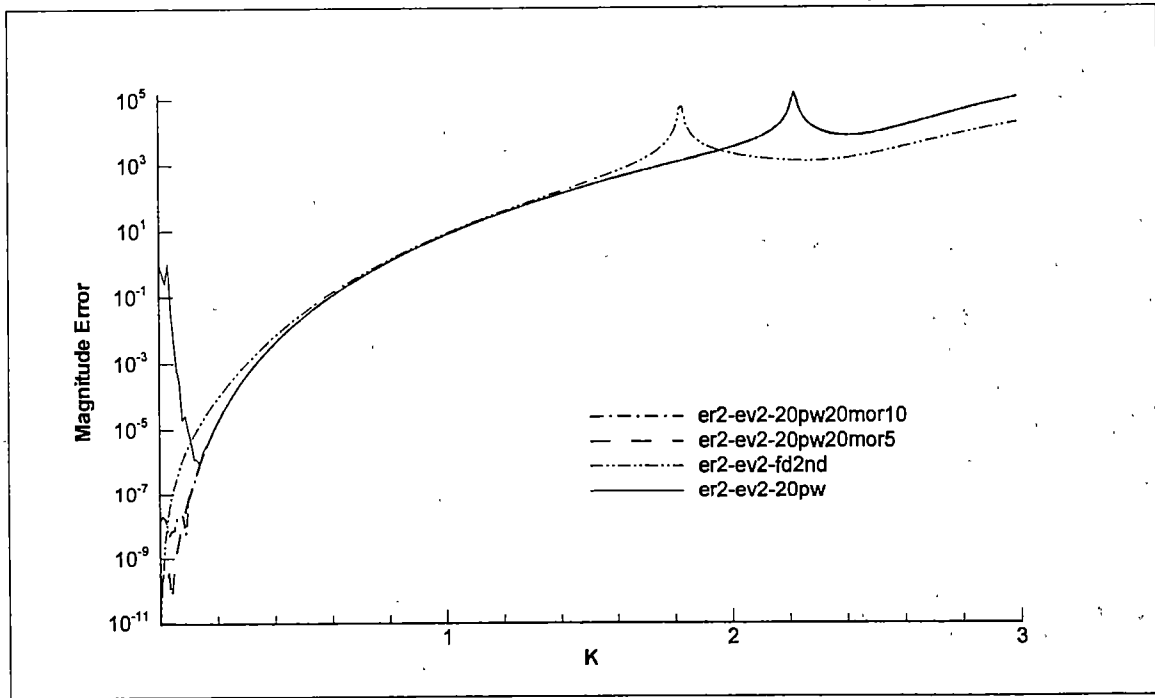
b)

Figure 3.2.5.2: Magnitude Error vs.  $k$  for various functions in interpolating an evanescent waves at phase Mach number = 0.5 (log-log plot).



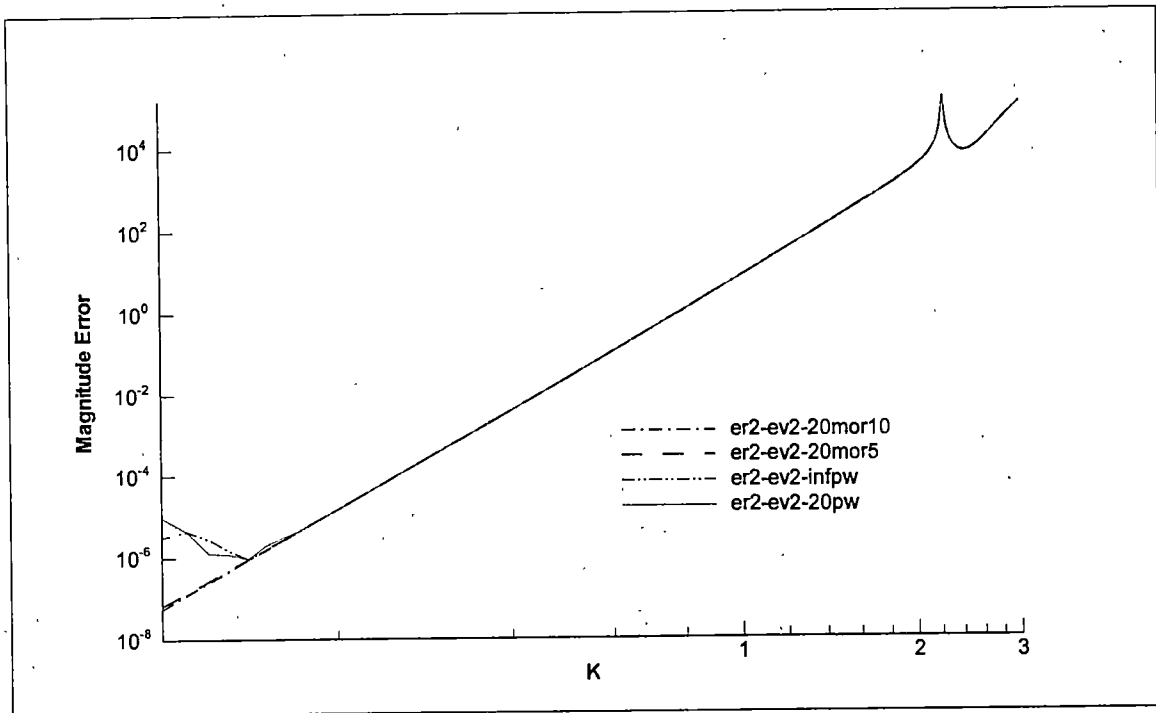


a)

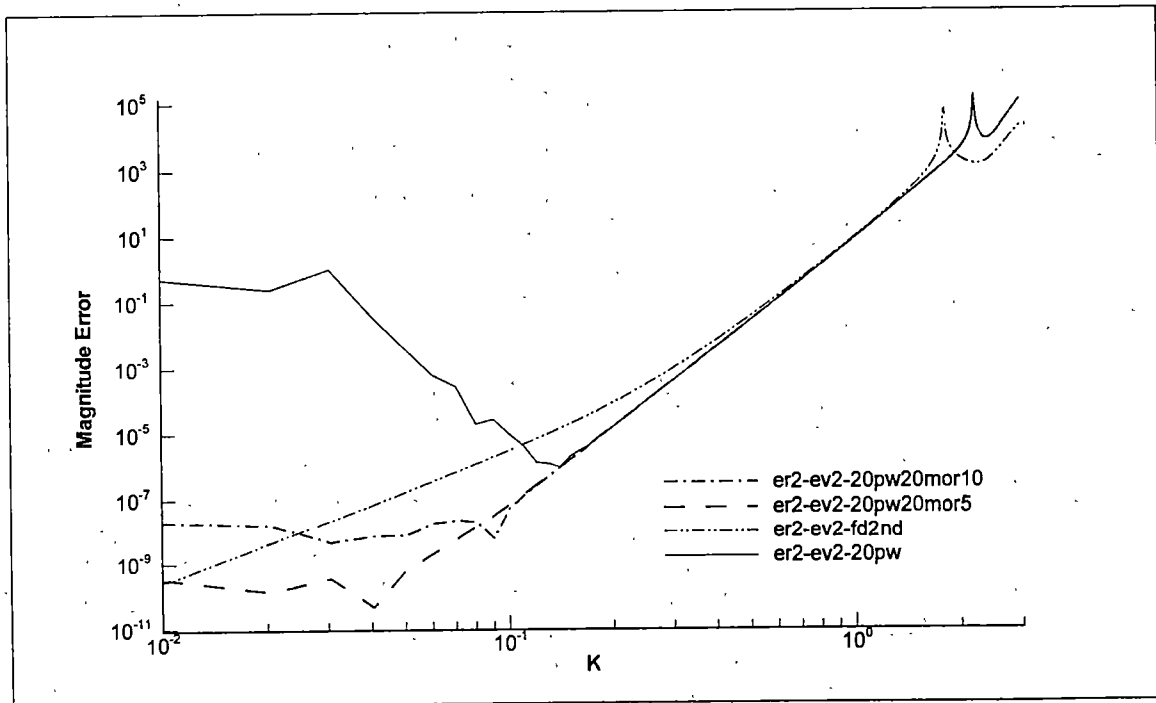


b)

Figure 3.2.5.3: Magnitude Error vs.  $k$  for various functions in interpolating an evanescent waves at phase Mach number = 0.25 (semi-log plot).



a)



b)

Figure 3.2.5.4: Magnitude Error vs.  $k$  for various functions in interpolating an evanescent waves at phase Mach number = 0.25 (log-log plot).

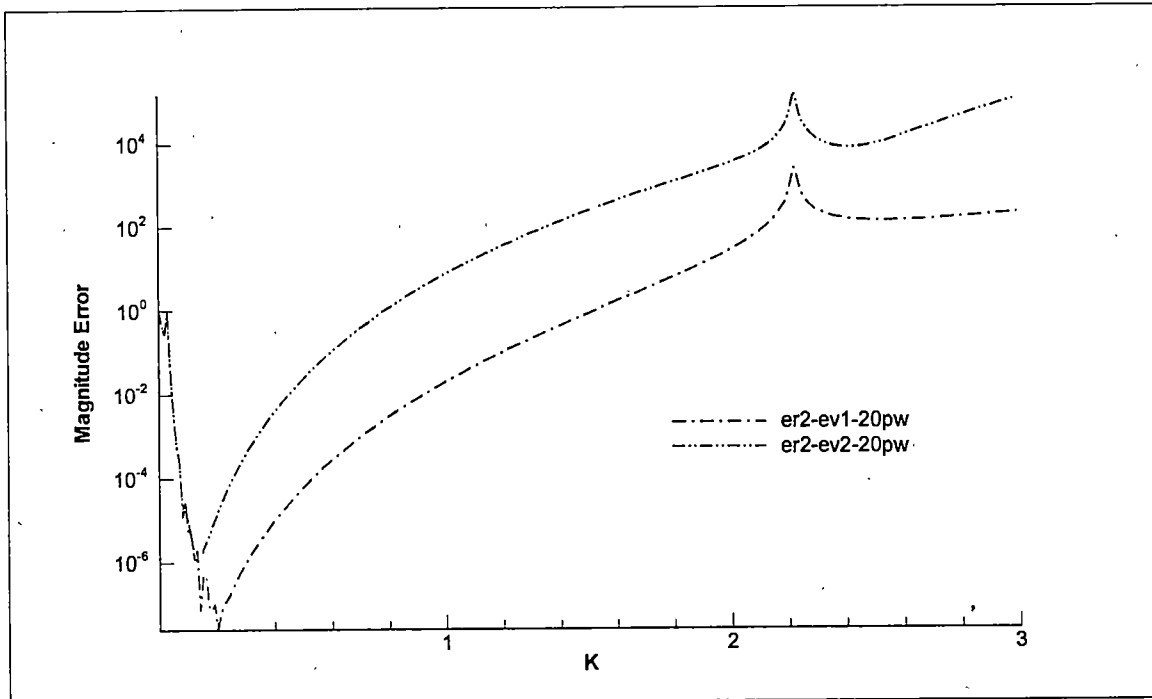


Figure 3.2.5.5: Magnitude Error vs.  $k$  for comparing the values for the 2 different interpolation evanescent waves, at phase Mach number 0.5 and 0.25 (semi-log plot).

### 3.3 Influence coefficient study

This section examines and compares how the influence coefficient vector,  $\mathbf{a}$  behaves for different functions used in the previous sections. Since a square stencil is being used for the interpolations, there must exist only two distinctive values of the coefficient components, namely  $a_1$  and  $a_2$  (see section 2.4). This is shown in figure 3.1.1.2.

Figures 3.3.1a – f show the plots of  $a_1$  and  $a_2$  for each of the interpolation functions and figure 3.3.1g shows the plot for 2<sup>nd</sup> order FD schemes. All the GFD interpolation functions show identical values of  $a_1$  and  $a_2$ . However, for 2D plane waves and infinite plane waves, the values start to have sharp discontinuities at very small values of  $k$ . Other interpolation functions show a very smooth convergence towards 0.05 and 0.2 for  $a_1$  and  $a_2$  respectively. It is worth noting that this is the well known 9 point FD formula for the two dimensional Laplace equation on a square stencil with 6<sup>th</sup> order accurate.

Caruthers et. al. [3] has shown analytically that for a square stencil with normalized spacing of 1, with infinite plane waves as its interpolating function, that the exact solution for  $\mathbf{a}$  is given by:

$$a_1 = -\frac{-2J_0(k\delta\sqrt{2})^2 - J_0(2k\delta)J_0(k\delta\sqrt{2}) - J_0(k\delta\sqrt{2}) + 2J_0(k\delta)^2 + 2J_0(k\delta\sqrt{5})J_0(k\delta)}{D}$$

$$a_2 = \frac{-2J_0(k\delta\sqrt{2})J_0(k\delta\sqrt{5}) - 2J_0(k\delta\sqrt{2})J_0(k\delta) + J_0(2k\delta\sqrt{2})J_0(k\delta) + J_0(k\delta) + 2J_0(2k\delta)J_0(k\delta)}{D}$$

where,

$$D = \det[\chi^H \chi] = 2J_0(2k\delta\sqrt{2})J_0(k\delta\sqrt{2}) + J_0(2k\delta\sqrt{2}) + J_0(2k\delta)J_0(2k\delta\sqrt{2}) + 1 \\ + 3J_0(2k\delta) - 8J_0(k\delta\sqrt{5})J_0(k\delta) - 4J_0(k\delta)^2 + 2J_0(k\delta\sqrt{2}) \\ - 4J_0(k\delta\sqrt{5})^2 + 4J_0(2k\delta)J_0(k\delta\sqrt{2}) + 2J_0(2k\delta)^2$$

Note that as  $k$  approaches 0, the exact solution approaches the limit form  $\frac{0}{0}$ . The existence of the sharp discontinuities at very small reduced frequencies in the plot, is due to round off error in evaluating these expression near the limit.

Taking the limit as  $k$  approaching zero yields:

$$\lim_{k \rightarrow 0} a_1 = \frac{1}{20}$$

$$\lim_{k \rightarrow 0} a_2 = \frac{1}{5}$$

which is the 9-point formula for Laplace's equation mentioned above.

For reduced frequencies,  $k > 0$ ,  $a_1$  and  $a_2$  were obtained by Caruthers et. al. [3] using Taylor Series expansion through 8<sup>th</sup> order term (to preserve the 6<sup>th</sup> order of accuracy). The expansion gives:

$$a_1 = \frac{1}{20} + \frac{17}{1000}(k\delta)^2 + \frac{801}{200000}(k\delta)^4 + \frac{76313}{90000000}(k\delta)^6 \\ + \frac{1091144231}{627200000000}(k\delta)^8 + O((k\delta)^{10})$$

$$a_2 = \frac{1}{5} + \frac{29}{500}(k\delta)^2 + \frac{2549}{200000}(k\delta)^4 + \frac{473849}{180000000}(k\delta)^6 \\ + \frac{10086892607}{18816000000000}(k\delta)^8 + O((k\delta)^{10})$$

Comparing this analytical result with the computed values (see table A3.1 and A3.2) shows that the values agree.

### 3.3.1 Figures reference codes

The interpolating functions used in this section are indicated as:

xx- 20pw	20 plane waves (the Standard case)
xx- 20mor5	20 monopoles at radius 5
xx- 20mor10	20 monopoles at radius 10
xx- 20pw20mor5	20 plane waves and 20 monopoles at radius 5
xx- 20pw20mor10	20 plane waves and 20 monopoles at radius 10
xx- infpw	Infinite number of plane waves
xx- fd2nd	The 2 <sup>nd</sup> order FD

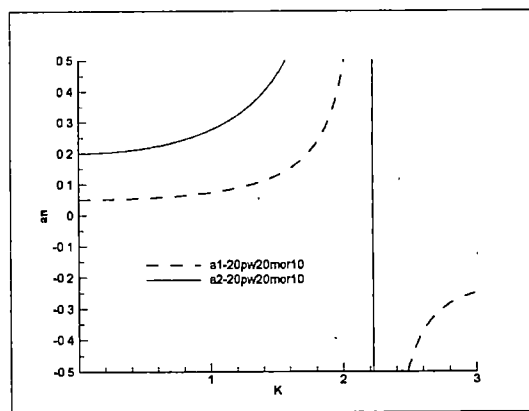
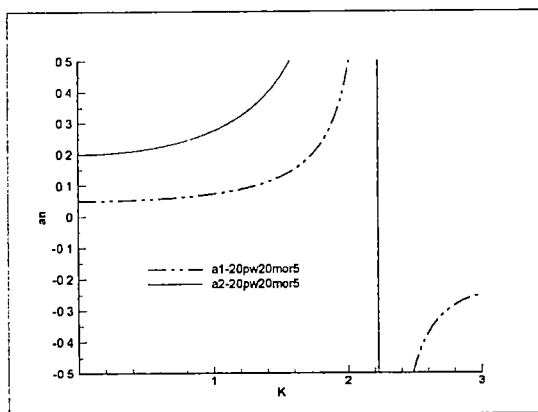
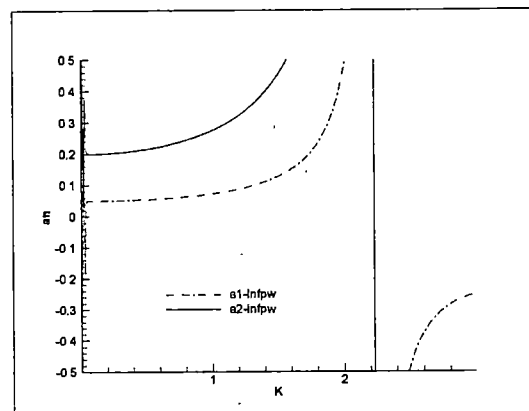
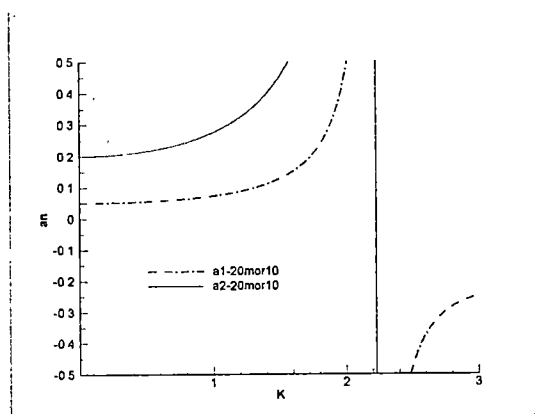
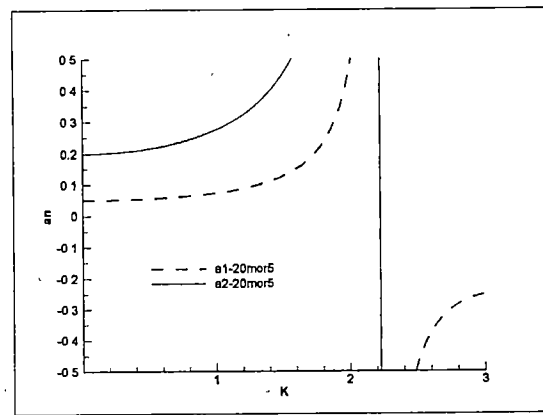
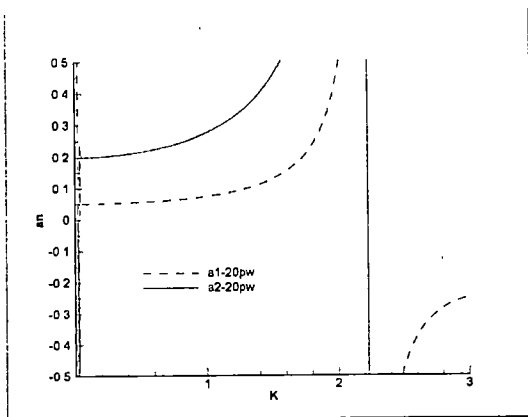


Figure 3.3.1:  $a_n$  vs.  $k$  plot for various functions.

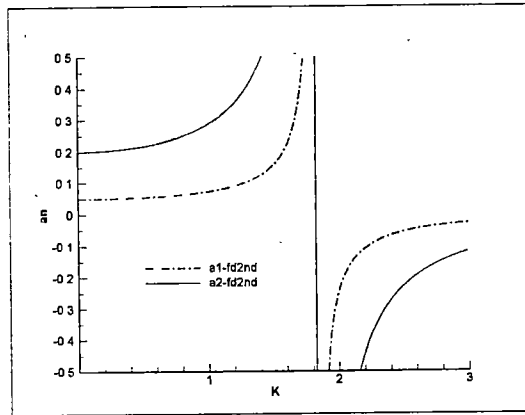


Figure 3.3.1(cont'd):



### 3.4 Evanescent Wave study

This section examines the effect of adding one or more evanescent waves to the interpolating function set. In this case, only the standard case of 20 plane waves is used as the interpolating function set. An evanescent wave is similar to a plane wave along one axis, but decays exponentially along the other. Section 3.2.3 has shown that interpolating evanescent waves at low phase Mach number using the previously used interpolation functions (i.e. with no evanescent wave included in the function) result in less accurate solution (relative to errors in interpolating a plane wave or monopole). It is intended in this section to see if the inclusion of one or more evanescent waves to the interpolation function could reduce the error. Two different combinations of evanescent waves are used for this purpose:

- One evanescent wave of phase Mach number,  $M = 1/2$ .
- Two evanescent waves of phase Mach numbers,  $M_1 = 1/2$  and  $M_2 = 1/3$ .

Figure 3.4.1 shows the average error plots. The error for functions with evanescent waves included is shown to be much poorer than the standard case. As the phase Mach number is increased, the average error reduces towards the one for the standard case. Since evanescent wave tends to become like a plane wave for supersonic speed ( $M \geq 1$ ), this is not a surprise.

Figures 3.4.2 and 3.4.4 show the magnitude errors in interpolating an evanescent wave, at  $M = 0.5$  and  $0.25$  respectively. Interpolating the larger phase Mach number with the evanescent waves seems to improve the error for up to  $4^{\circ}$  of magnitude. This is true when the evanescent wave used in the interpolation function is high in the phase Mach

number ( $M = 1/2$ ). As evanescent waves of smaller phase Mach number is added, the error starts to increase. It is also interesting to note that for larger values of the reduced frequencies, interpolating this large phase Mach number using evanescent waves causes the error to come to a constant value.

However, interpolating the smaller phase Mach number wave with evanescent waves does not seem to improve the error. The error tends to be almost similar to the standard case for most of the  $k$  range.

Both figure 3.4.3 and 3.4.5 show that the slopes of the error are still maintained at 8 thus, maintaining the order of accuracy of 6.

### 3.4.1 Figures reference codes.

There are generally two types of plots in this section, namely average error plot and magnitude error plot. They are indicated as:

er-xxx	Average error in interpolating its function
er2-xxx-xxx	Magnitude error in interpolating a certain oncoming wave function different than the interpolating function.

The interpolating functions are indicated as:

xx-xxx-20pw	20 plane waves (the Standard case)
xx-xxx-20pw1ev	20 plane waves and 1 evanescent wave, $n_x = 2$ ( $M = 0.5$ )
xx-xxx-20pw2ev	21 plane waves and 2 evanescent waves, $n_{x1} = 2$ ( $M = 0.5$ ), $n_{x2} = 3$ ( $M = 1/3$ )

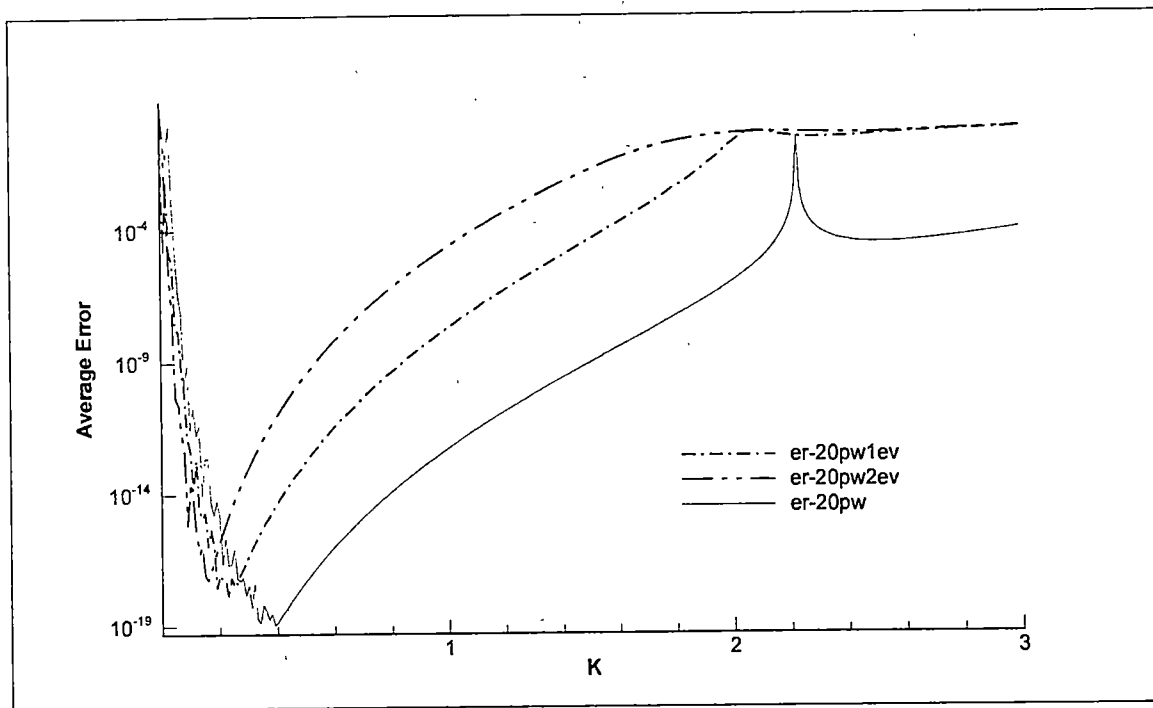


Figure 3.4.1: Average Error vs.  $k$  for various interpolating functions with evanescent wave(s) added.

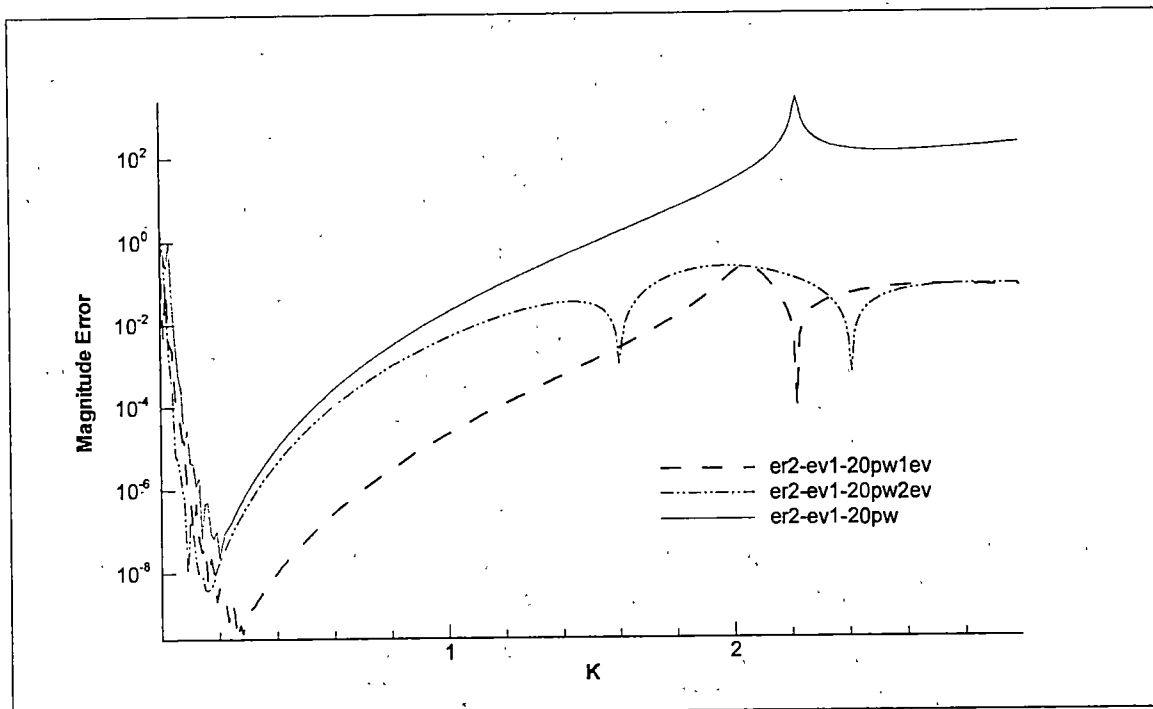


Figure 3.4.2: Magnitude Error vs.  $k$  for various functions with evanescent wave(s) added, in interpolating an evanescent waves at phase Mach number = 0.5 (semi-log plot).

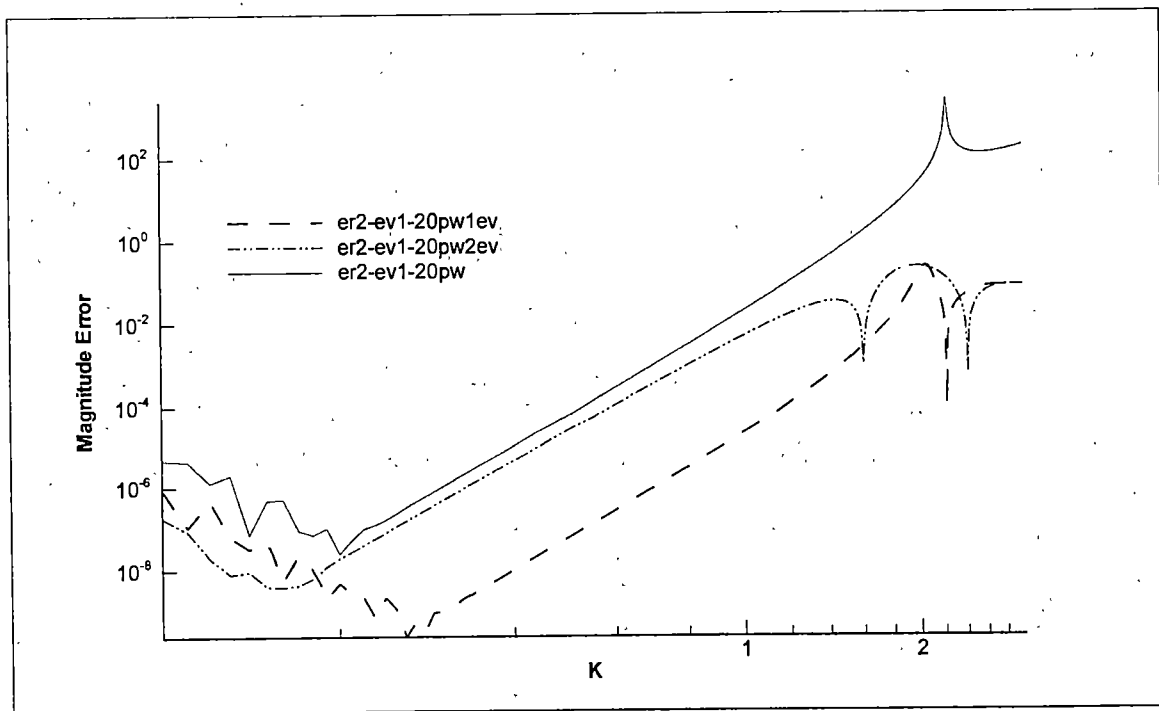


Figure 3.4.3: Magnitude Error vs.  $k$  for various functions with evanescent wave(s) added, in interpolating an evanescent waves at phase Mach number = 0.5 (log-log plot).

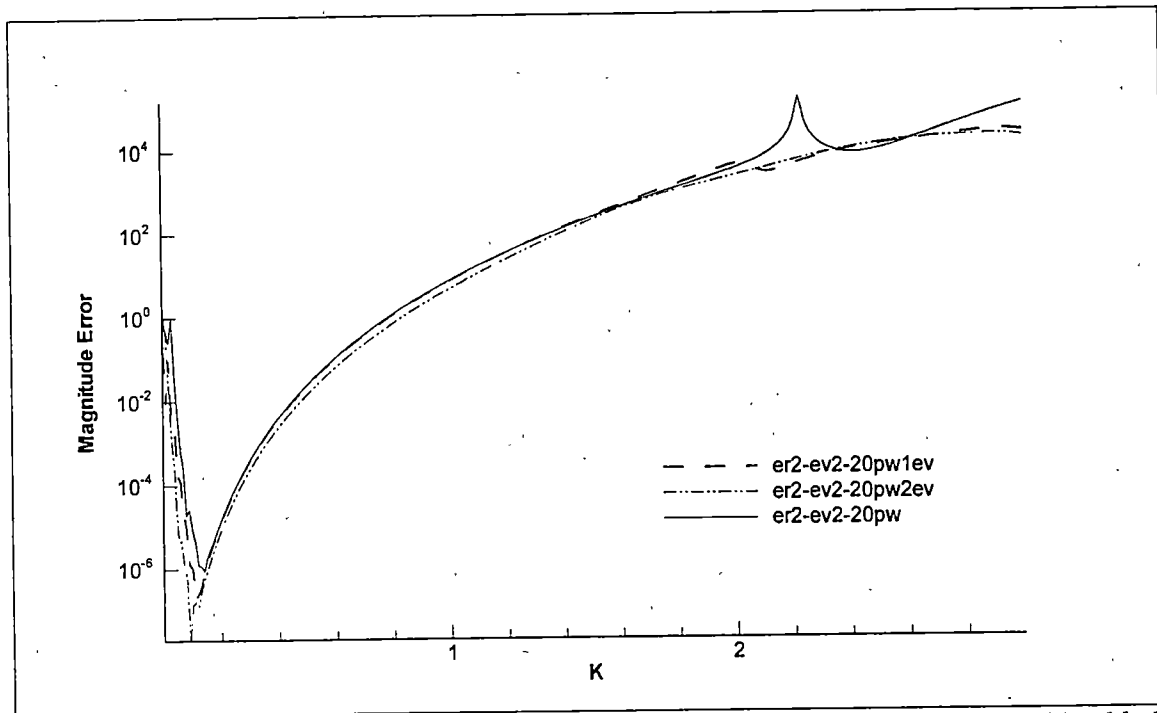


Figure 3.4.4: Magnitude Error vs.  $k$  for various functions with evanescent wave(s) added, in interpolating an evanescent waves at phase Mach number = 0.25 (semi-log plot).

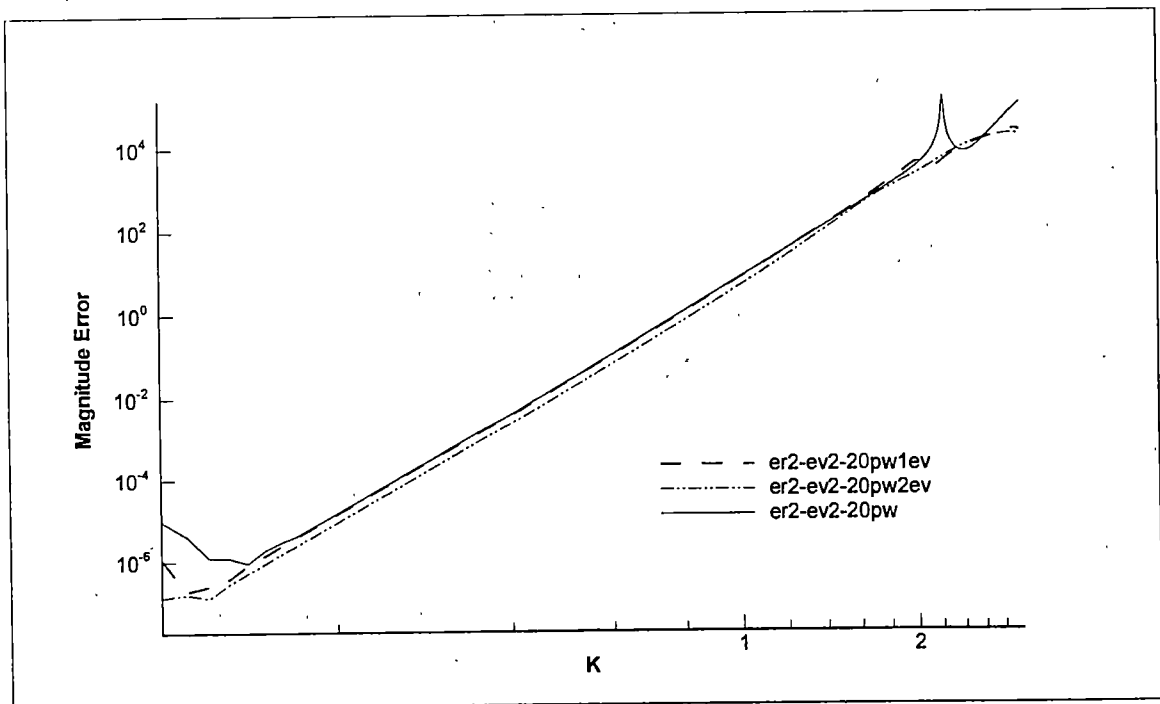


Figure 3.4.5: Magnitude Error vs.  $k$  for various functions with evanescent wave(s) added, in interpolating an evanescent waves at phase Mach number = 0.25 (log-log plot).

### 3.5 Multiple monopole set study

In this section, the effect of having multiple sets of monopoles in the interpolating functions is studied. In the previous sections (sections 3.2.1 – 3.2.4), an addition of a set of monopoles has shown to improve the error of the solutions at very small  $k$  (as compared to merely using the standard, 20 plane waves function). This is particularly apparent in interpolating an evanescent wave in section 3.2.4. This addition also has shown to cause the influence coefficient to converge smoothly as  $k$  approaches zero. Therefore, it is intended in this section to find out if having multiple sets of monopoles in the interpolating function could further improve the solution.

3 different cases are used in this study. This can be described as the following:

1. A function of 2 sets of monopoles; 20 at  $r/\delta = 5$  and 30 at  $r/\delta = 10$ . A total of 50 monopoles are used.
2. A function of 20 plane waves with 2 sets of monopoles; 20 monopoles at  $r/\delta = 5$  and 30 monopoles at  $r/\delta = 10$ . A total of 50 monopoles are used.
3. A function of 20 plane waves with 3 sets of monopoles; 20 at  $r/\delta = 5$ , 30 at  $r/\delta = 10$ , and 40 at  $r/\delta = 20$ . A total of 90 monopoles are used.

The influence coefficient for each case are plotted and compared with the standard case. This is shown in figure 3.5.1. Average errors are compared with the previous cases of single monopole sets, besides the standard case. Similar waves used in section 3.2 are rerun here for finding the magnitude error and again compared with the three functions (standard case and the two single sets of monopoles functions).

Figures 3.5.1 show that the values of the influence coefficients,  $a_1$  and  $a_2$  is again retained. The smoothness of the curves as  $k$  approaching zero, similar to the case of single monopoles sets are also obtained.

The average errors shown in figure 3.5.2 seem to have significant affect from the monopoles set at  $r/\delta = 5$ ; having larger error at small reduced frequencies than the standard case, and smooth curves as the frequency approaches zero. However, the addition (of extra sets of monopoles functions) slightly reduces the error than if only monopoles at  $r/\delta = 5$  are used. The error tends to become smaller as more sets of monopole functions are introduced:

Figures 3.5.3 and 3.5.4 both show the magnitude error in interpolating a plane wave approaching at  $15^\circ$  angle from the right, with semi-log and log-log plot respectively. A very similar result to the previous sections is obtained. The influence of the smaller radius set of monopoles ( $r/\delta = 5$ ) is also apparent at small values of reduced frequencies. The magnitude errors lie between the one obtained for the single monopoles sets of  $r/\delta = 10$  and  $r/\delta = 5$ , i.e. the errors of multiple sets of monopoles are slightly higher than the  $r/\delta = 5$  case, but lower than the case with  $r/\delta = 10$ . Beyond this range, no significant improvement is obtained. The log-log plots also show that the order of accuracy is still retained. Similar conclusions can also be drawn for other plots of magnitude error, shown in figures 3.5.5 – 3.5.12.

In general, there is no significant advantage can be obtained in adding some extra sets of monopoles in the interpolating function. However, by adding more sources to the interpolating function, the amount of computation load is increased. Therefore, it is not worthwhile to have multiple sets of monopoles in the interpolation function.

### 3.4.1 Figures reference codes

There are generally three types of plots in this section, namely influence coefficient, average error and magnitude error plots. They are indicated as:

an-xxx	Influence coefficient for each interpolating function.
er-xxx	Average error in interpolating its function.
er2-xxx-xxx	Magnitude error in interpolating a certain oncoming wave function different than the interpolating function.

The interpolating functions are indicated as:

xx-xxx-20pw	20 plane waves (the Standard case).
xx-xxx-20mor5	20 monopoles at radius 5.
xx-xxx-20mor10	20 monopoles at radius 10.
xx-xxx-mo20r530r10	20 monopoles at radius 5 and 30 monopoles at radius 10.
xx-xxx-20pwmo20r530r10	20 plane waves, 20 monopoles at radius 5 and 30 monopoles at radius 10.
xx-xxx-20pwmo20r530r1040r20	20 plane waves, 20 monopoles at radius 5, 30 monopoles at radius 10 and 40 monopoles at radius 20.



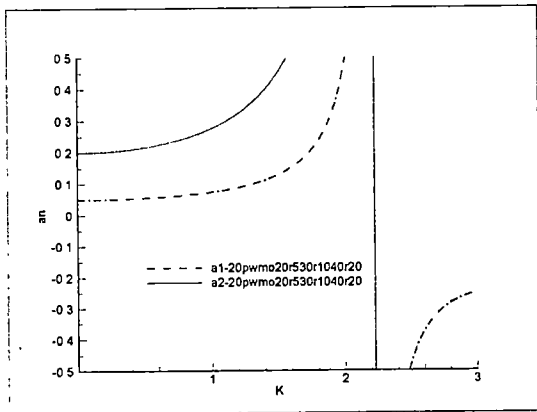
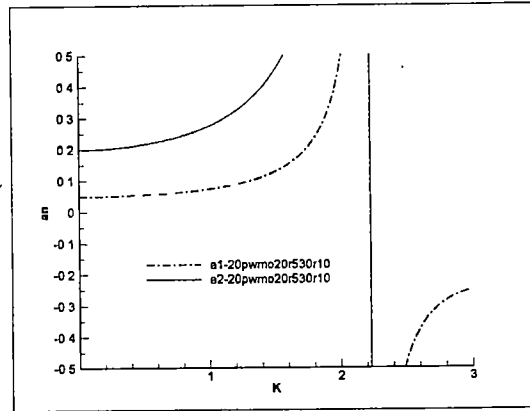
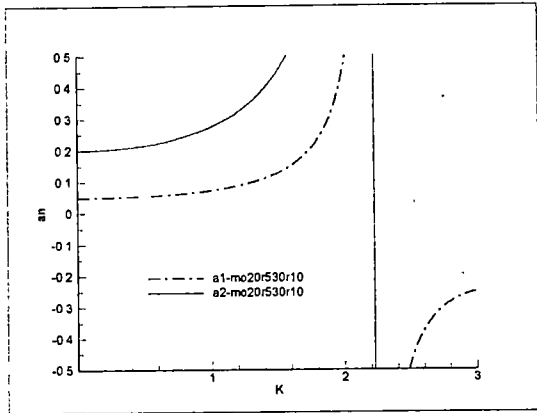


Figure 3.5.1:  $a_n$  vs.  $k$  plot for functions with additional set(s) of monopoles.

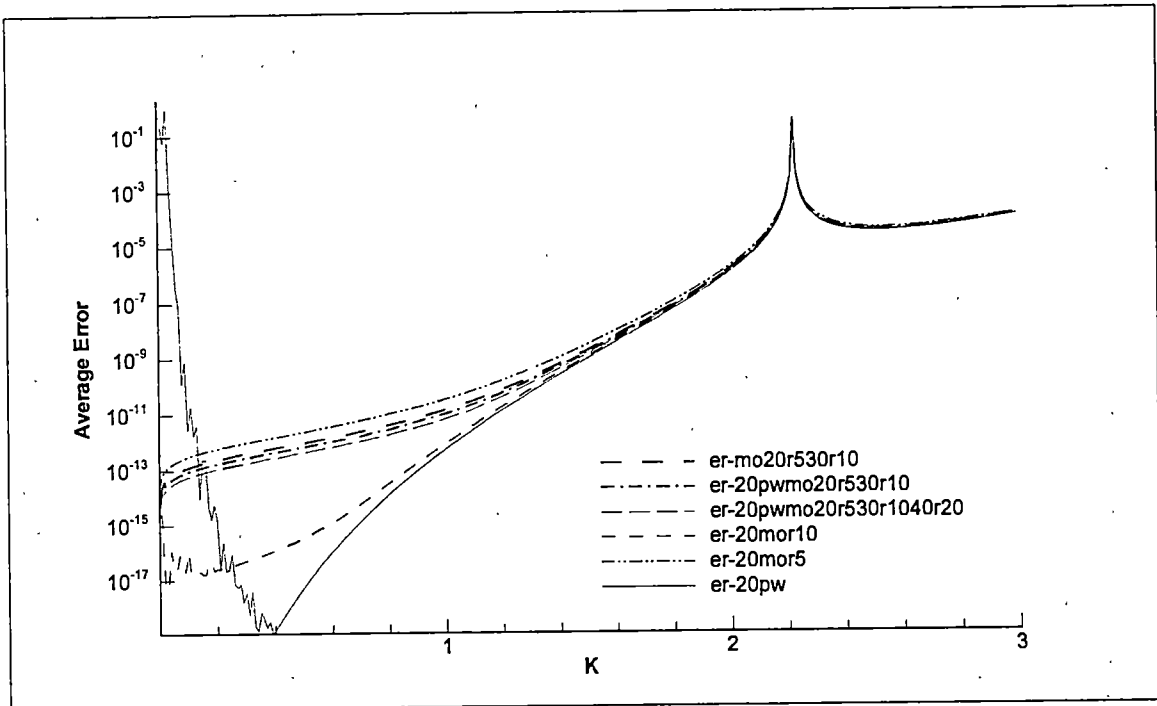


Figure 3.5.2: Average Error vs.  $k$  for functions with additional set(s) of monopoles.

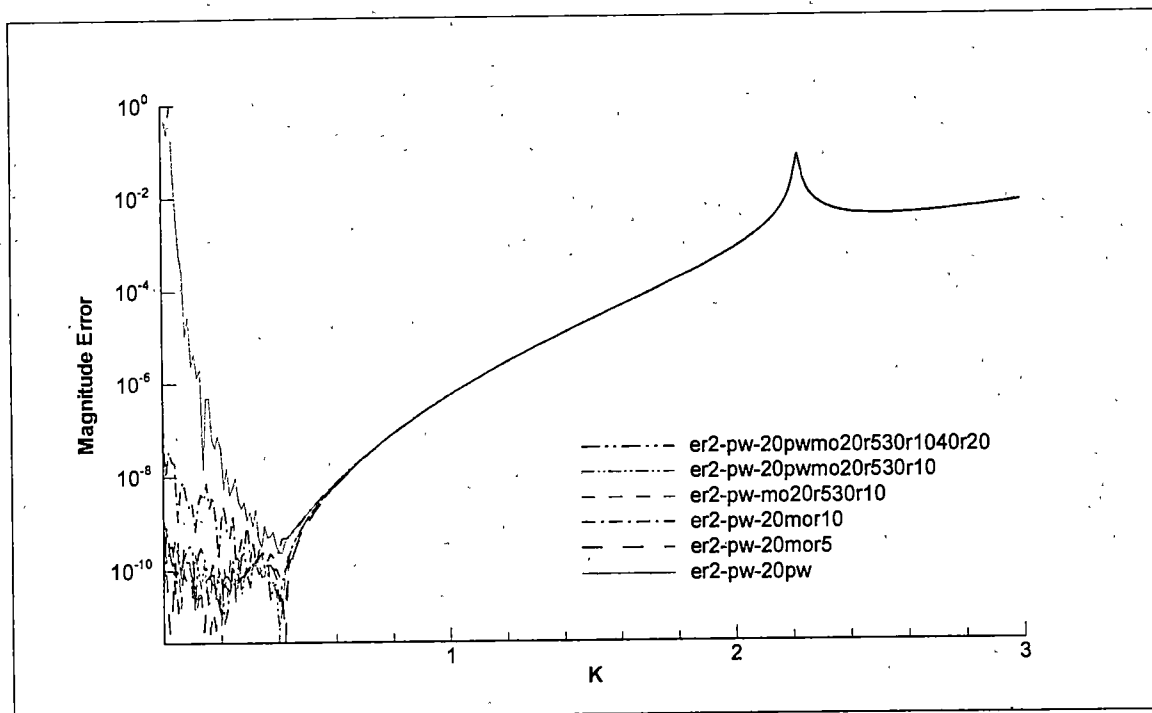


Figure 3.5.3: Magnitude Error vs.  $k$  for functions with additional set(s) of monopoles, in interpolating a plane wave approaching at  $15^\circ$  angle from the right (semi-log plot).

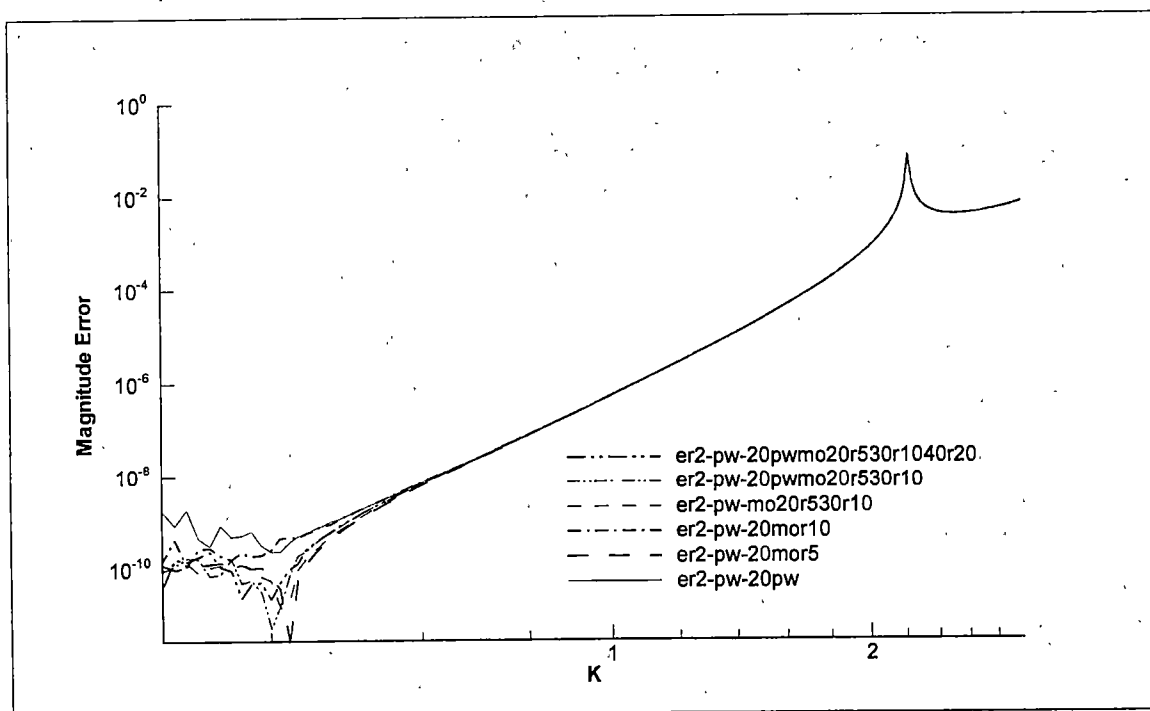


Figure 3.5.4: Magnitude Error vs.  $k$  for functions with additional set(s) of monopoles, in interpolating a plane wave approaching at  $15^\circ$  angle from the right (log-log plot).

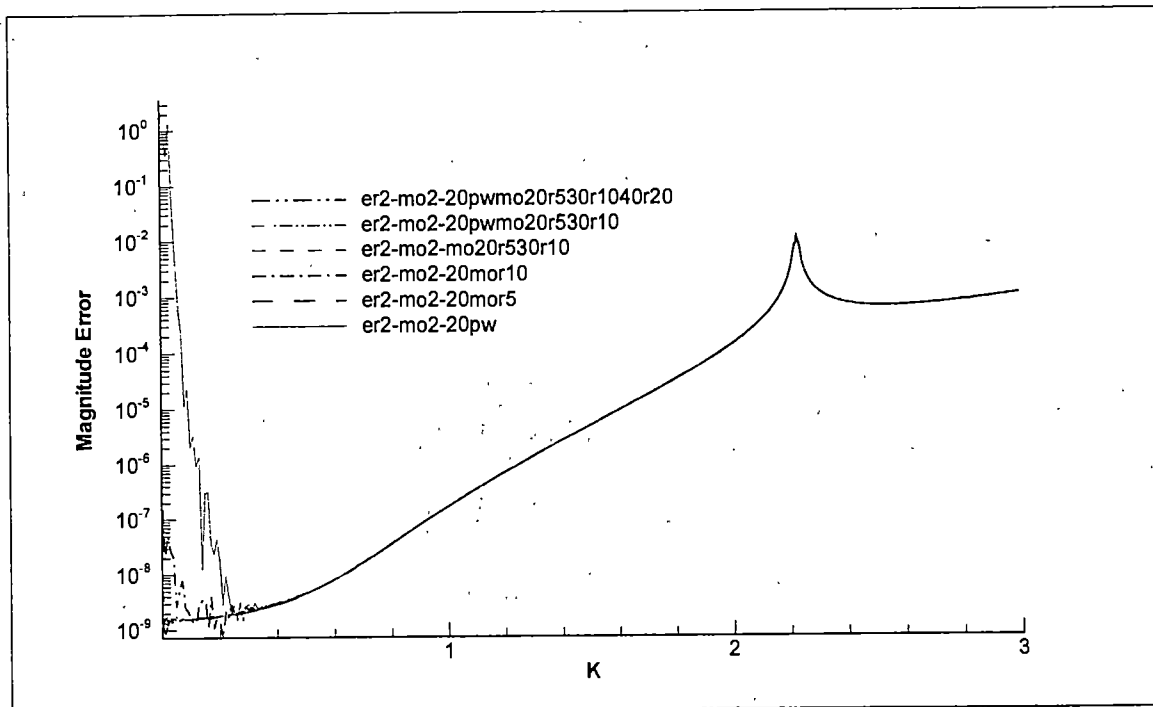


Figure 3.5.5: Magnitude Error vs.  $k$  for functions with additional set(s) of monopoles, in interpolating a monopole at radius  $R/\delta=10$ , at  $15^\circ$  angle from the right (semi-log plot).

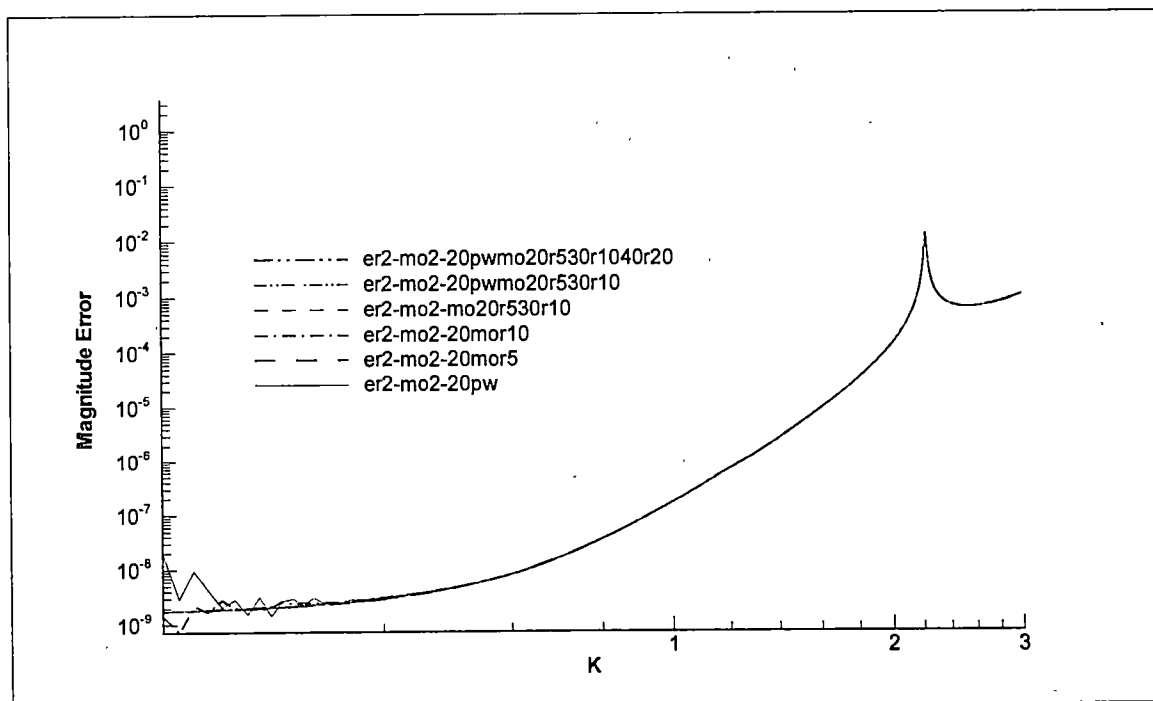


Figure 3.5.6: Magnitude Error vs.  $k$  for functions with additional set(s) of monopoles, in interpolating a monopole at radius  $R/\delta=10$ , at  $15^\circ$  angle from the right (log-log plot).

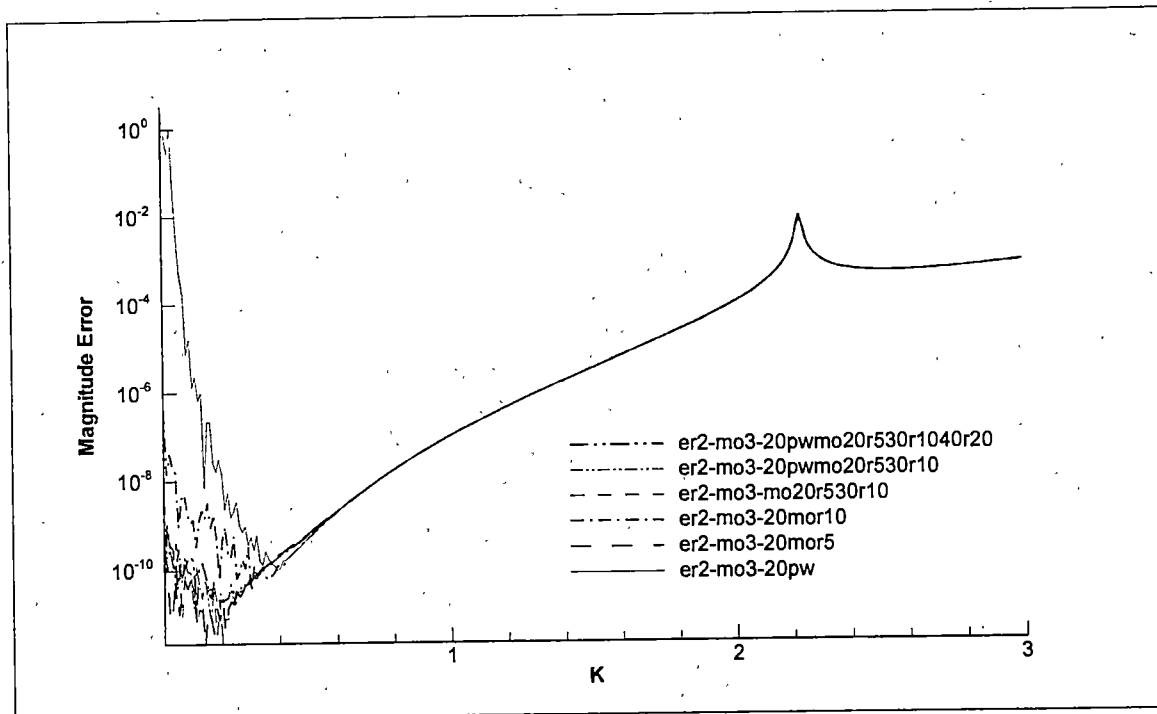


Figure 3.5.7: Magnitude Error vs.  $k$  for functions with additional set(s) of monopoles, in interpolating a monopole at radius  $R/\delta=20$ , at  $15^\circ$  angle from the right (semi-log plot)

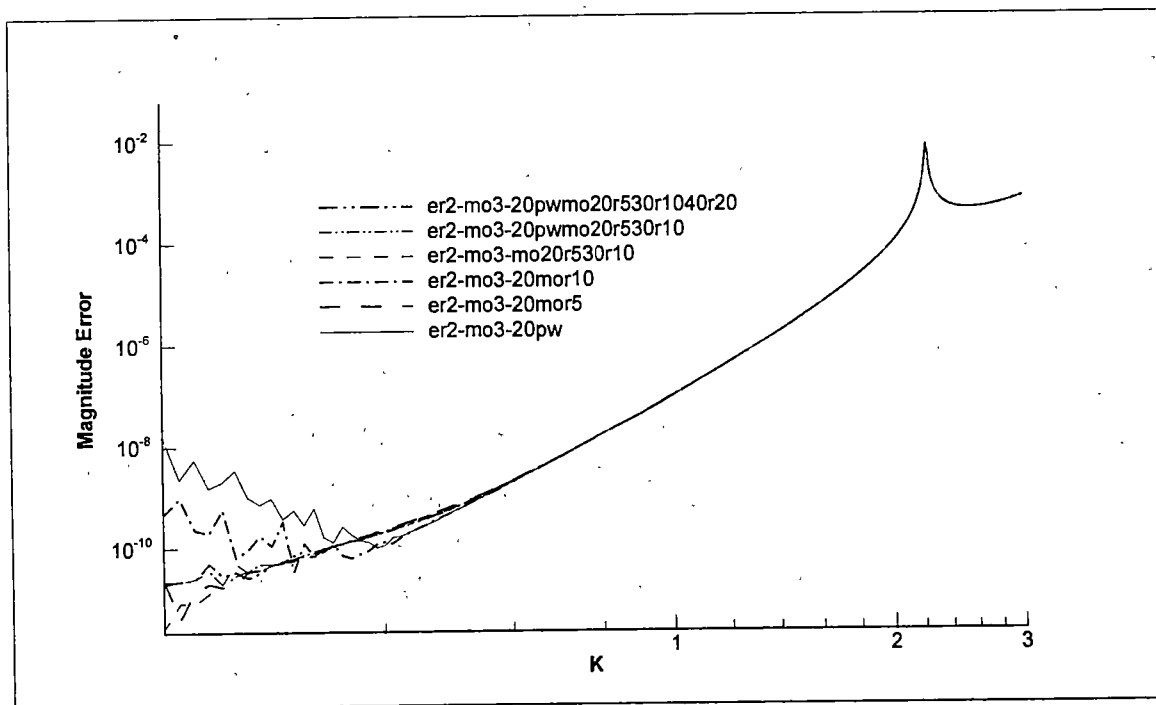


Figure 3.5.8: Magnitude Error vs.  $k$  for functions with additional set(s) of monopoles, in interpolating a monopole at radius  $R/\delta=20$ , at  $15^\circ$  angle from the right (log-log plot).

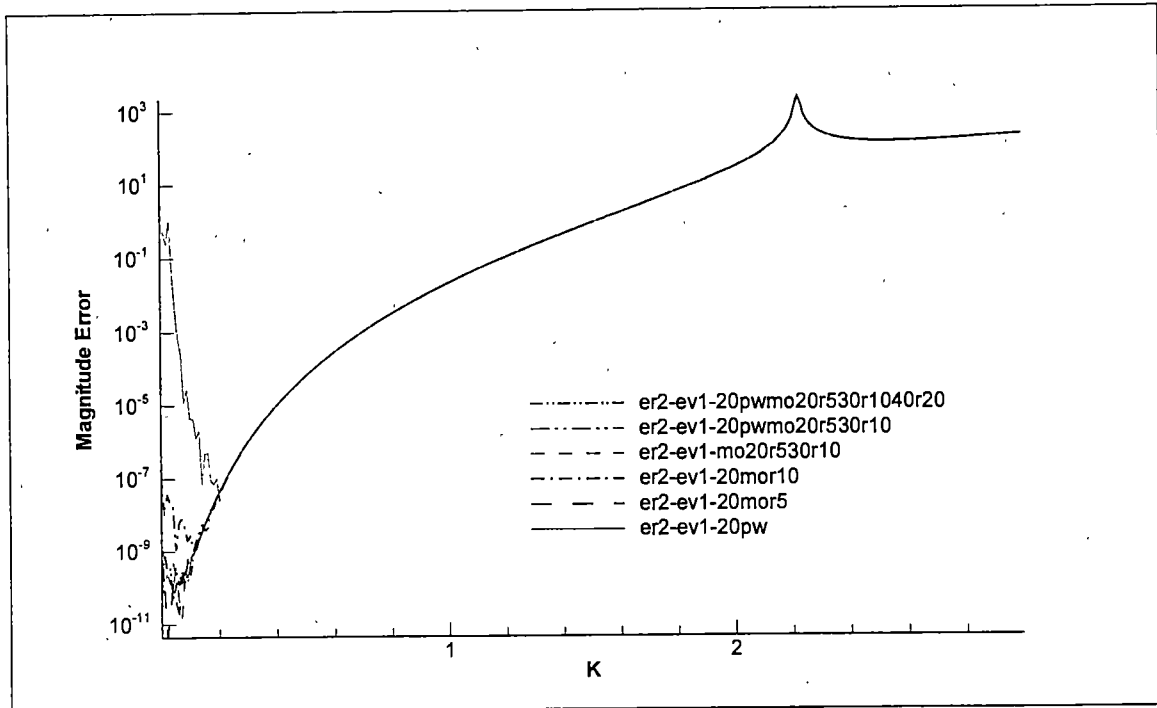


Figure 3.5.9: Magnitude Error vs.  $k$  for functions with additional set(s) of monopoles, in interpolating an evanescent waves at phase Mach number = 0.5 (semi-log plot).

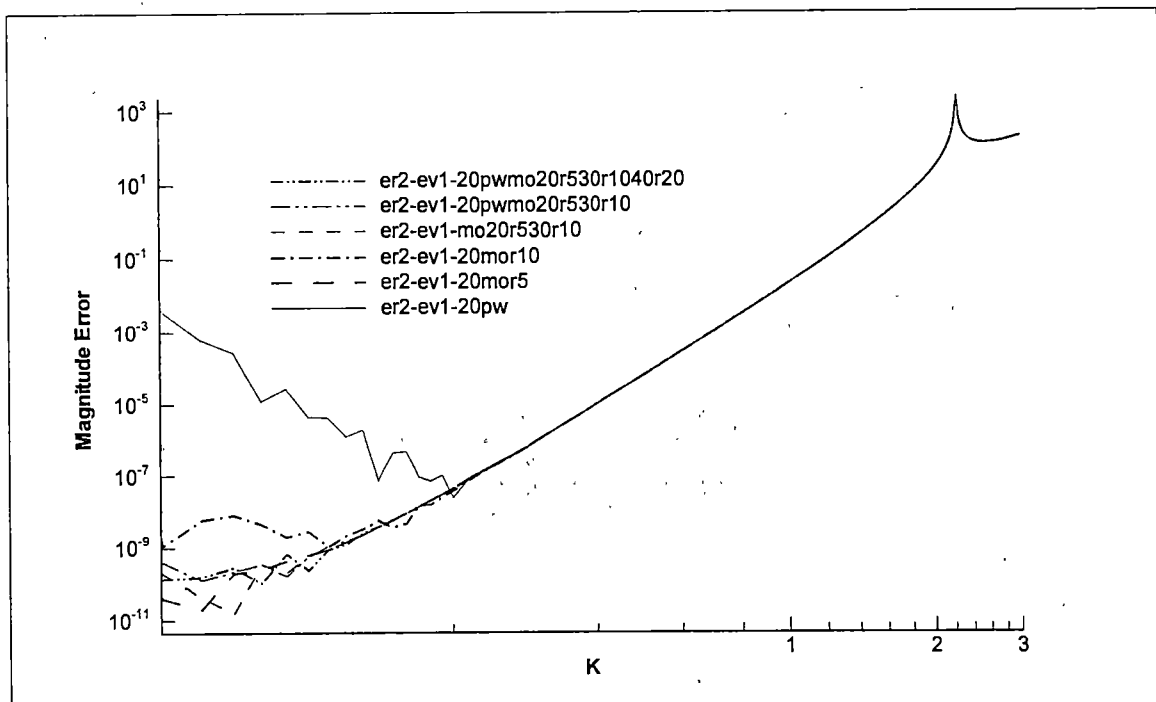


Figure 3.5.10: Magnitude Error vs.  $k$  for functions with additional set(s) of monopoles, in interpolating an evanescent waves at phase Mach number = 0.5 (log-log plot).

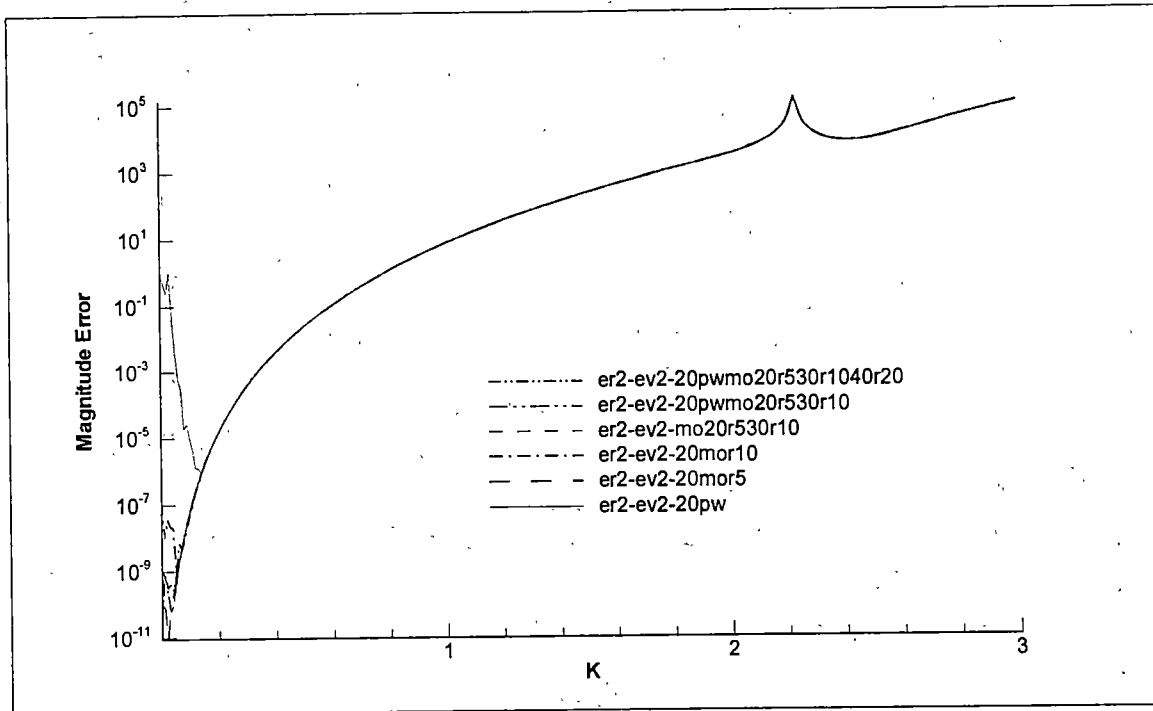


Figure 3.5.11: Magnitude Error vs.  $k$  for functions with additional set(s) of monopoles, in interpolating an evanescent waves at phase Mach number = 0.25 (semi-log plot).

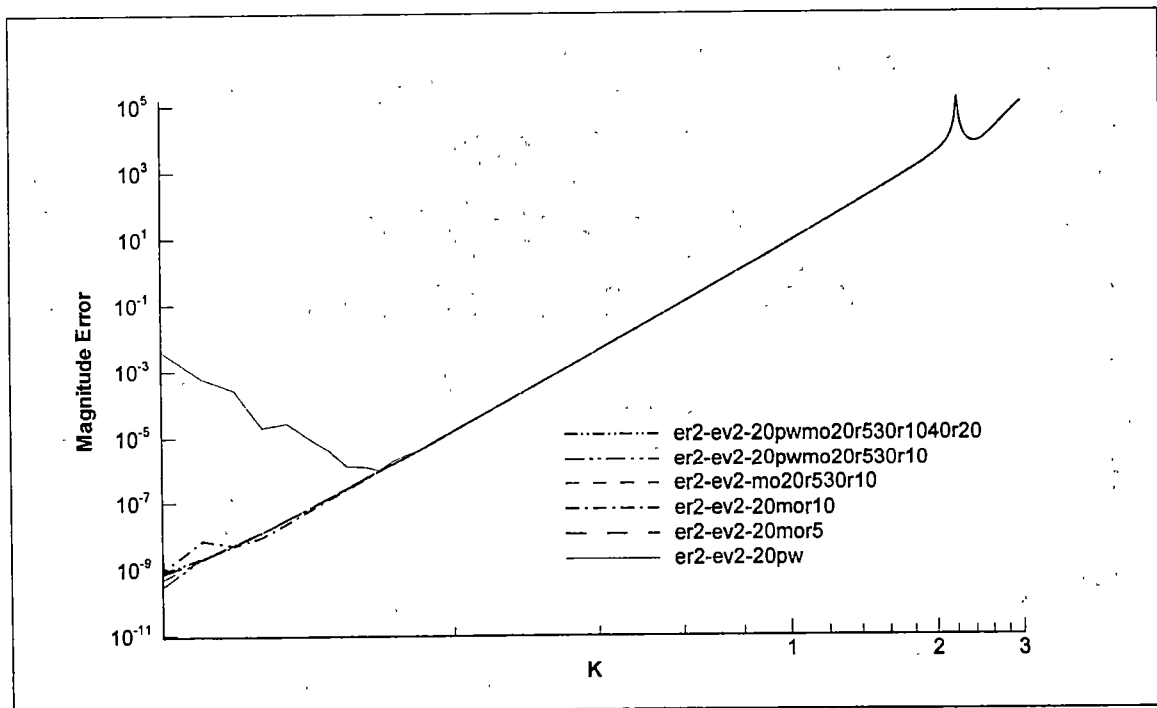


Figure 3.5.12: Magnitude Error vs.  $k$  for functions with additional set(s) of monopoles, in interpolating an evanescent waves at phase Mach number = 0.25 (log-log plot).

### 3.6 Irregular stencil grid study

In this section, the effect of different stencil configurations on the accuracy is studied. In constructing a grid for discretizing any given domain, there are generally 2 options to consider. One is to simply embed the geometry of interest within a regular rectangular grid arrangement. The other option is to use a so-called body fitted grid, where the regular grid points fall along the physical boundaries of the domain. This usually results in some nonuniformity of the grid such as skewed and variation in spacing [8].

As noted in the previous section, one of the advantages of having a uniform grid is that identical stencil is used throughout the domain. Therefore, only one discretization is sufficient for all grid points, which reduces the computation time. By having irregular grid points (therefore irregular stencil configuration), the discretization must be repeated for each of the points.

Two different types of skew grids are used in this study. Both grids are skewed at  $45^\circ$  angle. In determining the stencil node location, two different conditions are used. In the first grid type (figure 3.6.1a), named case 1, the height of the stencil is maintained as  $2\delta$ . This is similar to stretching the grid in y direction while sliding the upper nodes to the right to make a  $45^\circ$  angle from the base. The second type, case 2 (figure 3.6.1b) is configured by retaining the ratio of the stencil to  $\delta$ . This is similar to sliding the upper nodes to the right without stretching.

In both cases, three different stencil node distance are obtained (as compared to two in the regular squared stencil grid), labeled as  $a_1, a_2, a_3$  and  $a'_1, a'_2, a'_3$  in the figures,



respectively. Hence, the 8 component influence coefficient,  $a$ 's is expected to consist of components with three different values. This is shown in figures 3.6.2 and 3.6.3. The first case (figure 3.6.2) has two identical nodes  $a_1$  values, two having  $a_2$  values, while the other four nodes have the same value,  $a_3$ . A slightly different order is obtained in the second case due to its configuration. Both  $a'_1$  and  $a'_3$  share two nodes and  $a'_2$  values are shared by four other nodes. This is consistent with figure 3.6.1.

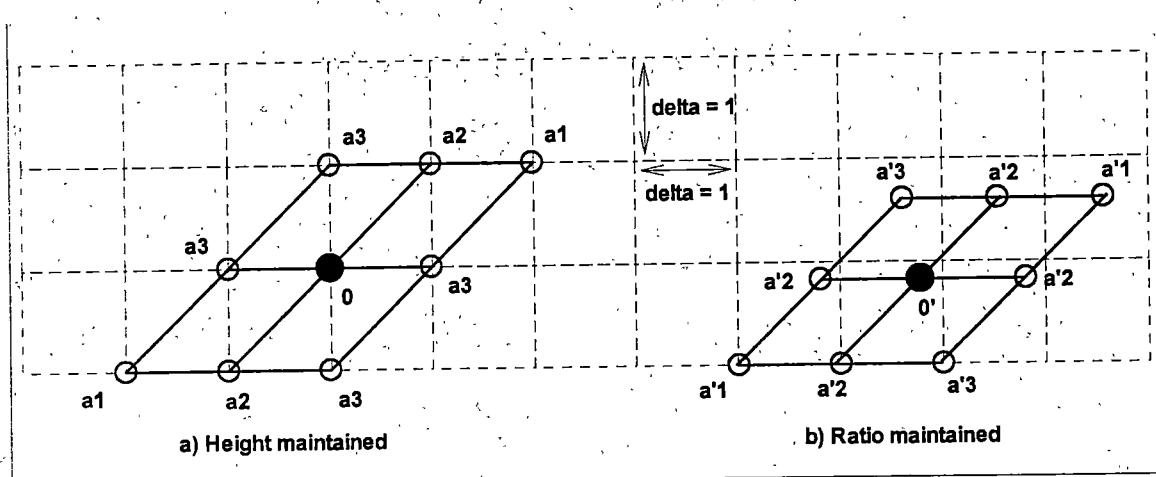


Figure 3.6.1: 45° skewed stencil grid configuration.

Average errors for both cases are shown in figure 3.6.4 and 3.6.5 respectively. In general, both cases are shown to have more erroneous solutions than the standard case with regular square stencil. Larger error of up to 10 orders of magnitude is noticed in case 1 as compared to the standard case. Case 2 produces lesser error but still significantly larger than the standard case. The characteristics of both plane waves and monopoles interpolation functions, which occur in the regular square stencil, are also retained in the skewed stencils.

Similar tests of interpolating different sources of sound are repeated here. Figures 3.6.6 and 3.6.7 show the magnitude errors in interpolating a plane wave approaching at

15° angle for case 1 and case 2 respectively. Similar result is observed where the errors on both cases appear to be more than the standard case and case 1 produces more error than case 2. The log-log plots for each case, in figure 3.6.8 and 3.6.9 shown the slope to be lower than the standard regular stencil case. Computing the slopes give the order of accuracy for case 1 and case 2 as 2 and 4 respectively. Hence, having irregular grid points would sacrifice the order of accuracy of the solution in Green's Function Discretization.

The rest of the tests also show similar trends. These are shown in the rest of the figures.

### 3.6.1 Figures reference codes

There are generally three types of plots in this section, namely influence coefficient, average error and magnitude error plots. They are indicated as:

an-xxx	Influence coefficient for each interpolating function.
er-xxx	Average error in interpolating its function.
er2-xxx-xxx	Magnitude error in interpolating a certain oncoming wave function different than the interpolating function.

The interpolating functions are indicated as:

xx-xxx-20pw	20 plane waves (the Standard case).
xx-xxx-g220pw	20 plane waves with skew grid of case 1.
xx-xxx-g220mor5	20 monopoles at radius 5 with skew grid of case 1.
xx-xxx-g220pw20mor5	20 plane waves and 20 monopoles at radius 5 with skew grid of case 1.

xx-xxx-g320pw

20 plane waves with skew grid of case 2.

xx-xxx-g320mor5

20 monopoles at radius 5 with skew grid of case 2.

xx-xxx-g320pw20mor5

20 plane waves and 20 monopoles at radius 5 with skew grid of case 2.

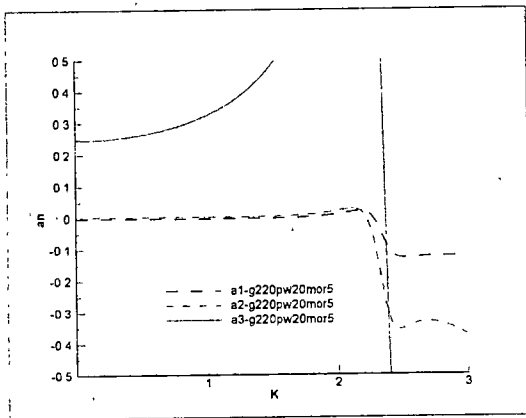
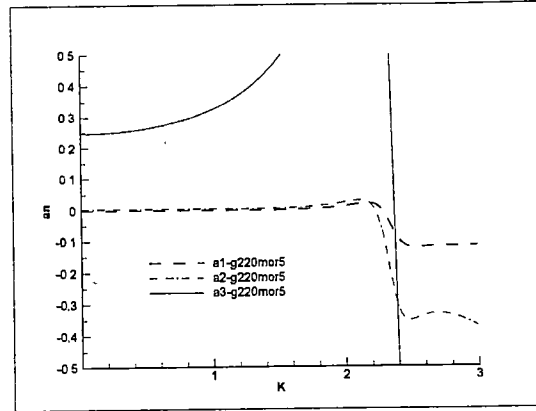
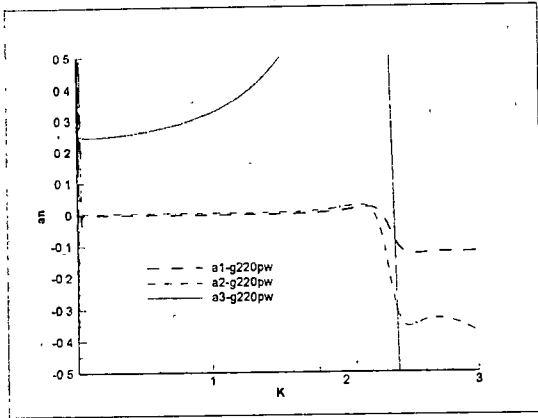


Figure 3.6.2:  $a_n$  vs.  $k$  plots for functions with skewed stencil grid of case 1.

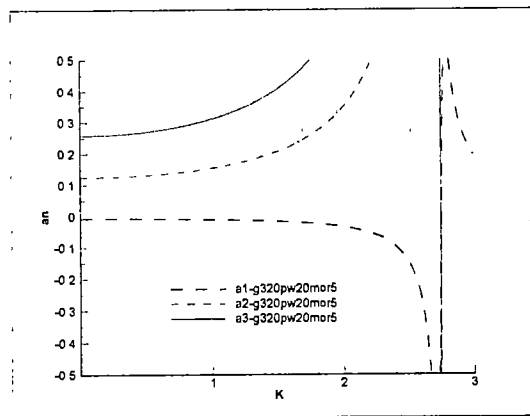
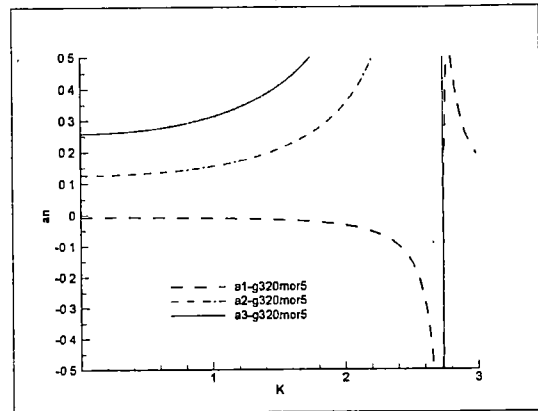
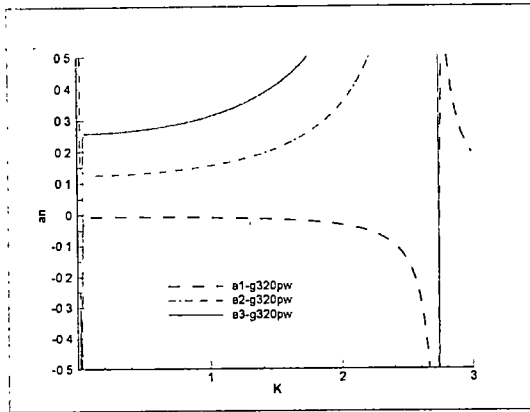


Figure 3.6.3:  $a_n$  vs.  $k$  plots for functions with skewed stencil grid of case 2.

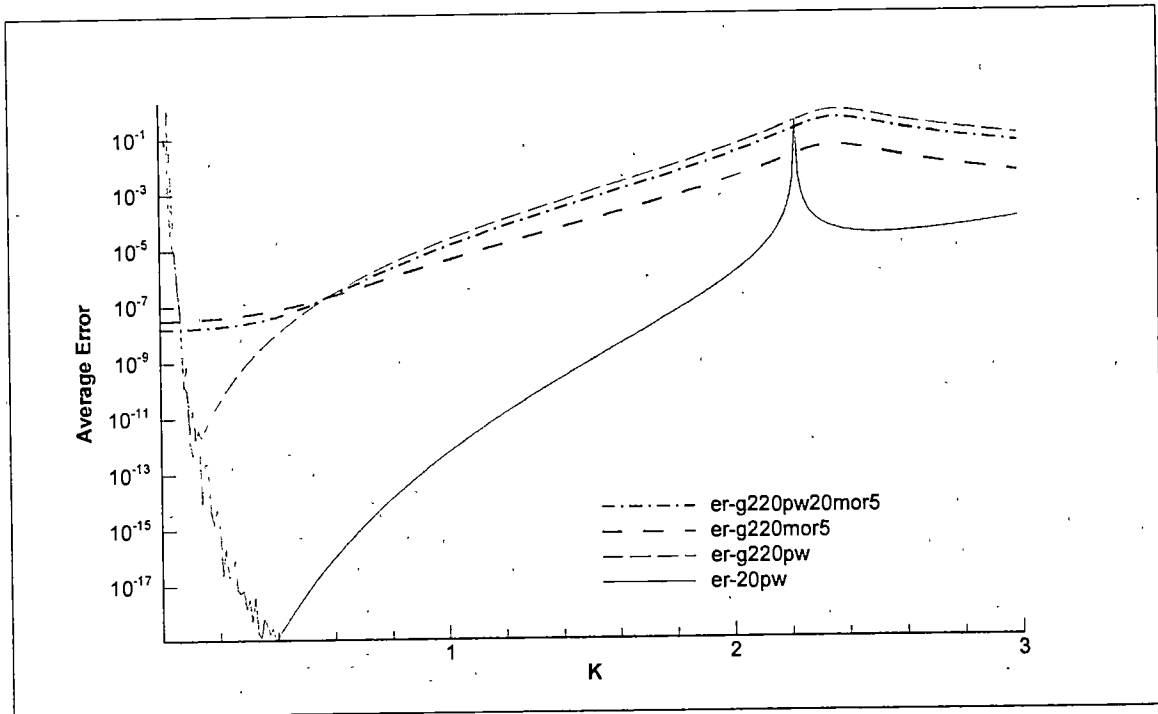


Figure 3.6.4: Average Error vs.  $k$  for functions with skewed stencil grid of case 1.

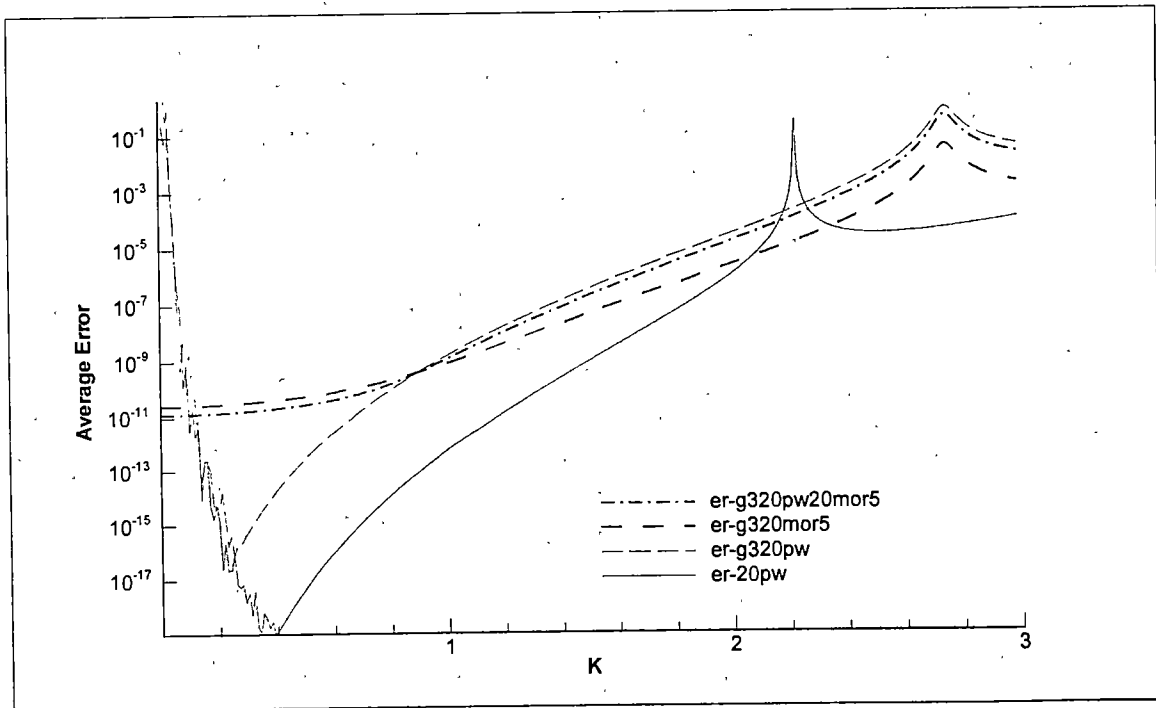


Figure 3.6.5: Average Error vs.  $k$  for functions with skewed stencil grid of case 2.

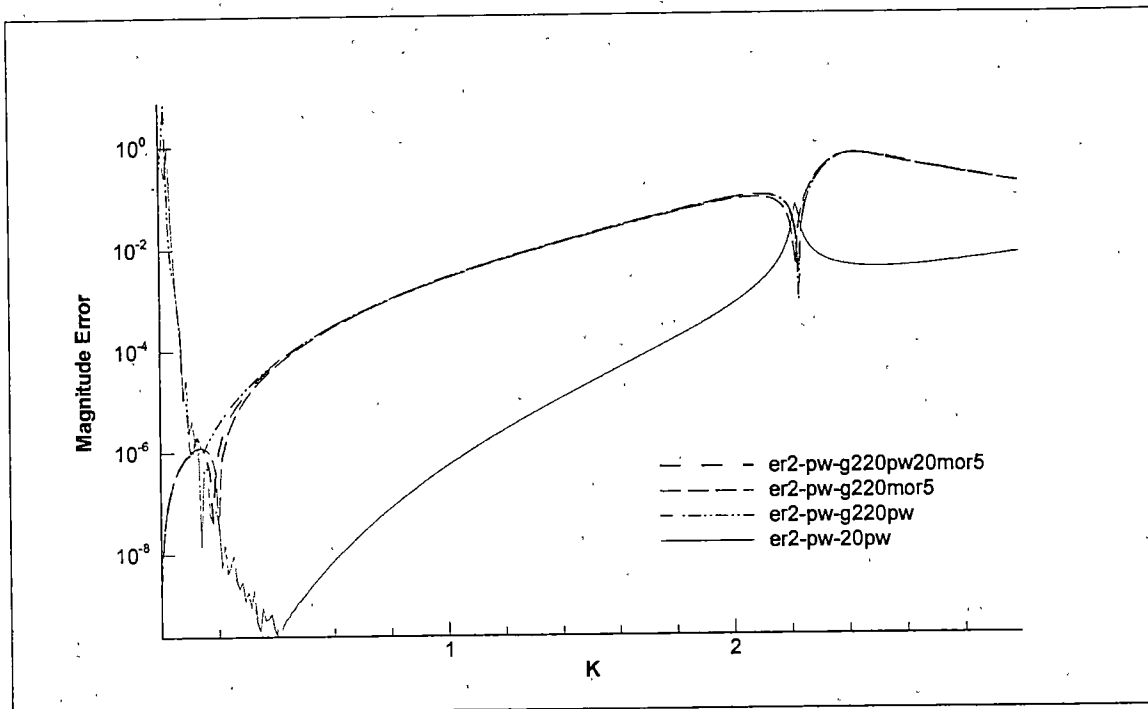


Figure 3.6.6: Magnitude Error vs.  $k$  for functions with skewed stencil grid of case 1, in interpolating a plane wave approaching at  $15^\circ$  angle from the right (semi-log plot).

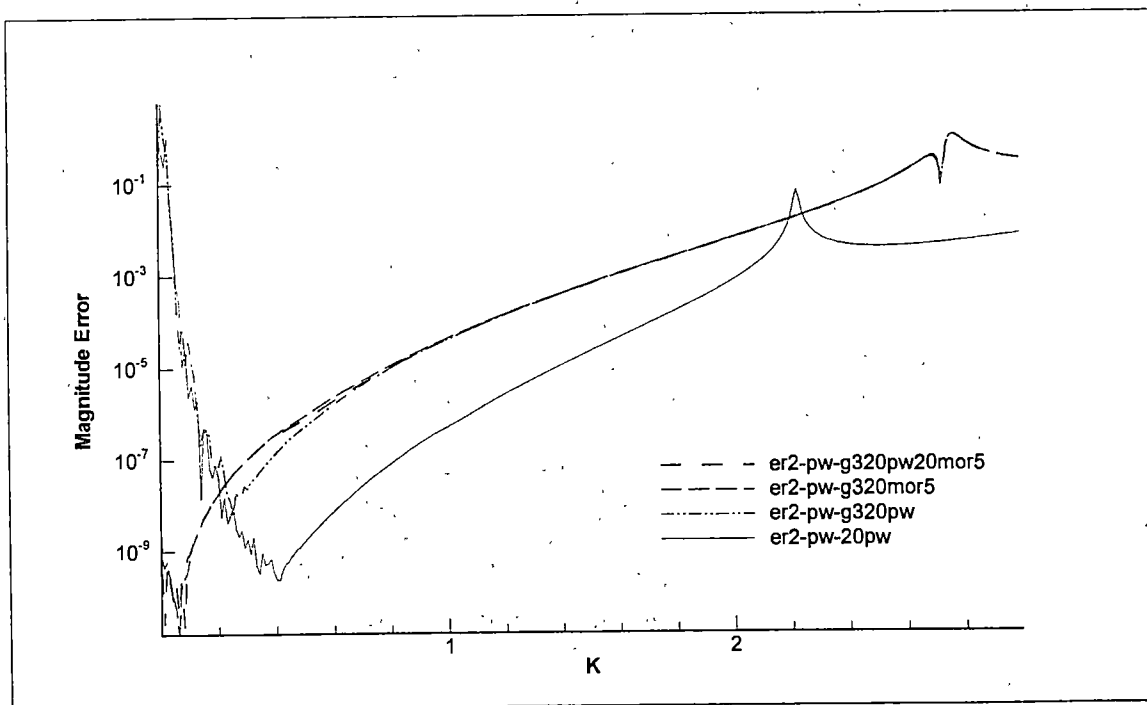


Figure 3.6.7: Magnitude Error vs.  $k$  for functions with skewed stencil grid of case 2, in interpolating a plane wave approaching at  $15^\circ$  angle from the right (semi-log plot).

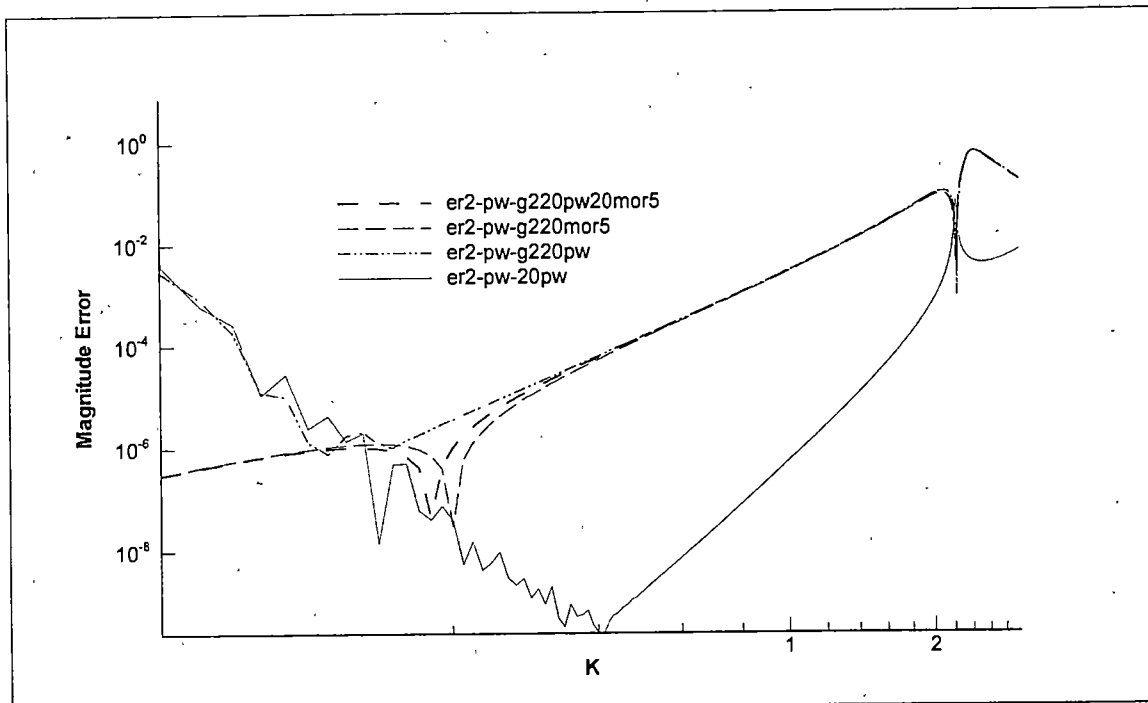


Figure 3.6.8: Magnitude Error vs.  $k$  for functions with skewed stencil grid of case 1, in interpolating a plane wave approaching at  $15^\circ$  angle from the right (log-log plot).

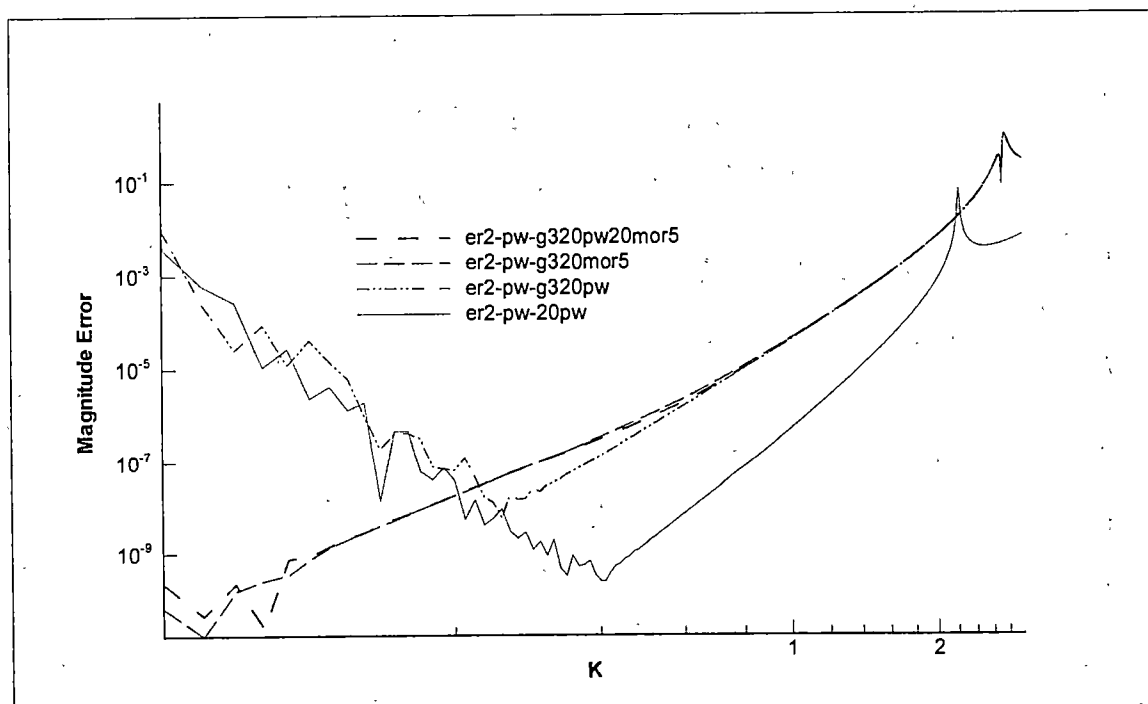


Figure 3.6.9: Magnitude Error vs.  $k$  for functions with skewed stencil grid of case 2, in interpolating a plane wave approaching at  $15^\circ$  angle from the right (log-log plot).



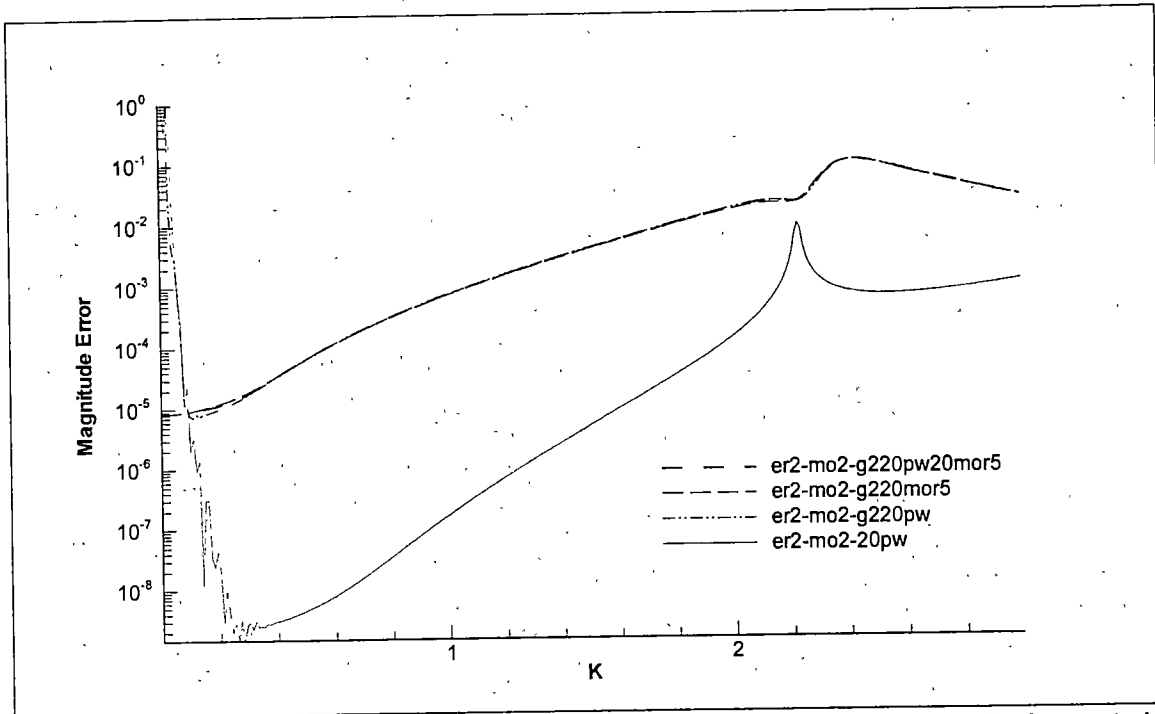


Figure 3.6.10: Magnitude Error vs.  $k$  for functions with skewed stencil grid of case 1, in interpolating a monopole at radius  $R/\delta = 10$ , at  $15^\circ$  angle from the right (semi-log plot).

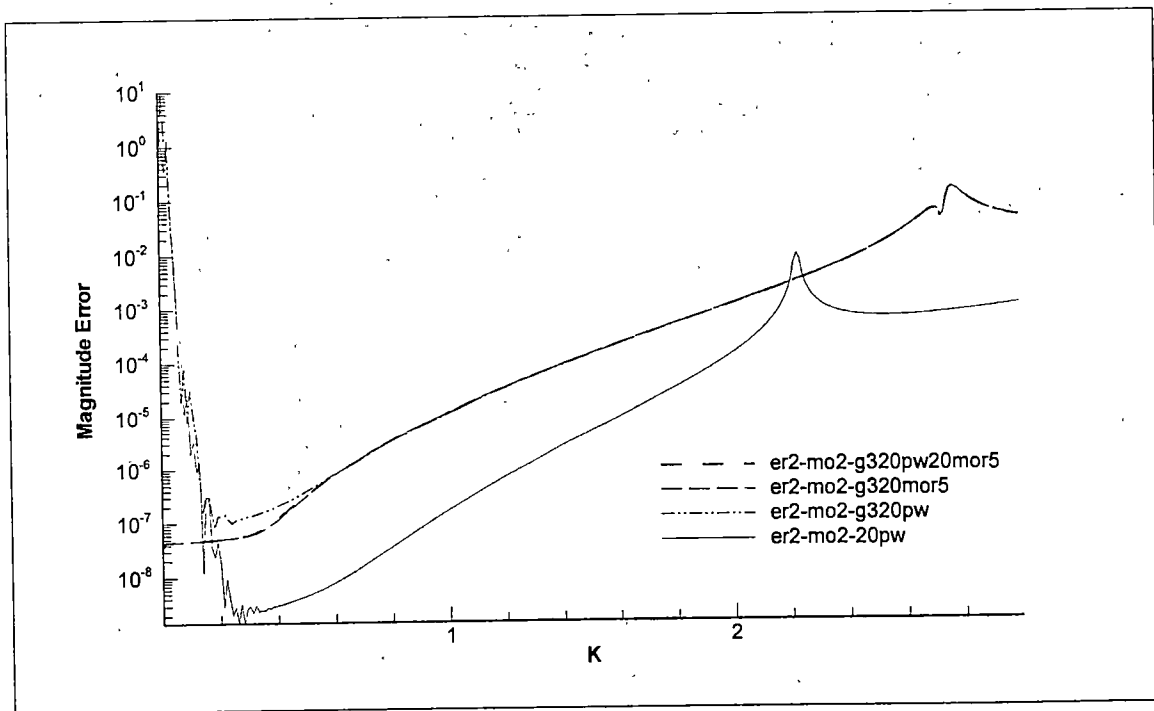


Figure 3.6.11: Magnitude Error vs.  $k$  for functions with skewed stencil grid of case 2, in interpolating a monopole at radius  $R/\delta = 10$ , at  $15^\circ$  angle from the right (semi-log plot).

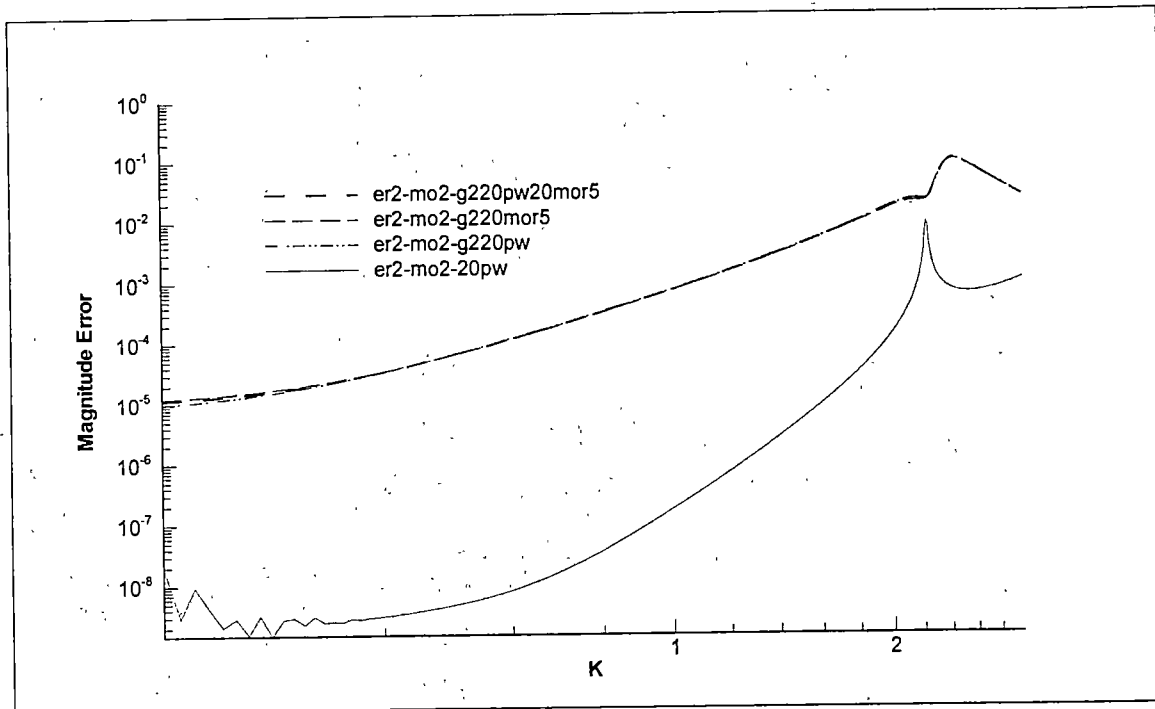


Figure 3.6.12: Magnitude Error vs.  $k$  for functions with skewed stencil grid of case 1, in interpolating a monopole at radius  $R/\delta = 10$ , at  $15^\circ$  angle from the right (log-log plot).

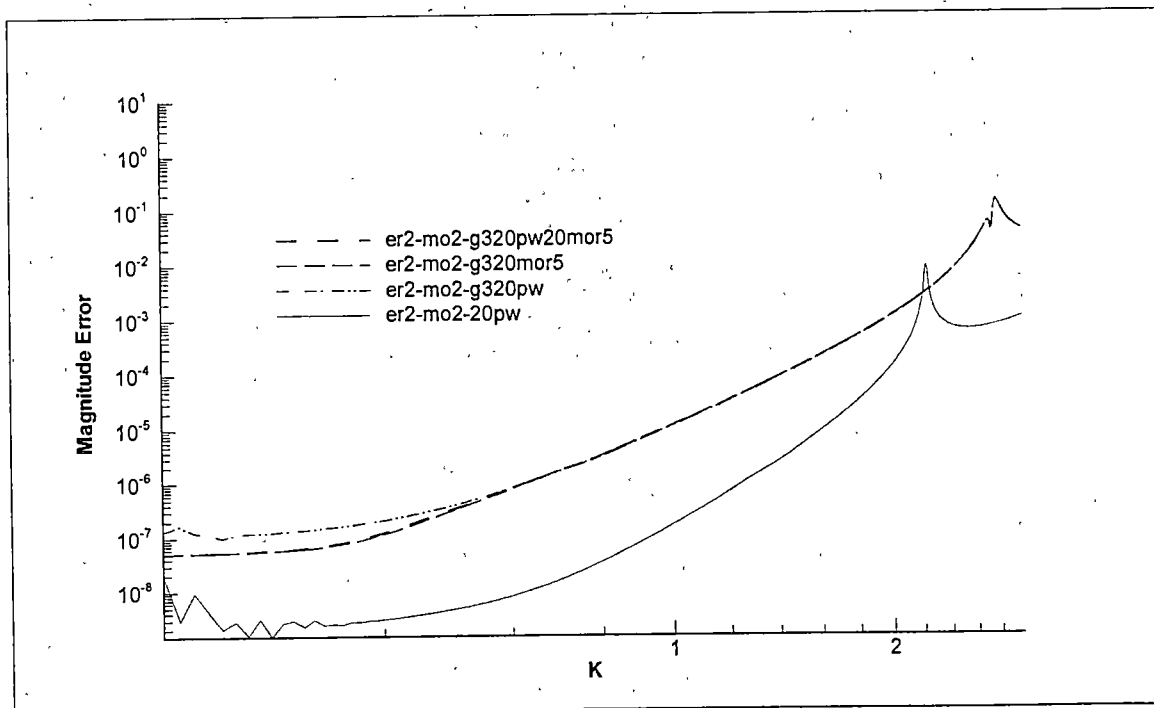


Figure 3.6.13: Magnitude Error vs.  $k$  for functions with skewed stencil grid of case 2, in interpolating a monopole at radius  $R/\delta = 10$ , at  $15^\circ$  angle from the right (log-log plot).

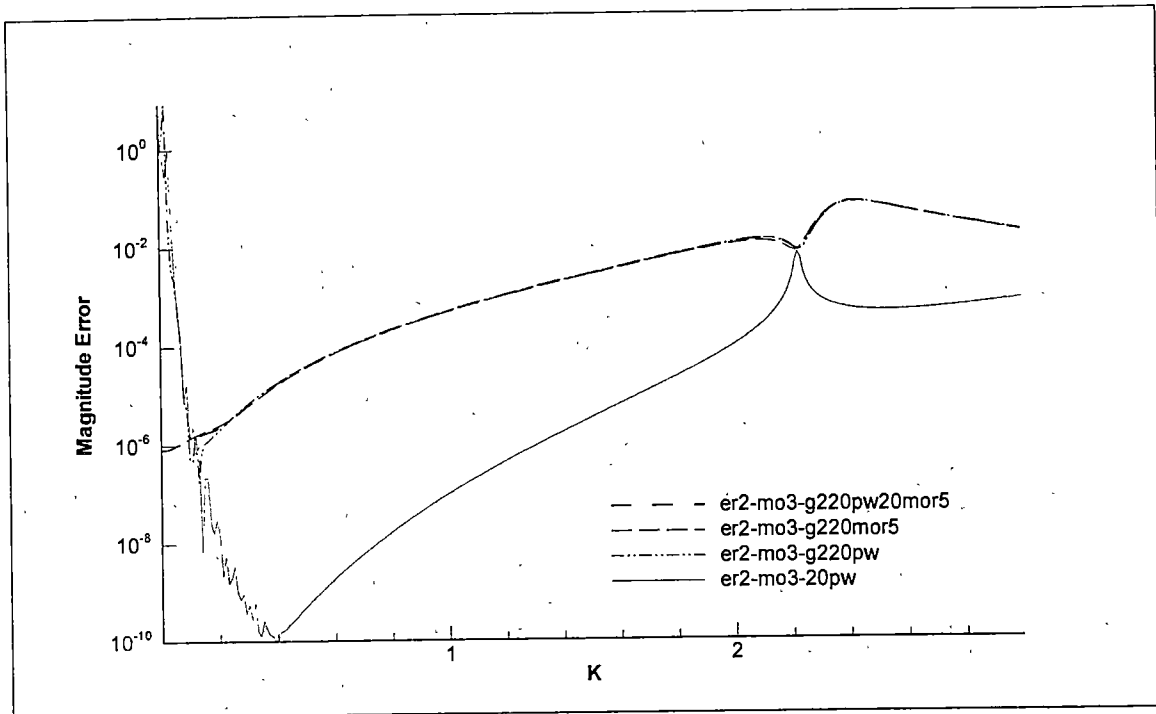


Figure 3.6.14: Magnitude Error vs.  $k$  for functions with skewed stencil grid of case 1, in interpolating a monopole at radius  $R/\delta=20$ , at  $15^\circ$  angle from the right (semi-log plot).

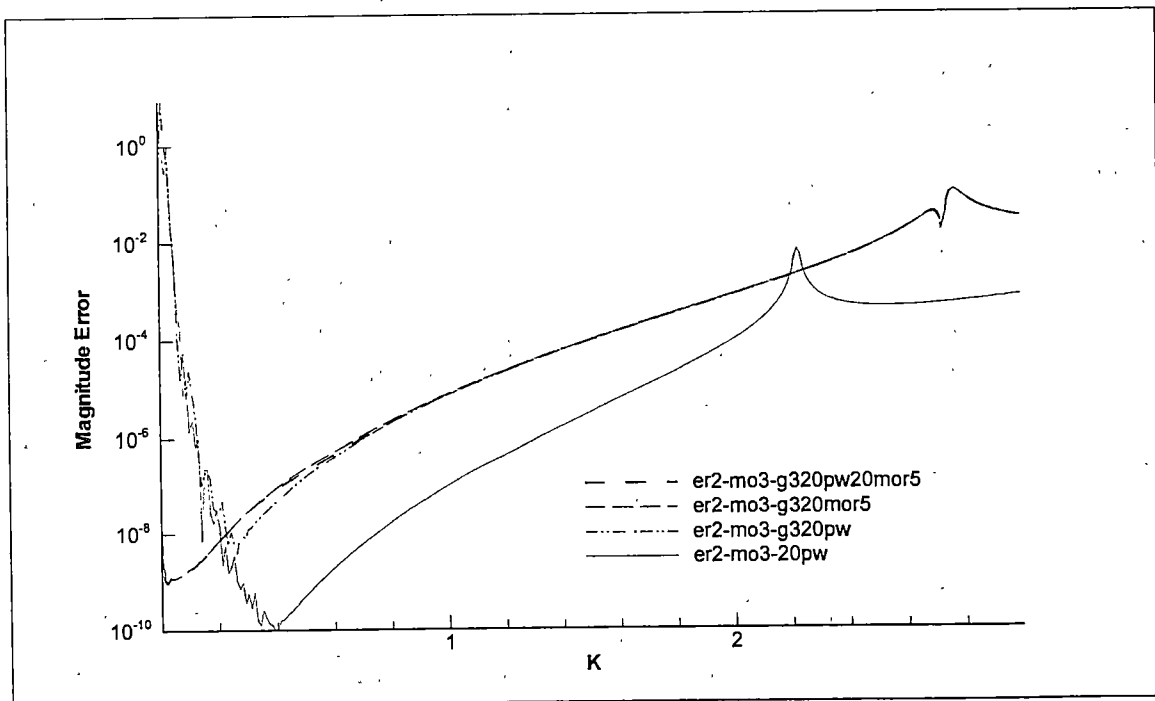


Figure 3.6.15: Magnitude Error vs.  $k$  for functions with skewed stencil grid of case 2, in interpolating a monopole at radius  $R/\delta=20$ , at  $15^\circ$  angle from the right (semi-log plot).

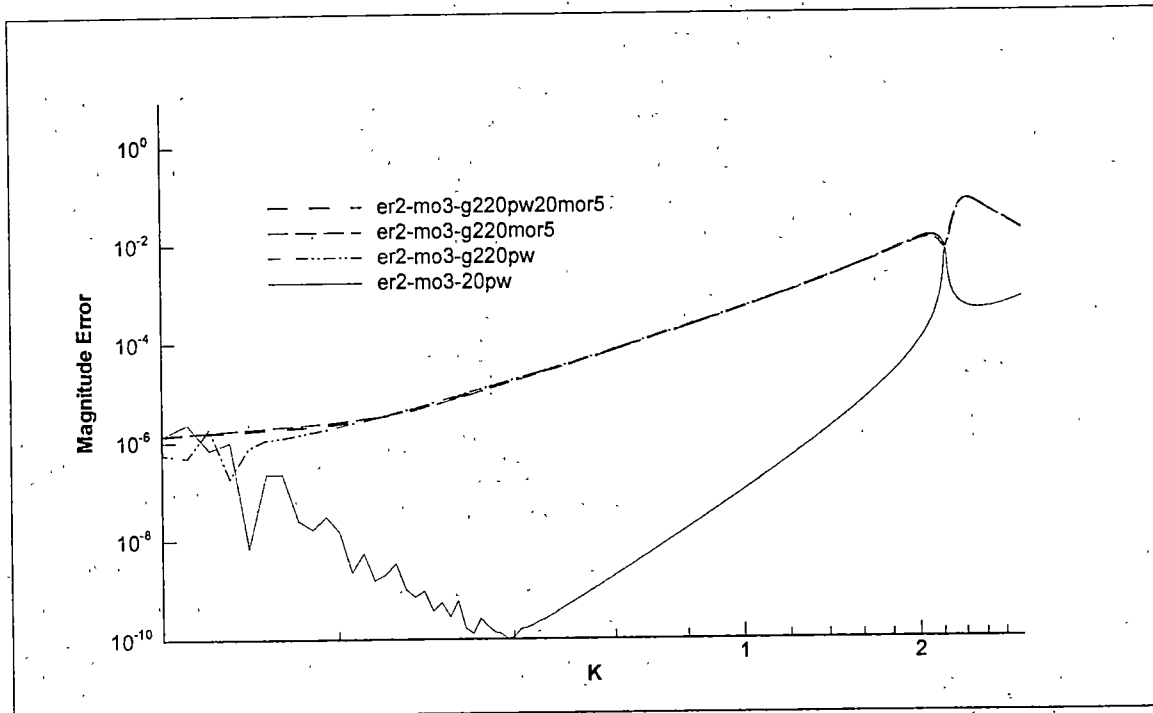


Figure 3.6.16: Magnitude Error vs.  $k$  for functions with skewed stencil grid of case 1, in interpolating a monopole at radius  $R/\delta=20$ , at  $15^\circ$  angle from the right (log-log plot).

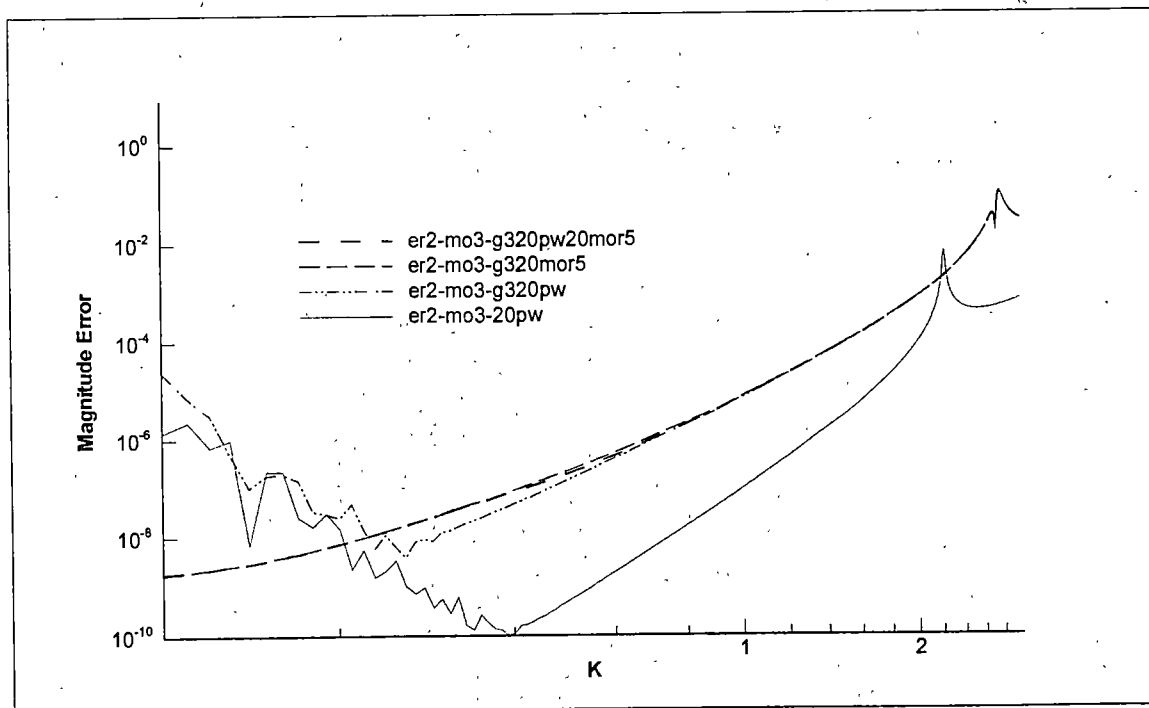


Figure 3.6.17: Magnitude Error vs.  $k$  for functions with skewed stencil grid of case 2, in interpolating a monopole at radius  $R/\delta=20$ , at  $15^\circ$  angle from the right (log-log plot).

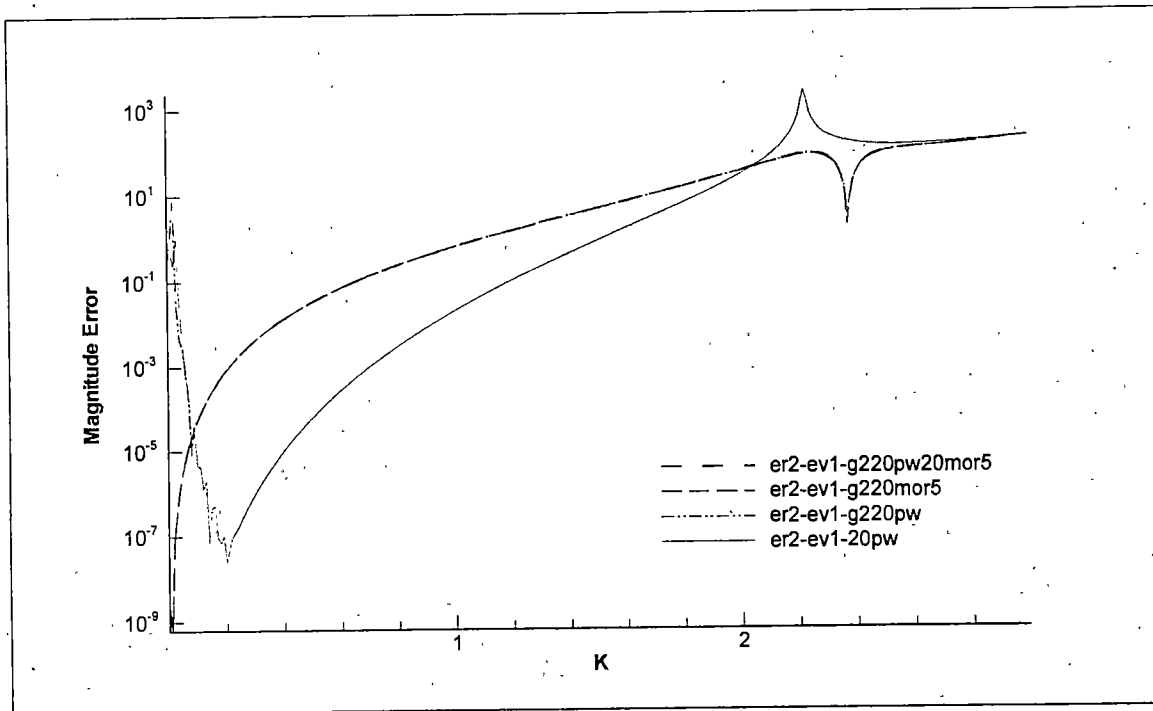


Figure 3.6.18: Magnitude Error vs.  $k$  for functions with skewed stencil grid of case 1, in interpolating an evanescent waves at phase Mach number = 0.5 (semi-log plot).

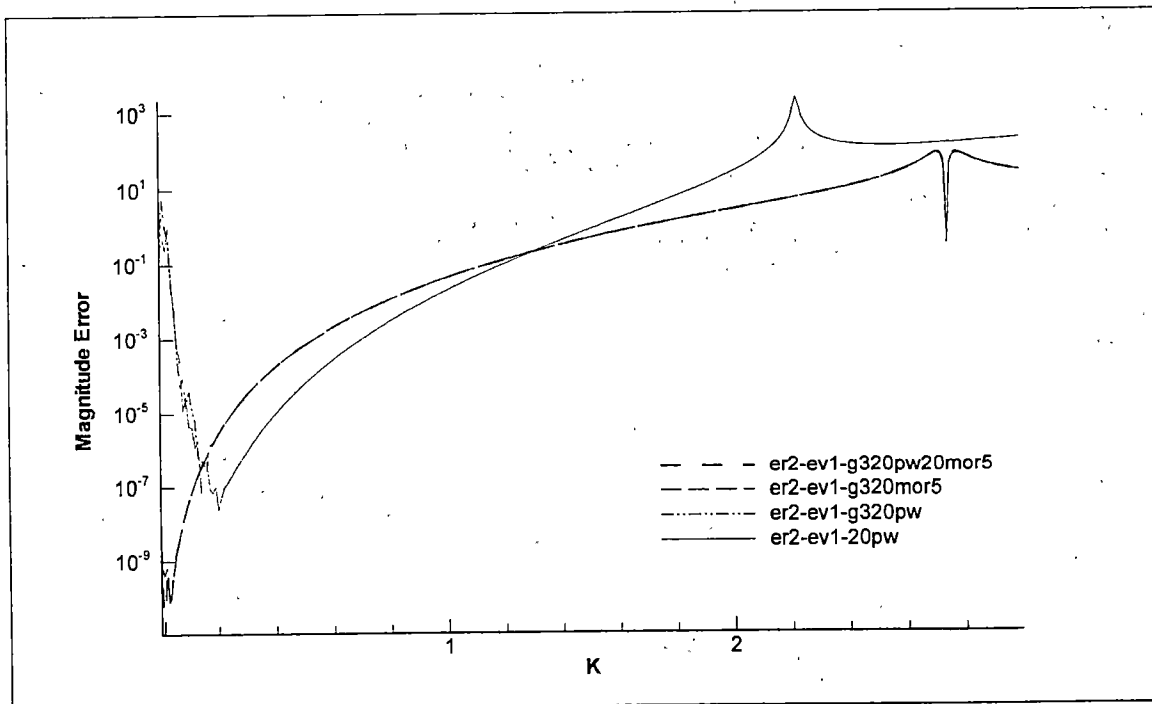


Figure 3.6.19: Magnitude Error vs.  $k$  for functions with skewed stencil grid of case 2, in interpolating an evanescent waves at phase Mach number = 0.5 (semi-log plot).

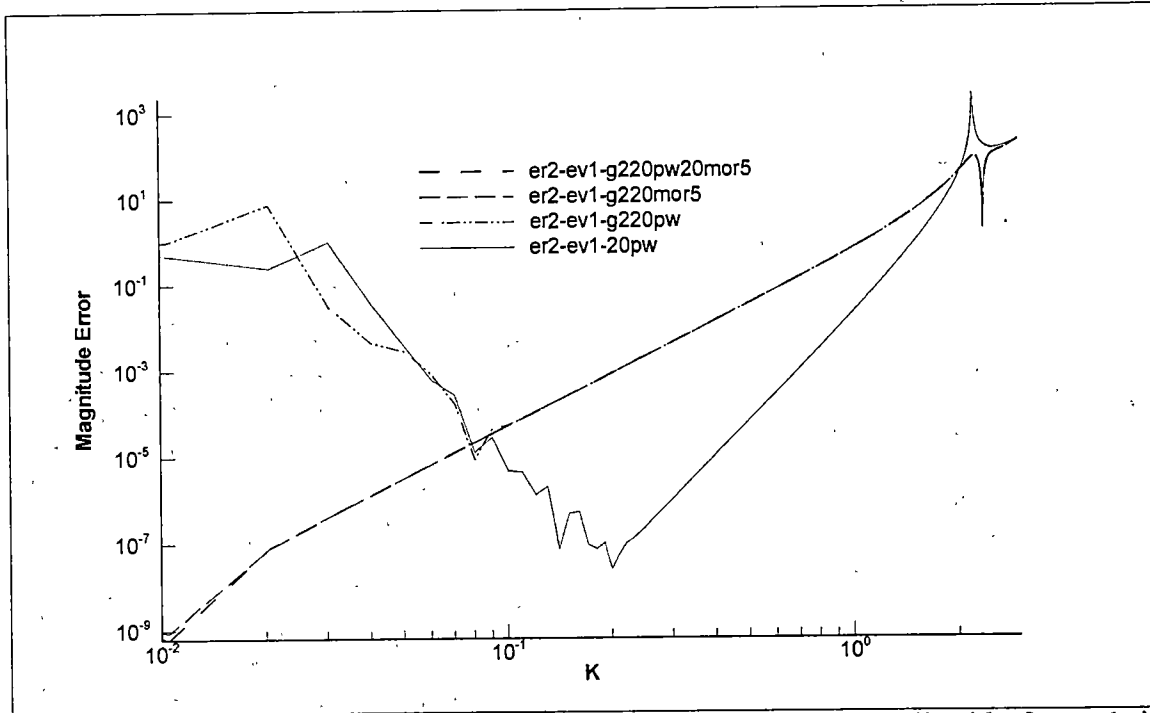


Figure 3.6.20: Magnitude Error vs.  $k$  for functions with skewed stencil grid of case 1, in interpolating an evanescent waves at phase Mach number = 0.5 (log-log plot).

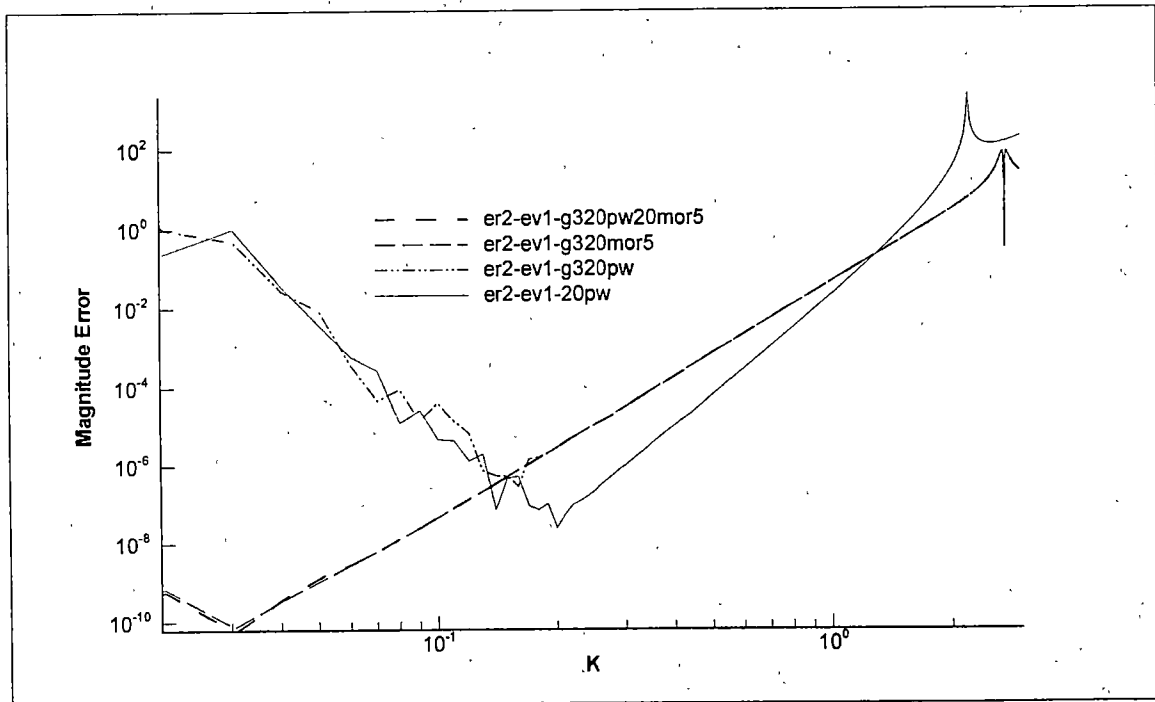


Figure 3.6.21: Magnitude Error vs.  $k$  for functions with skewed stencil grid of case 2, in interpolating an evanescent waves at phase Mach number = 0.5 (log-log plot).

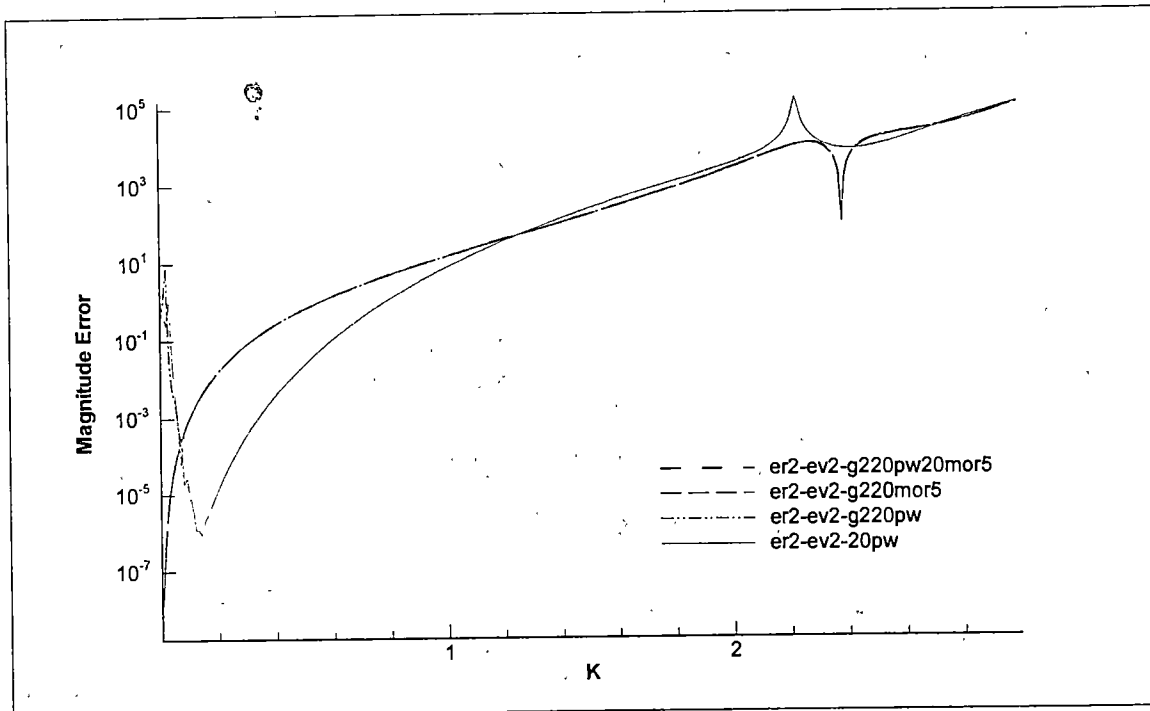


Figure 3.6.22: Magnitude Error vs.  $k$  for functions with skewed stencil grid of case 1, in interpolating an evanescent waves at phase Mach number = 0.25 (semi-log plot).

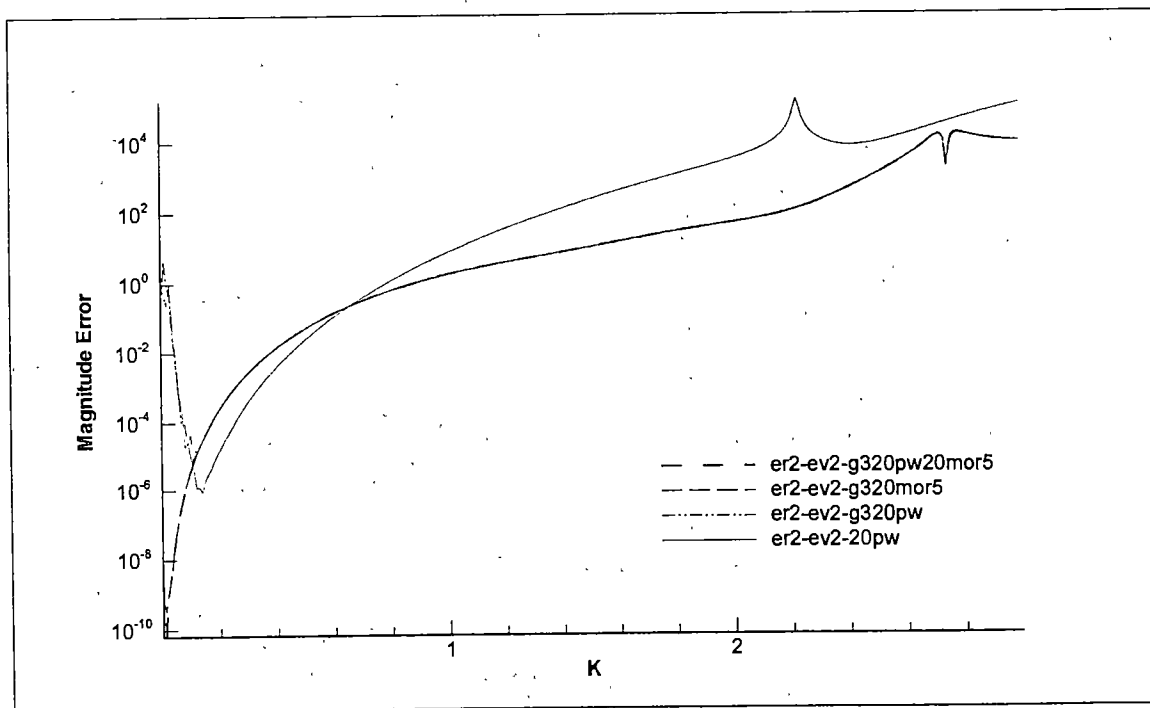


Figure 3.6.23: Magnitude Error vs.  $k$  for functions with skewed stencil grid of case 2, in interpolating an evanescent waves at phase Mach number = 0.25 (semi-log plot).

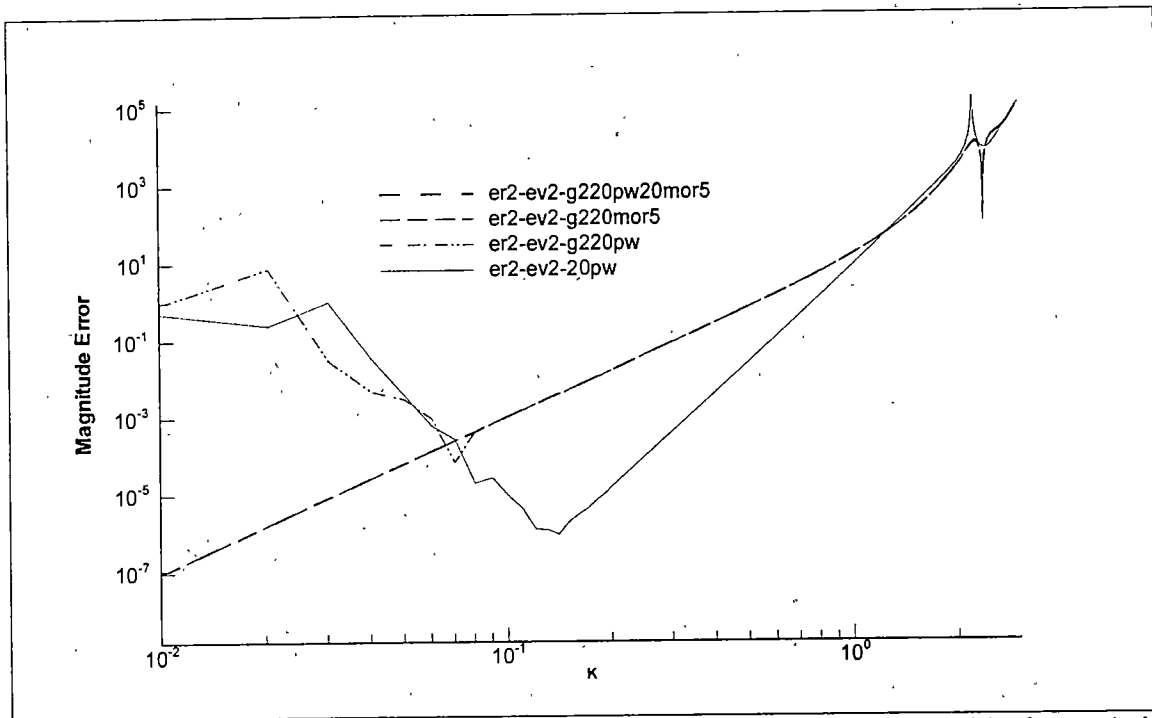


Figure 3.6.24: Magnitude Error vs.  $k$  for functions with skewed stencil grid of case 1, in interpolating an evanescent waves at phase Mach number = 0.25 (log-log plot).

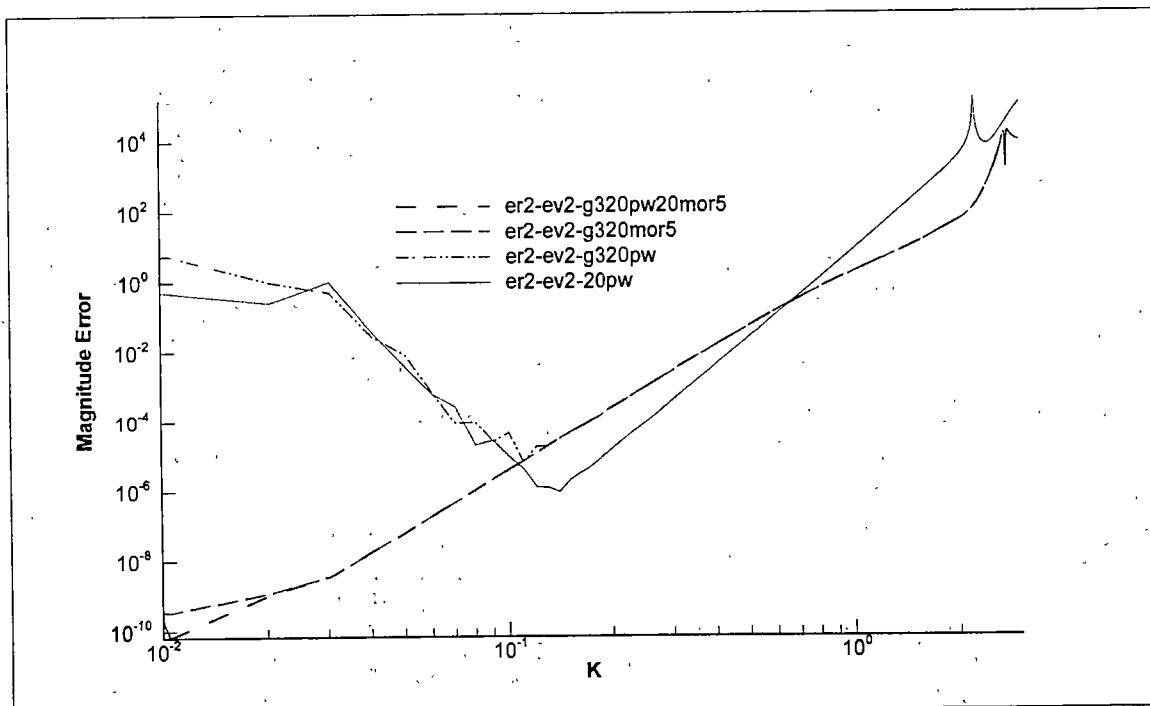


Figure 3.6.25: Magnitude Error vs.  $k$  for functions with skewed stencil grid of case 2, in interpolating an evanescent waves at phase Mach number = 0.25 (log-log plot).



### 3.7 Preliminary study on 3-D interpolation using GFD method

This section is intended to provide some preliminary results obtained in performing the Green's Function Discretization method in 3-D. Until now, there has been virtually no attempt to numerically prove that the GFD method works and produces the same 6<sup>th</sup> order result as for the 2-D case. It is of great importance to have this method to work as well in 3-D.

Thus far, only a minimal study has been accomplished on this dimension, and as stated above, this section only dealt this issue with very preliminary results. There are still many aspects that need to be refined and expanded further in the future. This study attempts to least assess the order of accuracy obtained in using this method in 3-D.

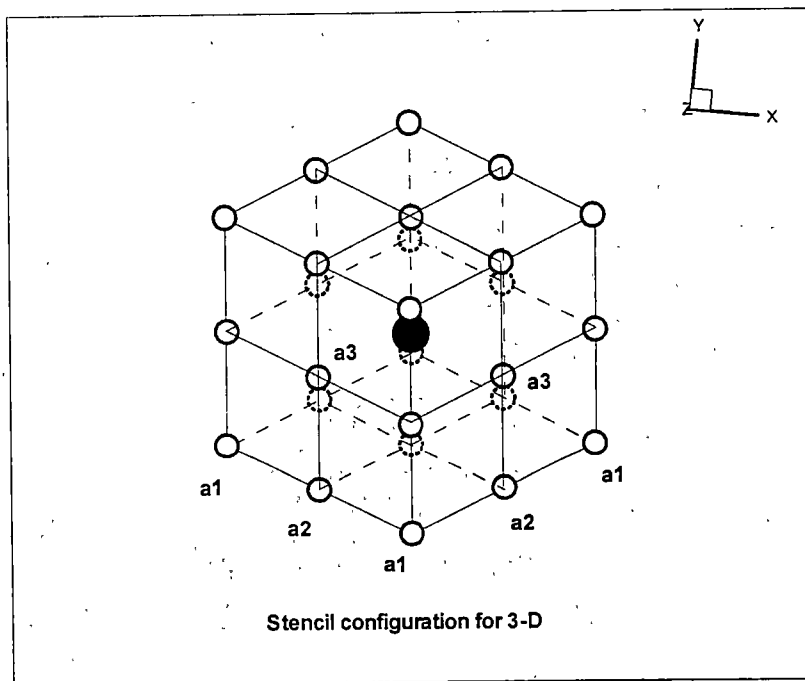


Figure 3.7.1: 3-D stencil grid configuration.

A standard 3-D coordinate representation is used. A cubic stencil is used with the normalized spacing,  $\Delta x = \Delta y = \Delta z = \delta = 1$ . This is shown in figure 3.7.1. Similar to the case of 2-D, the computed node is located at the center of the stencil and neighboring points of 26 are used as approximation to the computed node. Since three different node distances (from the center node) exist, it is therefore expected that 3 different values for the influence coefficients should be obtained. A set of 40 plane waves is used as the interpolating function. These waves are uniformly distributed on a spherical surface. For test function, a plane wave coming from a direction of  $\theta = 45^\circ$  and  $\phi = 15^\circ$  is used. The test is also run for the reduced frequencies of 0 to 3.

Figure 3.7.2 shows the influence coefficient values. As expected, 3 different values are obtained and shown. The average error is shown in figure 3.7.3 and the 2-D standard case of interpolating a plane wave is also attached as comparison. The error seems to show a quite similar trend as in the 2-D case. The plane wave behavior in 2-D of having sharp discontinuities in the error values at small reduced frequencies, is also retained and turns out to start at larger values of the reduced frequencies, which is around 1.2 instead of 0.4 in the standard 2-D case.

Figures 3.7.4 and 3.7.5 show the magnitude error in interpolating a plane wave. Larger error of up to 2 orders of magnitude is obtained for the 3-D case as compared to the 2-D case. As the slope on the log-log plot is measured, a remarkable and expected value of 6 is obtained for the order of accuracy. It is then shown that the order of accuracy to the GFD method in 3-D is maintained.

### 3.7.1 Figures reference codes

There are generally three types of plots in this section, namely influence coefficient, average error and magnitude error plots. They are indicated as:

an-3D-xxx	Influence coefficient for each interpolating function.
er-xxx	Average error in interpolating its function.
er2-xxx-xxx	Magnitude error in interpolating a certain oncoming wave function different than the interpolating function.

The interpolating functions are indicated as:

xx-xxx-20pw	20 plane waves (the Standard case).
xx-xxx-3D40pw	40 plane waves in 3-D.

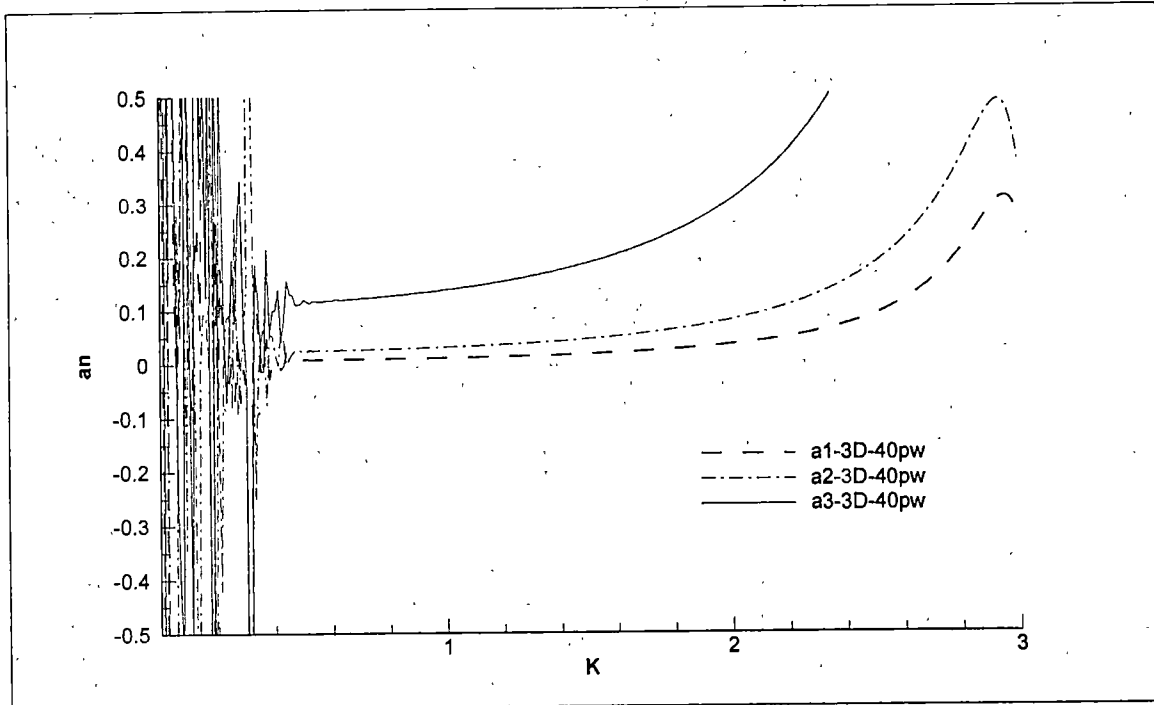


Figure 3.7.2:  $a_n$  vs.  $k$  plot for 3-D functions.

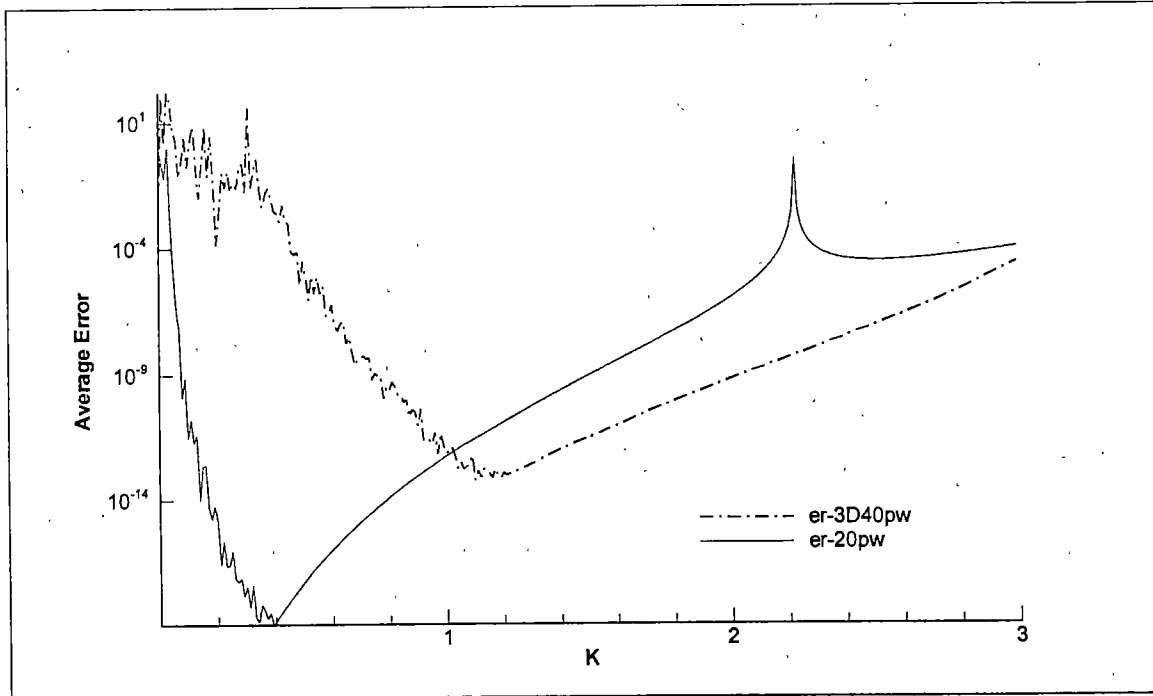


Figure 3.7.3: Average Error vs.  $k$  for 3-D functions.

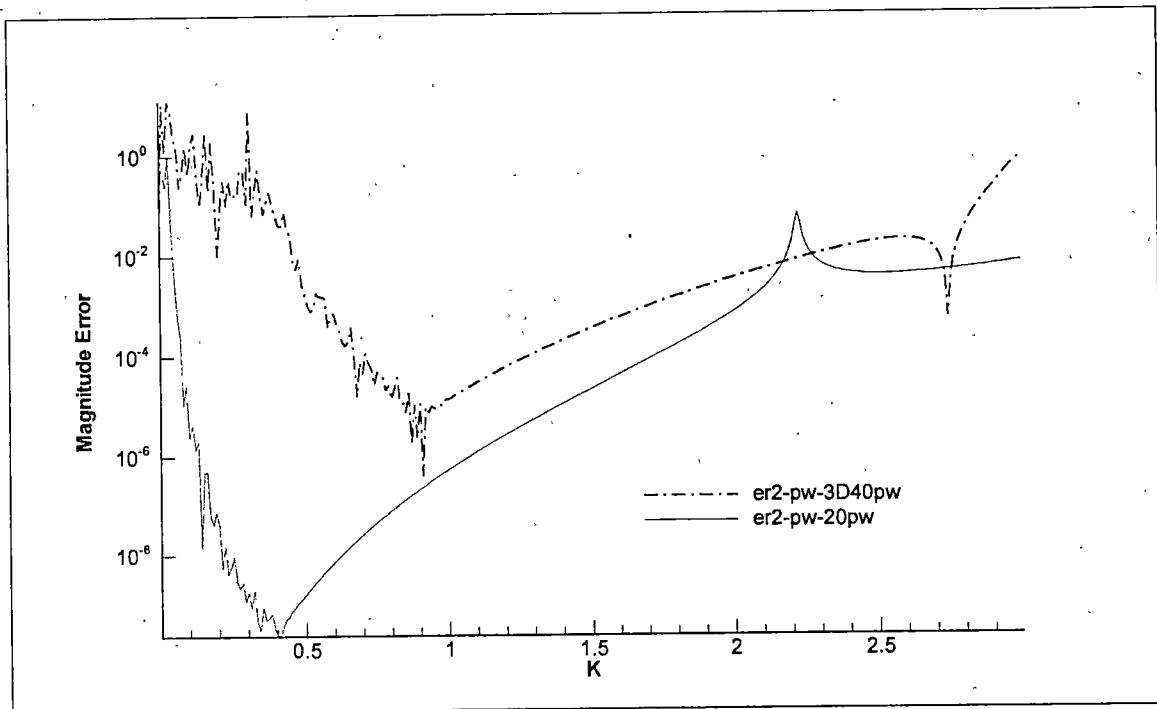


Figure 3.7.4: Magnitude Error vs.  $k$  for 3-D functions, in interpolating a plane wave approaching at  $\theta = 15^\circ$  and  $\phi = 15^\circ$  angles (semi-log plot).

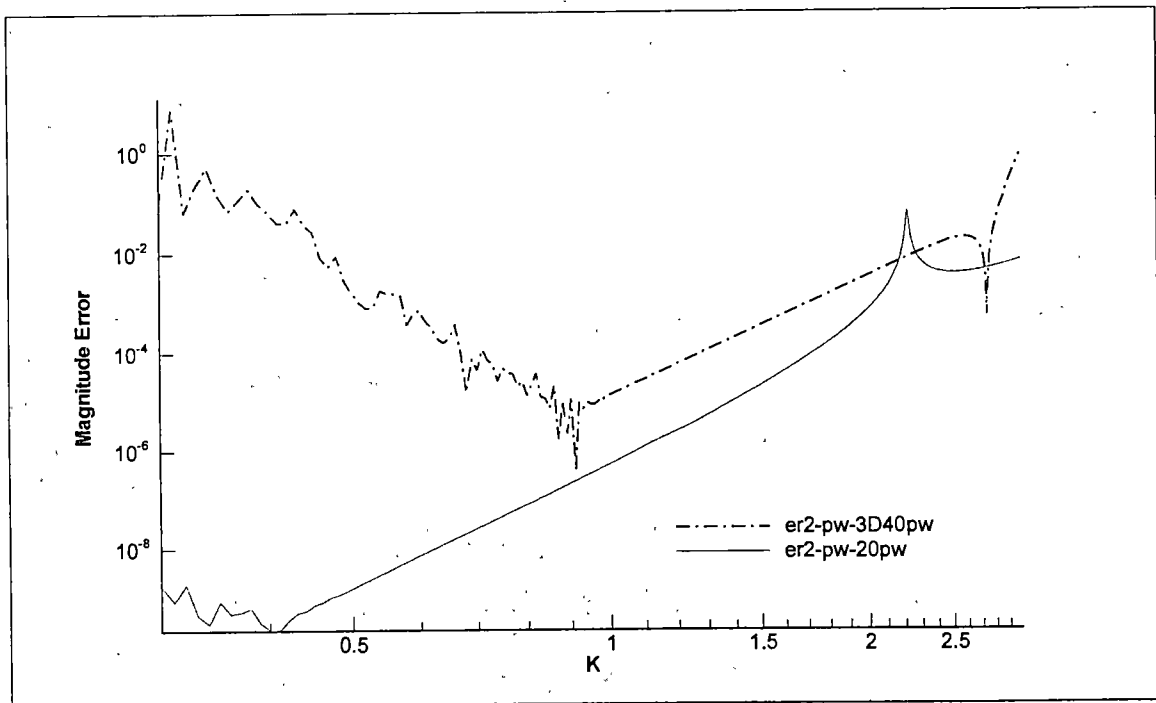


Figure 3.7.5: Magnitude Error vs.  $k$  for 3-D functions, in interpolating a plane wave approaching at  $\theta = 15^\circ$  and  $\phi = 15^\circ$  angles (log-log plot).

## CHAPTER 4

### CONCLUSIONS

Using various interpolating function sets, namely plane wave, monopole wave and evanescent wave, and combinations of them as the interpolating functions, does not seem to significantly affect the accuracy of GFD solutions. The errors show similar behavior for all interpolating functions, particularly at large reduced frequencies,  $k$ . As  $k$  approaches 0, the error is shown to vary due to the difference in the nature of the functions used; smoother variation for monopoles and sharp changes for plane waves.

Interpolating a monopole test function (different than the ones in the function set) introduced another variable,  $R/\delta$  that needs to be taken into account. In interpolating an evanescent wave, it was shown that the error in the solutions strongly depends on the phase Mach number of the wave. The error was found to decrease towards that of the plane wave as the phase Mach number increases. This is expected since an evanescent wave at Mach number greater than 1 is literally a plane wave.

The influence coefficients,  $a_n$  have been shown to be very similar to the 9 point Finite Difference formula for the 2-D Laplace equation on a square stencil, with 6<sup>th</sup> order accuracy. As shown in the log-log plots of the interpolations, 6<sup>th</sup> order of accuracy is maintained for the Helmholtz equations in all the square stencil solutions.

The addition of high phase Mach number evanescent waves in the interpolating function could improve the interpolation error of another high phase Mach number evanescent wave. However, no significant improvement is observed in interpolating a

low phase Mach number evanescent wave. The use of multiple sets of monopoles as interpolating functions has no apparent advantage in the solution. It is obvious however that these additional functions increase the computation time. It is worth noting that this computation effort for a stencil is negligibly small relative to the global solution effort involved in any given problem. Therefore, even if a small improvement could be gained in the solution by adding more sets of monopoles while increasing the stencil computation time, this is still an advantage.

The GFD method has shown to be quite sensitive to the stencil configuration. Using skew grids, instead of the standard square grid, reduces the order of accuracy quite significantly. The 3-D preliminary study on this method reveals that for a cubic stencil configuration, the 6<sup>th</sup> order of accuracy is maintained, even though only for a smaller region of the reduced frequencies.

## CHAPTER 5

### RECOMMENDATIONS FOR FURTHER WORK

Among other issues that are still needing to be addressed and answered are:

1. The problem with sharp discontinuities at small values of the reduced frequencies in the magnitude error plots. It is assumed that this phenomenon is due to the round off error. Analytical as well as numerical analyses needed to be able to explain this issue and further improve.
2. The lost in order of accuracy for skew grids should also be investigated further.
3. Obviously, the 3-D problem needs to be extended. Similar tests done on the 2-D could also be repeated for the 3-D.
4. Lastly, the time dependant problem should also be tackled.



## **LIST OF REFERENCES**

## LIST OF REFERENCES

- [1] Caruthers, J.E., French, J.C. and Raviprakash, G.K., Green Function Discretization for Numerical Solution of the Helmholtz Equation, "Journal of Sound and Vibration", October 1994, vol. 187, no. 4, p. 553-568.
- [2] French, J.C., "Evaluation of a Hypothetical Source Method for Discretization of the Helmholtz Equation", M.S. Thesis, UTK, Dec. 1993.
- [3] Caruthers, J.E., Steinhoff, J.S. and Engels, R.C., "Optimal Finite Difference Representation for the Helmholtz Equation using Green's Function Discretization", UTISI 98/04, Nov. 1998.
- [4] Dowling, A.P. and Williams, J.E.F., "Sound and Sources of Sound", Ellis Inc., New Jersey, © 1983.
- [5] Strang, G., "Linear Algebra and Its Applications", 3<sup>rd</sup> Edition, Harcourt-brace-Jovanovich, San Diego, 1988.
- [6] Caruthers, J.E. and Steinhoff, J.S., "Minimum Error Property of Green's Function Discretization", UTISI 98/05, Nov. 1997.
- [7] Tam, C.K.W and Webb, J.C., Dispersion-Relation-Preserving Finite Difference Schemes for Computational Acoustics, "Journal of Computational Physics", vol. 107, p. 262-281, 1993
- [8] Caruthers, J.E., French, J.C. and Raviprakash, G.K., "Recent Developments Concerning a new Discretization Method for the Helmholtz Equation", 1<sup>st</sup> CEAS/AIAA Aeroacoustics Conference, Munich, Germany, 1995.
- [9] Tam, C.K.W., "Computational Aeroacoustics: Issues and Methods", AIAA Journal, October 1995, vol. 33, no. 10, p. 1788-1796.
- [10] Hirsch, C., "Numerical Computation of Internal and External Flows", John Wiley and Sons Ltd., Great Britain, vol. 1, 1989.
- [11] Caruthers, J.E., and Dalton, W.N., Unsteady Aerodynamic Response of a Cascade to Nonuniform Inflow, "Journal of Turbomachinery", January 1993, vol. 115, no. 1, p. 79.
- [12] Dongara, J. J., Moler, C.B., Bunch, J.R., and Stewart, G.W., "Linpack User's Guide", SIAM Publication, 1979.

- [13] Raviprakash, G.K., "A Computational method for the Analysis of Acoustic Radiation from Turbofan Blades", Doctoral Dissertation, UTK, May 1992.
- [14] Anderson, D.A., Tannehill, J.C., and Pletcher, R.H., "Computational Fluid Mechanics and Heat Transfer", Hemisphere Publishing Corp., New York, ©1984.
- [15] Mayo, William E., Cwiakala, Martin, "Schaum's Outline on Theory and Problems of Programming with Fortran 77", McGraw-Hill Companies, 1995.

## **APPENDICES**

## APPENDIX 1

### DERIVATION OF THE SECOND ORDER FINITE DIFFERENCE SCHEME

This equation was derived in [14] for a Laplacian differential equation. To modify for the Helmholtz equation, the two sets of central difference in the x and y directions need to be weighed. According to the reference, the central difference containing the computed node is weighed by a multiplier of 10/12 and the two central difference around it by a multiplier of 1/12. Applying these weighs, the computed node and the minimum error coefficient can be obtained as follows:

$$\begin{aligned}
 & \frac{1}{12} \left( \frac{\phi_{i+1,j+1} - 2\phi_{i,j+1} + \phi_{i-1,j+1}}{(\Delta x)^2} \right) + \frac{5}{6} \left( \frac{\phi_{i+1,j} - 2\phi_{i,j} + \phi_{i-1,j}}{(\Delta x)^2} \right) + \\
 & \frac{1}{12} \left( \frac{\phi_{i+1,j-1} - 2\phi_{i,j-1} + \phi_{i-1,j-1}}{(\Delta x)^2} \right) + \frac{1}{12} \left( \frac{\phi_{i+1,j+1} - 2\phi_{i+1,j} + \phi_{i+1,j-1}}{(\Delta y)^2} \right) + \quad (A1.1) \\
 & \frac{5}{6} \left( \frac{\phi_{i,j+1} - 2\phi_{i,j} + \phi_{i,j-1}}{(\Delta y)^2} \right) + \frac{1}{12} \left( \frac{\phi_{i-1,j+1} - 2\phi_{i-1,j} + \phi_{i-1,j-1}}{(\Delta y)^2} \right) + k^2 \phi_{i,j} = 0
 \end{aligned}$$

For a square stencil, where  $\Delta x = \Delta y = \delta$ , we get

$$\begin{aligned}
 & \frac{1}{12} \left( \frac{\phi_{i+1,j+1} - 2\phi_{i,j+1} + \phi_{i-1,j+1}}{(\delta)^2} \right) + \frac{5}{6} \left( \frac{\phi_{i+1,j} - 2\phi_{i,j} + \phi_{i-1,j}}{(\delta)^2} \right) + \\
 & \frac{1}{12} \left( \frac{\phi_{i+1,j-1} - 2\phi_{i,j-1} + \phi_{i-1,j-1}}{(\delta)^2} \right) + \frac{1}{12} \left( \frac{\phi_{i+1,j+1} - 2\phi_{i+1,j} + \phi_{i+1,j-1}}{(\delta)^2} \right) + \quad (A1.2) \\
 & \frac{5}{6} \left( \frac{\phi_{i,j+1} - 2\phi_{i,j} + \phi_{i,j-1}}{(\delta)^2} \right) + \frac{1}{12} \left( \frac{\phi_{i-1,j+1} - 2\phi_{i-1,j} + \phi_{i-1,j-1}}{(\delta)^2} \right) + k^2 \phi_{i,j} = 0
 \end{aligned}$$

$$\begin{aligned}
& (\phi_{i+1,j+1} - 2\phi_{i,j+1} + \phi_{i-1,j+1}) + 10(\phi_{i+1,j} - 2\phi_{i,j} + \phi_{i-1,j}) + \\
& (\phi_{i+1,j-1} - 2\phi_{i,j-1} + \phi_{i-1,j-1}) + (\phi_{i+1,j+1} - 2\phi_{i+1,j} + \phi_{i+1,j-1}) + \\
& 10(\phi_{i,j+1} - 2\phi_{i,j} + \phi_{i,j-1}) + (\phi_{i-1,j+1} - 2\phi_{i-1,j} + \phi_{i-1,j-1}) + \\
& 12(\delta)^2 k^2 \phi_{i,j} = 0
\end{aligned} \tag{A1.3}$$

$$\begin{aligned}
& 2(\phi_{i+1,j+1} + \phi_{i-1,j+1} + \phi_{i+1,j-1} + \phi_{i-1,j-1}) + \\
& 8(\phi_{i,j+1} + \phi_{i+1,j} + \phi_{i,j-1} + \phi_{i-1,j}) \\
& = (40 - 12(\delta)^2 k^2) \phi_{i,j}
\end{aligned} \tag{A1.4}$$

Rearrange to finally obtain the computed node as:

$$\phi_{i,j} = \frac{1}{(40 - 12(\delta)^2 k^2)} \left[ \frac{2(\phi_{i+1,j+1} + \phi_{i-1,j+1} + \phi_{i+1,j-1} + \phi_{i-1,j-1}) + 8(\phi_{i,j+1} + \phi_{i+1,j} + \phi_{i,j-1} + \phi_{i-1,j})}{8(\phi_{i,j+1} + \phi_{i+1,j} + \phi_{i,j-1} + \phi_{i-1,j})} \right] \tag{A1.5}$$

$$\phi_{i,j} = \frac{1}{(20 - 6(\delta)^2 k^2)} \left[ \frac{(\phi_{i+1,j+1} + \phi_{i-1,j+1} + \phi_{i+1,j-1} + \phi_{i-1,j-1}) + 4(\phi_{i,j+1} + \phi_{i+1,j} + \phi_{i,j-1} + \phi_{i-1,j})}{4(\phi_{i,j+1} + \phi_{i+1,j} + \phi_{i,j-1} + \phi_{i-1,j})} \right] \tag{A1.6}$$

The minimum error coefficient is therefore:

$$a_1 = \frac{1}{(20 - 6(\delta)^2 k^2)} \tag{A1.7}$$

$$a_2 = \frac{4}{(20 - 6(\delta)^2 k^2)} \tag{A1.8}$$

## APPENDIX 2

### PLOTS OF INTERPOLATION ERROR FOR FUNCTION AT VARIOUS ANGLE

This appendix is to show that the error in interpolating an incoming wave function does not significantly affected by the angle in which it is approaching. This test is done in only the standard case of interpolating function (20 plane waves), and the result is shown in figure A3.1 below. Five plane waves, each approaching at various angle as follows:

- er2-pw-20pw a plane wave approaching at  $15^\circ$  angle from the right
- er2-pw2-20pw a plane wave approaching at  $75^\circ$  angle from the right
- er2-pw2-20pw a plane wave approaching at  $140^\circ$  angle from the right
- er2-pw2-20pw a plane wave approaching at  $200^\circ$  angle from the right
- er2-pw2-20pw a plane wave approaching at  $275^\circ$  angle from the right

The result shows that the difference in the error is insignificant, and some of them are even exactly on top of each other.

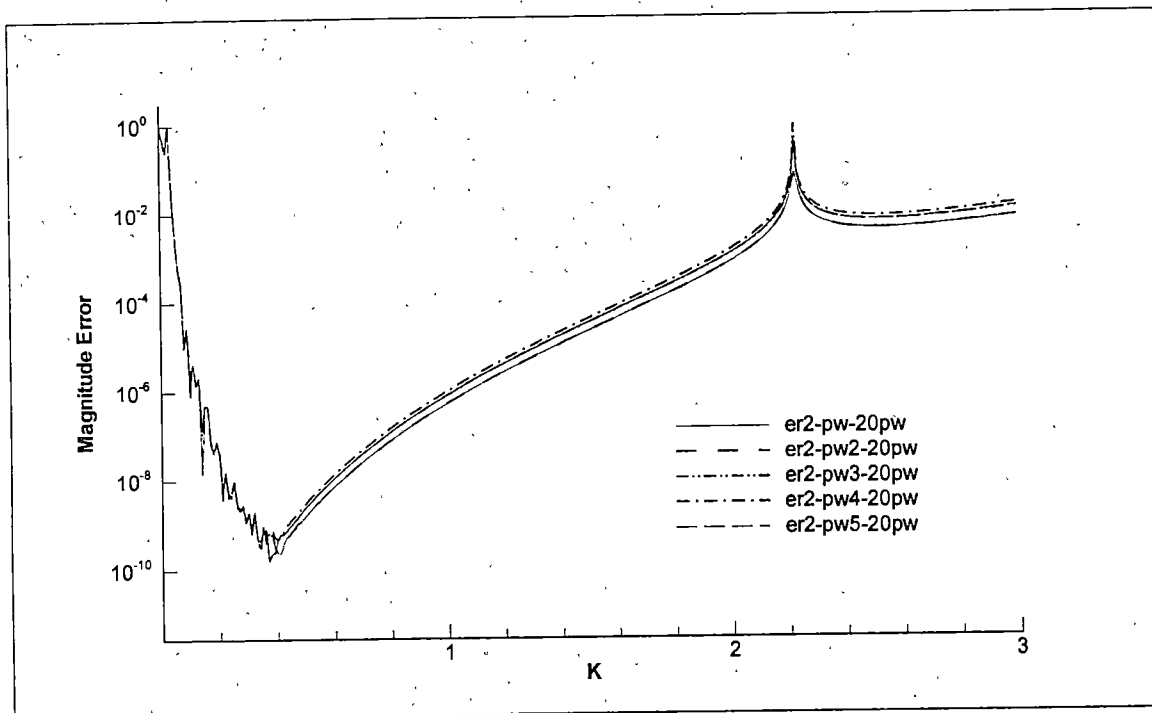


Figure A2.1: Magnitude error in interpolating a plane wave at various angle.



## APPENDIX 3

# TABLES OF INFLUENCE COEFFICIENT FOR VARIOUS INTERPOLATING FUNCTIONS

Table A3.1: Table of  $a_1$

vector coefficient, $a_1$ for various functions							
			20 monopoles	20 monopoles	20 p.w. and 20	20 p.w. and 20	
k	20 plane waves	infinite p.w.	at r = 5	at r = 10	mono at r = 5	mono at r = 10	2nd order FD
5.00E-04	0.390625	0.375	0.049999626	0.049999893	0.049999623	0.049999416	0.050000004
1.05E-02	-1.75	-0.25	0.050001496	0.050001927	0.050001496	0.050001919	0.050001654
2.05E-02	0	0.28125	0.050006767	0.050007179	0.050006767	0.050007164	0.050006305
3.05E-02	1	-0.1875	0.05001544	0.050015874	0.05001544	0.050015733	0.050013958
4.05E-02	0.015625	0.0390625	0.050027518	0.050027907	0.050027518	0.050028034	0.050024616
5.05E-02	0.046386719	0.05078125	0.050043004	0.050043397	0.050043004	0.050043456	0.050038283
6.05E-02	0.051025391	0.050048828	0.050061902	0.050062314	0.050061902	0.050062366	0.050054964
7.05E-02	0.049621582	0.049804688	0.050084218	0.050084585	0.050084218	0.050084546	0.050074665
8.05E-02	0.050186157	0.050231934	0.050109959	0.050110323	0.050109959	0.05011037	0.050097393
9.05E-02	0.050132751	0.050140381	0.050139131	0.0501395	0.05013913	0.050139476	0.050123156
0.1005	0.050167084	0.05014801	0.050171743	0.050172105	0.050171743	0.050172098	0.050151964
0.1105	0.050209045	0.050211906	0.050207803	0.050208161	0.050207803	0.050208185	0.050183827
0.1205	0.050247192	0.050244808	0.050247323	0.050247695	0.050247323	0.050247677	0.050218757
0.1305	0.050285816	0.050291538	0.050290314	0.050290684	0.050290314	0.050290707	0.050256766
0.1405	0.050337315	0.050338268	0.050336787	0.050337152	0.050336787	0.050337166	0.050297868
0.1505	0.050387144	0.050386071	0.050386757	0.050387118	0.050386757	0.050387081	0.050342078
0.1605	0.050441086	0.050440907	0.050440236	0.050440593	0.050440237	0.050440617	0.050389413
0.1705	0.050497442	0.050497293	0.050497242	0.050497602	0.050497242	0.05049758	0.05043989
0.1805	0.050557733	0.050558239	0.05055779	0.050558138	0.05055779	0.050558114	0.050493528
0.1905	0.050622314	0.050622165	0.050621897	0.050622255	0.050621897	0.050622271	0.050550345
0.2005	0.050689936	0.050689906	0.050689582	0.050689935	0.050689583	0.050689951	0.050610365
0.2105	0.050761245	0.050761141	0.050760865	0.050761212	0.050760866	0.050761219	0.050673608
0.2205	0.050836105	0.050836101	0.050835767	0.050836108	0.050835767	0.05083611	0.050740099
0.2305	0.050914682	0.050914649	0.050914308	0.050914648	0.050914309	0.050914657	0.050809862
0.2405	0.050996808	0.050996859	0.050996512	0.050996849	0.050996513	0.050996842	0.050882924
0.2505	0.051082755	0.051082747	0.051082403	0.051082738	0.051082405	0.051082733	0.050959313
0.2605	0.051172327	0.05117234	0.051172006	0.051172334	0.051172009	0.051172338	0.051039057
0.2705	0.051265678	0.051265667	0.051265348	0.051265672	0.051265351	0.051265673	0.051122187
0.2805	0.051362774	0.05136278	0.051362456	0.051362775	0.051362459	0.051362779	0.051208735
0.2905	0.05146368	0.051463671	0.051463358	0.051463675	0.051463362	0.051463672	0.051298734
0.3005	0.051568399	0.051568395	0.051568085	0.051568397	0.05156809	0.051568397	0.051392219
0.3105	0.051676972	0.051676976	0.051676667	0.051676976	0.051676674	0.051676977	0.051489227
0.3205	0.051789438	0.051789442	0.051789138	0.051789441	0.051789146	0.051789441	0.051589795
0.3305	0.051905828	0.051905827	0.05190553	0.051905829	0.051905541	0.051905827	0.051693963
0.3405	0.052026175	0.052026174	0.05202588	0.052026173	0.052025892	0.052026175	0.051801773
0.3505	0.05215051	0.052150513	0.052150222	0.052150511	0.052150237	0.052150511	0.051913267
0.3605	0.05227888	0.052278879	0.052278596	0.052278879	0.052278613	0.05227888	0.052028491
0.3705	0.052411318	0.052411317	0.052411039	0.052411317	0.05241106	0.052411318	0.05214749
0.3805	0.052547866	0.052547866	0.052547594	0.052547866	0.052547617	0.052547867	0.052270313
0.3905	0.052688567	0.052688567	0.0526883	0.052688567	0.052688327	0.052688567	0.05239701

0.4005	0.052833464	0.052833464	0.052833203	0.052833464	0.052833233	0.052833464	0.052527634
0.4105	0.052982602	0.052982602	0.052982346	0.052982601	0.05298238	0.052982601	0.052662238
0.4205	0.053136026	0.053136027	0.053135776	0.053136026	0.053135814	0.053136026	0.052800879
0.4305	0.053293786	0.053293786	0.053293542	0.053293786	0.053293584	0.053293786	0.052943616
0.4405	0.05345593	0.053455931	0.053455693	0.053455931	0.053455738	0.053455931	0.053090509
0.4505	0.053622511	0.053622511	0.053622279	0.053622511	0.053622329	0.053622511	0.05324162
0.4605	0.053793581	0.053793581	0.053793355	0.053793581	0.053793408	0.053793581	0.053397015
0.4705	0.053969194	0.053969194	0.053968975	0.053969194	0.053969031	0.053969194	0.053556762
0.4805	0.054149408	0.054149408	0.054149194	0.054149408	0.054149254	0.054149408	0.053720931
0.4905	0.05433428	0.05433428	0.054334072	0.054334279	0.054334135	0.05433428	0.053889593
0.5005	0.05452387	0.05452387	0.054523668	0.05452387	0.054523734	0.05452387	0.054062825
0.5105	0.05471824	0.05471824	0.054718045	0.05471824	0.054718113	0.05471824	0.054240705
0.5205	0.054917455	0.054917455	0.054917265	0.054917455	0.054917336	0.054917455	0.054423313
0.5305	0.05512158	0.05512158	0.055121396	0.05512158	0.055121469	0.05512158	0.054610734
0.5405	0.055330683	0.055330683	0.055330505	0.055330683	0.05533058	0.055330683	0.054803053
0.5505	0.055544834	0.055544834	0.055544661	0.055544834	0.055544738	0.055544834	0.055000362
0.5605	0.055764106	0.055764106	0.055763938	0.055764106	0.055764016	0.055764106	0.055202753
0.5705	0.055988572	0.055988572	0.05598841	0.055988572	0.055988488	0.055988572	0.055410324
0.5805	0.05621831	0.05621831	0.056218153	0.05621831	0.056218232	0.05621831	0.055623173
0.5905	0.056453398	0.056453398	0.056453246	0.056453398	0.056453325	0.056453398	0.055841406
0.6005	0.056693918	0.056693918	0.056693771	0.056693918	0.05669385	0.056693918	0.05606513
0.6105	0.056939953	0.056939953	0.056939811	0.056939953	0.05693989	0.056939953	0.056294456
0.6205	0.057191591	0.057191591	0.057191454	0.057191591	0.057191533	0.057191591	0.056529501
0.6305	0.05744892	0.05744892	0.057448787	0.05744892	0.057448866	0.05744892	0.056770383
0.6405	0.057712032	0.057712032	0.057711904	0.057712032	0.057711981	0.057712032	0.057017229
0.6505	0.057981022	0.057981022	0.057980897	0.057981022	0.057980974	0.057981022	0.057270165
0.6605	0.058255986	0.058255986	0.058255866	0.058255986	0.058255942	0.058255986	0.057529328
0.6705	0.058537026	0.058537026	0.058536909	0.058537026	0.058536984	0.058537026	0.057794854
0.6805	0.058824244	0.058824244	0.058824131	0.058824244	0.058824205	0.058824244	0.058066889
0.6905	0.059117747	0.059117747	0.059117638	0.059117747	0.059117711	0.059117747	0.058345581
0.7005	0.059417645	0.059417645	0.059417539	0.059417645	0.059417611	0.059417645	0.058631087
0.7105	0.059724051	0.059724051	0.059723948	0.059724051	0.059724019	0.059724051	0.058923566
0.7205	0.060037081	0.060037081	0.060036981	0.060037081	0.060037051	0.060037081	0.059223187
0.7305	0.060356855	0.060356855	0.060356758	0.060356855	0.060356827	0.060356855	0.059530122
0.7405	0.060683497	0.060683497	0.060683403	0.060683497	0.060683471	0.060683497	0.059844553
0.7505	0.061017135	0.061017135	0.061017044	0.061017135	0.06101711	0.061017135	0.060166667
0.7605	0.0613579	0.0613579	0.061357811	0.0613579	0.061357876	0.0613579	0.060496659
0.7705	0.061705927	0.061705927	0.06170584	0.061705926	0.061705904	0.061705927	0.060834731
0.7805	0.062061355	0.062061355	0.062061271	0.062061355	0.062061334	0.062061355	0.061181094
0.7905	0.06242433	0.06242433	0.062424248	0.062424329	0.062424309	0.06242433	0.061535968
0.8005	0.062794998	0.062794998	0.062794918	0.062794998	0.062794979	0.062794998	0.06189958
0.8105	0.063173514	0.063173514	0.063173436	0.063173514	0.063173496	0.063173514	0.062272168
0.8205	0.063560034	0.063560034	0.063559958	0.063560034	0.063560017	0.063560034	0.062653978
0.8305	0.063954723	0.063954723	0.063954648	0.063954722	0.063954706	0.063954723	0.063045269
0.8405	0.064357746	0.064357746	0.064357673	0.064357746	0.06435773	0.064357746	0.063446308
0.8505	0.064769279	0.064769279	0.064769207	0.064769278	0.064769263	0.064769279	0.063857374
0.8605	0.065189498	0.065189498	0.065189428	0.065189498	0.065189484	0.065189498	0.06427876
0.8705	0.065618589	0.065618589	0.065618521	0.065618589	0.065618575	0.065618589	0.064710769
0.8805	0.066056742	0.066056742	0.066056675	0.066056742	0.066056729	0.066056742	0.065153717
0.8905	0.066504154	0.066504154	0.066504087	0.066504153	0.066504141	0.066504154	0.065607936
0.9005	0.066961026	0.066961026	0.066960961	0.066961026	0.066961014	0.066961026	0.066073771
0.9105	0.067427569	0.067427569	0.067427505	0.067427569	0.067427557	0.067427569	0.066551583
0.9205	0.067903999	0.067903999	0.067903935	0.067903998	0.067903987	0.067903999	0.06704175
0.9305	0.068390538	0.068390538	0.068390476	0.068390538	0.068390527	0.068390538	0.067544664
0.9405	0.068887419	0.068887419	0.068887357	0.068887418	0.068887408	0.068887419	0.068060739
0.9505	0.069394878	0.069394878	0.069394817	0.069394878	0.069394868	0.069394878	0.068590406
0.9605	0.069913163	0.069913163	0.069913103	0.069913163	0.069913153	0.069913163	0.069134116

0.9705	0.070442529	0.070442529	0.070442469	0.070442528	0.070442519	0.070442529	0.069692343
0.9805	0.070983237	0.070983237	0.070983178	0.070983237	0.070983228	0.070983237	0.070265583
0.9905	0.071535562	0.071535562	0.071535503	0.071535562	0.071535553	0.071535562	0.070854355
1.0005	0.072099784	0.072099784	0.072099726	0.072099784	0.072099775	0.072099784	0.071459204
1.0105	0.072676196	0.072676196	0.072676137	0.072676195	0.072676187	0.072676196	0.072080704
1.0205	0.073265097	0.073265097	0.073265039	0.073265097	0.073265088	0.073265097	0.072719453
1.0305	0.073866802	0.073866802	0.073866743	0.073866801	0.073866793	0.073866802	0.073376085
1.0405	0.074481632	0.074481632	0.074481574	0.074481631	0.074481623	0.074481632	0.074051264
1.0505	0.075109922	0.075109922	0.075109864	0.075109921	0.075109914	0.075109922	0.074745686
1.0605	0.075752019	0.075752019	0.075751961	0.075752019	0.075752011	0.075752019	0.075460089
1.0705	0.076408283	0.076408283	0.076408224	0.076408282	0.076408274	0.076408283	0.076195245
1.0805	0.077079084	0.077079084	0.077079026	0.077079083	0.077079076	0.077079084	0.076951972
1.0905	0.077764809	0.077764809	0.077764751	0.077764808	0.077764801	0.077764809	0.077731131
1.1005	0.078465858	0.078465858	0.078465799	0.078465857	0.07846585	0.078465858	0.078533629
1.1105	0.079182646	0.079182646	0.079182586	0.079182644	0.079182638	0.079182646	0.079360428
1.1205	0.079915602	0.079915602	0.079915542	0.079915601	0.079915594	0.079915602	0.080212541
1.1305	0.080665174	0.080665174	0.080665114	0.080665173	0.080665166	0.080665174	0.081091041
1.1405	0.081431826	0.081431826	0.081431765	0.081431824	0.081431818	0.081431826	0.081997065
1.1505	0.082216038	0.082216038	0.082215976	0.082216036	0.08221603	0.082216038	0.082931815
1.1605	0.083018311	0.083018311	0.083018248	0.083018309	0.083018303	0.083018311	0.083896569
1.1705	0.083839164	0.083839164	0.083839101	0.083839162	0.083839156	0.083839164	0.084892681
1.1805	0.084679138	0.084679138	0.084679074	0.084679136	0.08467913	0.084679138	0.085921589
1.1905	0.085538794	0.085538794	0.085538729	0.085538792	0.085538786	0.085538794	0.086984822
1.2005	0.086418716	0.086418716	0.08641865	0.086418714	0.086418708	0.086418716	0.088084009
1.2105	0.087319512	0.087319512	0.087319446	0.08731951	0.087319504	0.087319512	0.089220882
1.2205	0.088241815	0.088241815	0.088241747	0.088241813	0.088241807	0.088241815	0.09039729
1.2305	0.089186283	0.089186283	0.089186214	0.08918628	0.089186275	0.089186283	0.091615207
1.2405	0.090153602	0.090153602	0.090153531	0.090153599	0.090153594	0.090153602	0.09287674
1.2505	0.091144487	0.091144487	0.091144415	0.091144484	0.091144479	0.091144487	0.094184143
1.2605	0.092159683	0.092159683	0.09215961	0.09215968	0.092159675	0.092159683	0.095539833
1.2705	0.093199968	0.093199968	0.093199893	0.093199965	0.09319996	0.093199968	0.096946397
1.2805	0.094266152	0.094266152	0.094266076	0.094266149	0.094266144	0.094266152	0.098406615
1.2905	0.095359082	0.095359082	0.095359003	0.095359078	0.095359073	0.095359081	0.099923474
1.3005	0.09647964	0.09647964	0.09647956	0.096479636	0.096479631	0.09647964	0.101500188
1.3105	0.09762875	0.09762875	0.097628668	0.097628746	0.097628741	0.09762875	0.103140223
1.3205	0.098807377	0.098807377	0.098807293	0.098807373	0.098807368	0.098807377	0.104847317
1.3305	0.100016529	0.100016529	0.100016442	0.100016525	0.10001652	0.100016529	0.106625512
1.3405	0.101257262	0.101257262	0.101257172	0.101257257	0.101257252	0.101257261	0.108479183
1.3505	0.102530678	0.102530678	0.102530586	0.102530673	0.102530669	0.102530678	0.110413074
1.3605	0.103837935	0.103837935	0.103837841	0.10383793	0.103837926	0.103837935	0.112432335
1.3705	0.105180244	0.105180244	0.105180147	0.105180239	0.105180234	0.105180244	0.114542571
1.3805	0.106558875	0.106558875	0.106558774	0.106558868	0.106558864	0.106558874	0.116749891
1.3905	0.107975158	0.107975158	0.107975054	0.107975151	0.107975147	0.107975157	0.119060964
1.4005	0.10943049	0.10943049	0.109430383	0.109430484	0.10943048	0.10943049	0.121483087
1.4105	0.11092634	0.11092634	0.110926229	0.110926333	0.110926329	0.11092634	0.124024262
1.4205	0.112464247	0.112464247	0.112464132	0.112464239	0.112464236	0.112464247	0.126693279
1.4305	0.114045831	0.114045831	0.114045712	0.114045823	0.114045819	0.11404583	0.129499819
1.4405	0.115672795	0.115672795	0.115672672	0.115672786	0.115672783	0.115672795	0.132454568
1.4505	0.117346932	0.117346932	0.117346805	0.117346923	0.11734692	0.117346932	0.135569351
1.4605	0.119070131	0.119070131	0.119069998	0.119070121	0.119070118	0.11907013	0.138857289
1.4705	0.120844379	0.120844379	0.120844241	0.120844368	0.120844366	0.120844378	0.142332981
1.4805	0.122671774	0.122671774	0.122671631	0.122671763	0.122671761	0.122671774	0.146012718
1.4905	0.124554531	0.124554531	0.124554382	0.124554519	0.124554517	0.12455453	0.149914732
1.5005	0.126494985	0.126494985	0.126494831	0.126494973	0.126494971	0.126494985	0.154059503
1.5105	0.128495608	0.128495608	0.128495447	0.128495595	0.128495593	0.128495607	0.158470104
1.5205	0.13055901	0.13055901	0.130558842	0.130558996	0.130558995	0.130559009	0.163172637
1.5305	0.132687955	0.132687955	0.13268778	0.13268794	0.13268794	0.132687955	0.168196738

1.5405	0.134885372	0.134885372	0.134885189	0.134885356	0.134885356	0.134885371	0.1735762
1.5505	0.137154363	0.137154363	0.137154172	0.137154346	0.137154347	0.137154362	0.179349726
1.5605	0.139498221	0.139498221	0.139498021	0.139498203	0.139498204	0.139498222	0.185561859
1.5705	0.141920442	0.141920442	0.141920232	0.141920423	0.141920424	0.141920441	0.192264119
1.5805	0.144424741	0.144424741	0.144424522	0.14442472	0.144424723	0.14442474	0.199516432
1.5905	0.147015071	0.147015071	0.147014841	0.147015049	0.147015052	0.14701507	0.207388914
1.6005	0.149695641	0.149695641	0.149695399	0.149695617	0.149695621	0.14969564	0.215964134
1.6105	0.152470935	0.152470935	0.152470682	0.15247091	0.152470914	0.152470934	0.225340001
1.6205	0.155345741	0.155345741	0.155345475	0.155345714	0.155345719	0.15534574	0.235633513
1.6305	0.158325169	0.158325169	0.158324889	0.15832514	0.158325146	0.158325168	0.246985633
1.6405	0.161414685	0.161414685	0.16141439	0.161414654	0.161414661	0.161414684	0.259567765
1.6505	0.164620138	0.164620138	0.164619827	0.164620105	0.164620113	0.164620137	0.273590438
1.6605	0.167947798	0.167947798	0.16794747	0.167947763	0.167947772	0.167947797	0.289315143
1.6705	0.171404391	0.171404391	0.171404045	0.171404353	0.171404364	0.17140439	0.307070749
1.6805	0.174997143	0.174997143	0.174996777	0.174997103	0.174997114	0.174997141	0.327276696
1.6905	0.178733826	0.178733826	0.17873344	0.178733783	0.178733796	0.178733824	0.350476482
1.7005	0.182622812	0.182622812	0.182622403	0.182622766	0.182622781	0.182622811	0.377387186
1.7105	0.186673132	0.186673132	0.186672699	0.186673082	0.186673098	0.18667313	0.408974788
1.7205	0.190894538	0.190894538	0.190894079	0.190894485	0.190894503	0.190894536	0.446572412
1.7305	0.195297583	0.195297583	0.195297095	0.195297525	0.195297546	0.195297581	0.492073072
1.7405	0.199893698	0.199893698	0.199893179	0.199893636	0.199893658	0.199893695	0.548258088
1.7505	0.20469529	0.20469529	0.204694738	0.204695223	0.204695248	0.204695287	0.619387383
1.7605	0.209715846	0.209715846	0.209715259	0.209715774	0.209715802	0.209715844	0.712332651
1.7705	0.214970054	0.214970054	0.214969428	0.214969977	0.214970008	0.214970052	0.838941306
1.7805	0.220473939	0.220473939	0.220473269	0.220473855	0.220473889	0.220473936	1.021535501
1.7905	0.226245016	0.226245016	0.2262443	0.226244926	0.226244964	0.226245013	1.307773339
1.8005	0.232302472	0.232302472	0.232301706	0.232302375	0.232302417	0.232302469	1.820835272
1.8105	0.238667368	0.238667368	0.238666546	0.238667262	0.238667309	0.238667364	3.007170598
1.8205	0.24536287	0.24536287	0.245361988	0.245362755	0.245362807	0.245362866	8.720030346
1.8305	0.252414525	0.252414524	0.252413575	0.2524144	0.252414457	0.252414521	-9.580241709
1.8405	0.259850567	0.259850566	0.259849544	0.259850431	0.259850494	0.259850562	-3.080320908
1.8505	0.267702286	0.267702285	0.267701182	0.267702138	0.267702208	0.267702281	-1.831161423
1.8605	0.27600445	0.276004449	0.276003256	0.276004288	0.276004366	0.276004445	-1.300793549
1.8705	0.284795801	0.2847958	0.284794507	0.284795624	0.284795711	0.284795795	-1.007433347
1.8805	0.294119639	0.294119638	0.294118235	0.294119445	0.294119542	0.294119633	-0.82123281
1.8905	0.304024515	0.304024514	0.304022987	0.304024302	0.30402441	0.304024508	-0.692548832
1.9005	0.314565048	0.314565046	0.314563381	0.314564814	0.314564934	0.31456504	-0.598300289
1.9105	0.325802904	0.325802902	0.325801081	0.325802646	0.32580278	0.325802895	-0.526298754
1.9205	0.337807971	0.337807969	0.337805972	0.337807686	0.337807836	0.337807962	-0.469500871
1.9305	0.350659775	0.350659773	0.350657577	0.350659459	0.350659627	0.350659765	-0.423552662
1.9405	0.3644492	0.364449197	0.364446775	0.364448848	0.364449038	0.364449188	-0.385617768
1.9505	0.379280589	0.379280586	0.379277906	0.379280197	0.379280411	0.379280577	-0.353769225
1.9605	0.395274335	0.395274331	0.395271353	0.395273895	0.395274138	0.39527432	-0.326652047
1.9705	0.41257008	0.412570076	0.412566755	0.412569587	0.412569862	0.412570065	-0.30328566
1.9805	0.431330734	0.431330729	0.431327009	0.431330177	0.431330491	0.431330716	-0.28294294
1.9905	0.451747517	0.451747512	0.451743326	0.451746886	0.451747246	0.451747497	-0.265073293
2.0005	0.474046399	0.474046393	0.474041658	0.47404568	0.474046094	0.474046376	-0.24925215
2.0105	0.498496358	0.498496351	0.498490964	0.498495535	0.498496013	0.498496333	-0.23514686
2.0205	0.525420128	0.525420119	0.525413952	0.525419179	0.525419735	0.525420098	-0.222493095
2.0305	0.555208327	0.555208317	0.555201207	0.555207225	0.555207876	0.555208293	-0.211078163
2.0405	0.588338299	0.588338286	0.588330025	0.58833701	0.588337778	0.588338259	-0.200728987
2.0505	0.625399587	0.625399572	0.62538989	0.625398067	0.625398981	0.625399541	-0.191303295
2.0605	0.667128962	0.667128944	0.667117482	0.667127151	0.667128248	0.667128907	-0.182683053
2.0705	0.714459428	0.714459405	0.714445684	0.714457246	0.714458578	0.714459362	-0.174769521
2.0805	0.768590211	0.768590182	0.768573544	0.768587548	0.768589186	0.76859013	-0.167479458
2.0905	0.831088998	0.831088962	0.831068484	0.831085701	0.831087744	0.831088899	-0.160742205
2.1005	0.904045209	0.904045162	0.904019517	0.904041055	0.904043648	0.904045085	-0.154497384

2.1105	0.990306705	0.990306644	0.990273865	0.990301365	0.990304722	0.990306547	-0.148693103
2.1205	1.09385824	1.093858157	1.093815221	1.093851205	1.093855658	1.093858032	-0.143284509
2.1305	1.220451585	1.22045147	1.220393529	1.220442037	1.220448121	1.220451305	-0.138232639
2.1405	1.37870696	1.378706794	1.378625666	1.378693514	1.378702138	1.378706566	-0.133503479
2.1505	1.582155469	1.58215522	1.58203617	1.582135627	1.582148436	1.582154891	-0.129067206
2.1605	1.853315966	1.853315567	1.853129793	1.853284832	1.853305058	1.853315064	-0.124897561
2.1705	2.232640095	2.232639401	2.232324091	2.232586962	2.232621694	2.232638563	-0.12097133
2.1805	2.800787711	2.800786349	2.800181948	2.800685308	2.800752656	2.800784772	-0.117267918
2.1905	3.745036748	3.745033512	3.743629991	3.744797653	3.744955842	3.745029919	-0.113768989
2.2005	5.621795973	5.621785097	5.617169321	5.621005229	5.621531478	5.6217735	-0.110458162
2.2105	11.13355126	11.13346689	11.09846681	11.12751243	11.13155419	11.13338042	-0.107320762
2.2205	19.58816172	19.57164458	14.54445004	18.48370653	19.21302761	19.55529294	-0.1043436
2.2305	-11.60434456	-11.60425047	-11.56671291	-11.59780052	-11.60223032	-11.60416125	-0.101514788
2.2405	-5.823850851	-5.823839122	-5.819233114	-5.823045463	-5.823593748	-5.823828412	-0.098823589
2.2505	-3.89612777	-3.896124283	-3.894778517	-3.895891366	-3.896053186	-3.896121217	-0.096260274
2.2605	-2.933969995	-2.933968513	-2.933406337	-2.933870763	-2.933939053	-2.933967257	-0.09381601
2.2705	-2.357538549	-2.357537783	-2.357251789	-2.357487823	-2.357522916	-2.357537157	-0.091482758
2.2805	-1.973732984	-1.973732534	-1.97356754	-1.973703578	-1.973724026	-1.973732181	-0.089253189
2.2905	-1.699892513	-1.699892225	-1.699788285	-1.6998739	-1.699886908	-1.699892007	-0.0871206
2.3005	-1.494728399	-1.494728201	-1.494658289	-1.49471582	-1.494724654	-1.494728058	-0.085078857
2.3105	-1.335321525	-1.335321383	-1.335271889	-1.335312579	-1.335318892	-1.335321284	-0.083122331
2.3205	-1.207929857	-1.207929749	-1.207893227	-1.207923225	-1.207927926	-1.207929679	-0.081245847
2.3305	-1.103813465	-1.103813381	-1.103785481	-1.103808376	-1.103812	-1.103813329	-0.079444641
2.3405	-1.017148548	-1.01714848	-1.017126527	-1.017144525	-1.017147402	-1.017148441	-0.077714319
2.3505	-0.94390491	-0.943904855	-0.94388713	-0.943901649	-0.943903991	-0.943904824	-0.076050824
2.3605	-0.881204876	-0.881204829	-0.881190189	-0.881202171	-0.881204121	-0.881204805	-0.074450399
2.3705	-0.826938815	-0.826938774	-0.826926433	-0.826936525	-0.826938182	-0.826938755	-0.072909565
2.3805	-0.779524948	-0.779524912	-0.779514316	-0.779522974	-0.779524407	-0.779524897	-0.071425095
2.3905	-0.737753985	-0.737753952	-0.737744702	-0.737752255	-0.737753515	-0.73775394	-0.069993987
2.4005	-0.700685583	-0.700685553	-0.700677355	-0.700684044	-0.700685169	-0.700685544	-0.068613452
2.4105	-0.667577526	-0.667577498	-0.667570132	-0.667576138	-0.667577155	-0.66757749	-0.06728089
2.4205	-0.637836157	-0.637836131	-0.637829428	-0.63783489	-0.637835821	-0.637836125	-0.065993875
2.4305	-0.610980989	-0.610980964	-0.610974794	-0.610979818	-0.610980681	-0.610980959	-0.064750142
2.4405	-0.586618968	-0.586618943	-0.586613205	-0.586617875	-0.586618682	-0.58661894	-0.063547576
2.4505	-0.564425453	-0.564425429	-0.564420041	-0.564424423	-0.564425186	-0.564425427	-0.062384193
2.4605	-0.544129959	-0.544129935	-0.544124834	-0.544128981	-0.544129707	-0.544129934	-0.061258139
2.4705	-0.525505319	-0.525505295	-0.525500426	-0.525504383	-0.525505079	-0.525505295	-0.06016767
2.4805	-0.508359348	-0.508359324	-0.508354645	-0.508358445	-0.508359118	-0.508359325	-0.059111152
2.4905	-0.492528364	-0.49252834	-0.492523814	-0.492527488	-0.492528142	-0.492528342	-0.058087049
2.5005	-0.477872095	-0.477872071	-0.477867668	-0.47787124	-0.47787188	-0.477872074	-0.057093915
2.5105	-0.464269641	-0.464269617	-0.464265312	-0.464268803	-0.464269431	-0.46426962	-0.056130388
2.5205	-0.451616245	-0.451616222	-0.451611991	-0.45161542	-0.45161604	-0.451616225	-0.055195188
2.5305	-0.439820688	-0.439820662	-0.439816491	-0.439819871	-0.439820486	-0.439820668	-0.054287103
2.5405	-0.428803172	-0.428803146	-0.428799016	-0.428802362	-0.428802973	-0.428803153	-0.053404991
2.5505	-0.418493593	-0.418493565	-0.418489463	-0.418492785	-0.418493395	-0.418493573	-0.052547775
2.5605	-0.408830108	-0.40883008	-0.408825992	-0.408829301	-0.408829912	-0.408830089	-0.051714433
2.5705	-0.399757964	-0.399757935	-0.39975385	-0.399757155	-0.399757768	-0.399757944	-0.050904
2.5805	-0.391228505	-0.391228475	-0.391224383	-0.391227693	-0.391228309	-0.391228485	-0.050115563
2.5905	-0.383198353	-0.383198321	-0.383194213	-0.383197535	-0.383198157	-0.383198333	-0.049348254
2.6005	-0.375628711	-0.375628678	-0.375624546	-0.375627886	-0.375628515	-0.375628691	-0.048601252
2.6105	-0.368484779	-0.368484745	-0.36848058	-0.368483945	-0.368484581	-0.368484759	-0.047873778
2.6205	-0.361735251	-0.361735215	-0.361731011	-0.361734407	-0.361735052	-0.361735231	-0.047165091
2.6305	-0.35535189	-0.355351853	-0.355347603	-0.355351035	-0.35535169	-0.35535187	-0.046474488
2.6405	-0.349309167	-0.349309128	-0.349304825	-0.349308299	-0.349308964	-0.349309146	-0.0458013
2.6505	-0.343583938	-0.343583898	-0.343579536	-0.343583056	-0.343583734	-0.343583918	-0.045144889
2.6605	-0.338155183	-0.338155141	-0.338150714	-0.338154286	-0.338154976	-0.338155162	-0.044504651
2.6705	-0.333003763	-0.333003718	-0.33299922	-0.333002849	-0.333003553	-0.333003742	-0.043880008

2.6805	-0.328112218	-0.328112171	-0.328107597	-0.328111286	-0.328112006	-0.328112197	-0.04327041
2.6905	-0.323464591	-0.323464542	-0.323459886	-0.32346364	-0.323464375	-0.323464569	-0.042675331
2.7005	-0.319046269	-0.319046218	-0.319041474	-0.319045298	-0.31904605	-0.319046247	-0.042094272
2.7105	-0.314843847	-0.314843793	-0.314838956	-0.314842854	-0.314843624	-0.314843824	-0.041526754
2.7205	-0.310845008	-0.310844951	-0.310840016	-0.310843992	-0.310844781	-0.310844984	-0.04097232
2.7305	-0.307038416	-0.307038356	-0.307033317	-0.307037376	-0.307038185	-0.307038392	-0.040430534
2.7405	-0.303413624	-0.303413561	-0.303408412	-0.303412559	-0.303413388	-0.303413599	-0.039900979
2.7505	-0.299960987	-0.299960921	-0.299955657	-0.299959895	-0.299960747	-0.299960962	-0.039383256
2.7605	-0.296671592	-0.296671522	-0.296666138	-0.296670472	-0.296671347	-0.296671566	-0.038876982
2.7705	-0.293537189	-0.293537116	-0.293531604	-0.29353604	-0.293536939	-0.293537163	-0.038381791
2.7805	-0.290550134	-0.290550057	-0.290544413	-0.290548955	-0.290549879	-0.290550107	-0.037897332
2.7905	-0.287703335	-0.287703254	-0.287697472	-0.287702124	-0.287703074	-0.287703308	-0.037423271
2.8005	-0.284990206	-0.284990121	-0.284984195	-0.284988962	-0.28498994	-0.284990178	-0.036959284
2.8105	-0.282404625	-0.282404535	-0.282398458	-0.282403346	-0.282404353	-0.282404596	-0.036505062
2.8205	-0.279940892	-0.279940798	-0.279934563	-0.279939578	-0.279940614	-0.279940863	-0.036060308
2.8305	-0.277593702	-0.277593603	-0.277587203	-0.277592349	-0.277593417	-0.277593672	-0.035624738
2.8405	-0.275358105	-0.275358001	-0.27535143	-0.275356713	-0.275357813	-0.275358074	-0.035198079
2.8505	-0.273229485	-0.273229376	-0.273222627	-0.273228052	-0.273229187	-0.273229454	-0.034780066
2.8605	-0.271203533	-0.271203418	-0.271196484	-0.271202058	-0.271203227	-0.271203501	-0.034370448
2.8705	-0.269276222	-0.2692761	-0.269268973	-0.269274702	-0.269275908	-0.269276189	-0.033968982
2.8805	-0.267443786	-0.267443658	-0.26743633	-0.26744222	-0.267443465	-0.267443752	-0.033575433
2.8905	-0.265702705	-0.26570257	-0.265695032	-0.26570109	-0.265702376	-0.26570267	-0.033189577
2.9005	-0.264049683	-0.26404954	-0.264041785	-0.264048017	-0.264049344	-0.264049647	-0.032811196
2.9105	-0.262481633	-0.262481483	-0.262473501	-0.262479915	-0.262481286	-0.262481597	-0.032440083
2.9205	-0.260995667	-0.260995509	-0.260987291	-0.260993895	-0.260995311	-0.260995629	-0.032076037
2.9305	-0.259589077	-0.259588911	-0.259580447	-0.259587247	-0.259588711	-0.259589038	-0.031718863
2.9405	-0.258259326	-0.25825915	-0.258250431	-0.258257437	-0.25825895	-0.258259286	-0.031368375
2.9505	-0.257004037	-0.257003851	-0.256994866	-0.257002085	-0.25700365	-0.257003995	-0.031024393
2.9605	-0.25582098	-0.255820784	-0.255811522	-0.255818964	-0.255820583	-0.255820937	-0.030686743
2.9705	-0.254708068	-0.254707861	-0.254698312	-0.254705985	-0.25470766	-0.254708024	-0.030355258
2.9805	-0.253663344	-0.253663126	-0.253653276	-0.25366119	-0.253662924	-0.253663298	-0.030029776
2.9905	-0.252684973	-0.252684743	-0.252674582	-0.252682747	-0.252684541	-0.252684927	-0.029710141

Table A3.2: Table of  $a_2$ 

vector coefficient, $a_2$ for various functions							
k	20 plane waves	infinite p.w.	20 monopoles	20 monopoles	20 p.w. and 20	20 p.w. and 20	
			at $r = 5$	at $r = 10$	mono at $r = 5$	mono at $r = 10$	2nd order FD
5.00E-04	-1.75	-1	0.200000393	0.200000107	0.200000396	0.200000584	0.200000015
1.05E-02	2.25	0.5	0.200006773	0.200006321	0.200006773	0.200006381	0.200006615
2.05E-02	0.5	3.13E-02	0.200024755	0.200024351	0.200024754	0.200024337	0.200025218
3.05E-02	-0.5	0.375	0.200054343	0.200053912	0.200054343	0.200054072	0.200055831
4.05E-02	0.23046875	0.2109375	0.200095546	0.200095166	0.200095545	0.200095043	0.200098463
5.05E-02	0.206542969	0.202148438	0.200148374	0.20014799	0.200148373	0.200147919	0.200153132
6.05E-02	0.199462891	0.200317383	0.200212841	0.200212441	0.200212841	0.200212374	0.200219856
7.05E-02	0.200805664	0.200500488	0.200288964	0.20028859	0.200288964	0.200288627	0.20029866
8.05E-02	0.200317383	0.200256348	0.200376764	0.200376399	0.200376763	0.200376354	0.200389572
9.05E-02	0.200492859	0.2004776	0.200476263	0.200475894	0.200476263	0.200475905	0.200492625
0.1005	0.200588226	0.200611115	0.200587487	0.20058712	0.200587487	0.200587127	0.200607857
0.1105	0.200709343	0.200703621	0.200710468	0.200710114	0.200710468	0.200710092	0.200735308
0.1205	0.200843811	0.200846672	0.200845236	0.200844863	0.200845237	0.200844891	0.200875027
0.1305	0.200995445	0.200989246	0.200991829	0.20099146	0.200991828	0.200991429	0.201027062
0.1405	0.201149702	0.201149225	0.201150284	0.201149926	0.201150284	0.201149914	0.201191471
0.1505	0.20132041	0.201321125	0.201320644	0.20132028	0.201320644	0.20132032	0.201368313
0.1605	0.201502323	0.201502323	0.201502955	0.201502602	0.201502955	0.201502571	0.201557653
0.1705	0.201697022	0.201697201	0.201697265	0.201696907	0.201697265	0.201696917	0.20175956
0.1805	0.201903701	0.201903194	0.201903627	0.201903278	0.201903627	0.201903302	0.20197411
0.1905	0.20212169	0.202121779	0.202122096	0.20212174	0.202122095	0.202121727	0.202201382
0.2005	0.202352345	0.202352405	0.20235273	0.202352381	0.202352729	0.202352371	0.202441459
0.2105	0.202595219	0.202595323	0.202595592	0.202595249	0.202595592	0.202595238	0.202694432
0.2205	0.20285042	0.202850416	0.202850748	0.202850412	0.202850747	0.202850409	0.202960396
0.2305	0.203117903	0.203117937	0.203118266	0.203117931	0.203118265	0.203117923	0.203239449
0.2405	0.20339792	0.203397883	0.20339822	0.203397888	0.203398219	0.203397895	0.203531697
0.2505	0.203690341	0.203690352	0.203690686	0.203690357	0.203690685	0.203690358	0.203837252
0.2605	0.203995429	0.203995416	0.203995744	0.203995422	0.203995741	0.203995416	0.204156228
0.2705	0.204313152	0.204313161	0.204313476	0.204313158	0.204313474	0.204313158	0.204488748
0.2805	0.204643656	0.204643653	0.204643972	0.204643659	0.204643968	0.204643654	0.204834939
0.2905	0.204987007	0.204987013	0.204987321	0.204987011	0.204987317	0.204987013	0.205194936
0.3005	0.205343314	0.205343315	0.20534362	0.205343315	0.205343614	0.205343315	0.205568876
0.3105	0.205712668	0.205712666	0.205712966	0.205712665	0.205712959	0.205712663	0.205956907
0.3205	0.206095171	0.206095167	0.206095463	0.206095167	0.206095454	0.206095168	0.20635918
0.3305	0.206490929	0.206490929	0.206491218	0.206490927	0.206491208	0.206490929	0.206775853
0.3405	0.206900055	0.206900056	0.206900342	0.206900057	0.20690033	0.206900056	0.207207093
0.3505	0.207322672	0.207322669	0.20732295	0.207322671	0.207322936	0.20732267	0.207653069
0.3605	0.207758889	0.207758889	0.207759163	0.207758889	0.207759146	0.207758888	0.208113963
0.3705	0.208208835	0.208208835	0.208209104	0.208208835	0.208209084	0.208208835	0.208589959
0.3805	0.208672638	0.208672638	0.208672901	0.208672639	0.208672878	0.208672638	0.209081251
0.3905	0.209150431	0.209150432	0.209150688	0.209150432	0.209150662	0.209150431	0.20958804
0.4005	0.209642352	0.209642352	0.209642602	0.209642352	0.209642573	0.209642352	0.210110535
0.4105	0.210148541	0.210148542	0.210148787	0.210148542	0.210148754	0.210148542	0.210648952
0.4205	0.210669149	0.210669149	0.210669388	0.210669149	0.210669351	0.210669149	0.211203518
0.4305	0.211204325	0.211204325	0.211204558	0.211204326	0.211204518	0.211204326	0.211774464
0.4405	0.211754228	0.211754228	0.211754455	0.211754228	0.211754411	0.211754228	0.212362035
0.4505	0.21231902	0.21231902	0.21231924	0.21231902	0.212319193	0.21231902	0.21296648
0.4605	0.212898868	0.212898868	0.212899082	0.212898869	0.212899032	0.212898868	0.213588061
0.4705	0.213493946	0.213493946	0.213494154	0.213493947	0.2134941	0.213493946	0.214227049
0.4805	0.214104432	0.214104432	0.214104634	0.214104433	0.214104577	0.214104432	0.214883722
0.4905	0.214730511	0.214730511	0.214730706	0.214730511	0.214730647	0.214730511	0.215558373

0.5005	0.215372372	0.215372372	0.215372561	0.215372372	0.215372499	0.215372372	0.216251302
0.5105	0.216030212	0.216030212	0.216030395	0.216030212	0.21603033	0.216030212	0.21696282
0.5205	0.216704232	0.216704232	0.216704409	0.216704232	0.216704343	0.216704232	0.217693253
0.5305	0.217394642	0.217394642	0.217394813	0.217394642	0.217394745	0.217394642	0.218442935
0.5405	0.218101655	0.218101655	0.21810182	0.218101655	0.218101751	0.218101655	0.219212213
0.5505	0.218825494	0.218825494	0.218825653	0.218825494	0.218825583	0.218825494	0.220001448
0.5605	0.219566386	0.219566386	0.21956654	0.219566386	0.219566469	0.219566386	0.220811013
0.5705	0.220324566	0.220324566	0.220324715	0.220324566	0.220324643	0.220324566	0.221641294
0.5805	0.221100277	0.221100277	0.22110042	0.221100277	0.221100348	0.221100277	0.222492693
0.5905	0.221893768	0.221893768	0.221893906	0.221893768	0.221893834	0.221893768	0.223365625
0.6005	0.222705296	0.222705296	0.22270543	0.222705297	0.222705358	0.222705296	0.22426052
0.6105	0.223535127	0.223535127	0.223535255	0.223535127	0.223535184	0.223535127	0.225177825
0.6205	0.224383531	0.224383531	0.224383655	0.224383531	0.224383584	0.224383531	0.226118003
0.6305	0.225250792	0.225250792	0.225250911	0.225250792	0.225250841	0.225250792	0.227081534
0.6405	0.226137197	0.226137197	0.226137312	0.226137197	0.226137243	0.226137197	0.228068915
0.6505	0.227043045	0.227043045	0.227043156	0.227043045	0.227043087	0.227043045	0.229080662
0.6605	0.227968643	0.227968643	0.22796875	0.227968643	0.227968683	0.227968643	0.230117311
0.6705	0.228914307	0.228914307	0.22891441	0.228914307	0.228914344	0.228914307	0.231179416
0.6805	0.229880363	0.229880363	0.229880462	0.229880363	0.229880397	0.229880363	0.232267555
0.6905	0.230867145	0.230867145	0.230867241	0.230867145	0.230867177	0.230867145	0.233382325
0.7005	0.231875	0.231875	0.231875093	0.231875001	0.23187503	0.231875	0.234524347
0.7105	0.232904284	0.232904284	0.232904373	0.232904284	0.232904312	0.232904284	0.235694264
0.7205	0.233955362	0.233955362	0.233955449	0.233955362	0.233955388	0.233955362	0.236892747
0.7305	0.235028613	0.235028613	0.235028697	0.235028613	0.235028638	0.235028613	0.238120489
0.7405	0.236124426	0.236124426	0.236124507	0.236124426	0.236124449	0.236124426	0.239378213
0.7505	0.237243201	0.237243201	0.237243279	0.237243201	0.237243223	0.237243201	0.240666668
0.7605	0.238385352	0.238385352	0.238385427	0.238385352	0.238385372	0.238385352	0.241986635
0.7705	0.239551303	0.239551303	0.239551376	0.239551303	0.239551322	0.239551303	0.243338924
0.7805	0.240741494	0.240741494	0.240741565	0.240741494	0.240741512	0.240741494	0.244724377
0.7905	0.241956377	0.241956377	0.241956446	0.241956377	0.241956394	0.241956377	0.246143872
0.8005	0.243196418	0.243196418	0.243196484	0.243196418	0.243196434	0.243196418	0.24759832
0.8105	0.244462096	0.244462096	0.244462161	0.244462096	0.244462111	0.244462096	0.24908867
0.8205	0.245753907	0.245753907	0.24575397	0.245753908	0.245753922	0.245753907	0.250615912
0.8305	0.247072362	0.247072362	0.247072423	0.247072362	0.247072376	0.247072362	0.252181075
0.8405	0.248417987	0.248417987	0.248418047	0.248417987	0.248418	0.248417987	0.253785231
0.8505	0.249791325	0.249791325	0.249791383	0.249791326	0.249791338	0.249791325	0.255429497
0.8605	0.251192936	0.251192936	0.251192993	0.251192937	0.251192948	0.251192936	0.25711504
0.8705	0.252623398	0.252623398	0.252623454	0.252623399	0.25262341	0.252623398	0.258843074
0.8805	0.254083308	0.254083308	0.254083361	0.254083308	0.254083318	0.254083308	0.260614868
0.8905	0.255573279	0.255573279	0.255573331	0.255573279	0.255573289	0.255573279	0.262431744
0.9005	0.257093947	0.257093947	0.257093999	0.257093948	0.257093957	0.257093947	0.264295085
0.9105	0.258645968	0.258645968	0.258646019	0.258645969	0.258645978	0.258645969	0.266206334
0.9205	0.260230019	0.260230019	0.260230068	0.260230019	0.260230028	0.260230019	0.268166998
0.9305	0.261846797	0.261846797	0.261846845	0.261846798	0.261846806	0.261846797	0.270178656
0.9405	0.263497025	0.263497025	0.263497073	0.263497026	0.263497034	0.263497025	0.272242956
0.9505	0.265181448	0.265181448	0.265181495	0.265181449	0.265181456	0.265181448	0.274361623
0.9605	0.266900837	0.266900837	0.266900883	0.266900837	0.266900845	0.266900837	0.276536465
0.9705	0.268655987	0.268655987	0.268656032	0.268655987	0.268655994	0.268655987	0.278769374
0.9805	0.270447721	0.270447721	0.270447765	0.270447721	0.270447728	0.270447721	0.281062333
0.9905	0.27227689	0.27227689	0.272276933	0.27227689	0.272276897	0.27227689	0.28341742
1.0005	0.274144372	0.274144372	0.274144415	0.274144373	0.274144379	0.274144372	0.285836818
1.0105	0.276051079	0.276051079	0.276051122	0.27605108	0.276051086	0.276051079	0.288322814
1.0205	0.27799795	0.27799795	0.277997992	0.277997951	0.277997957	0.27799795	0.290877814
1.0305	0.27998596	0.27998596	0.279986002	0.279985961	0.279985967	0.27998596	0.293504342
1.0405	0.282016117	0.282016117	0.282016158	0.282016117	0.282016123	0.282016117	0.296205054
1.0505	0.284089463	0.284089463	0.284089504	0.284089463	0.284089469	0.284089463	0.298982745
1.0605	0.286207079	0.286207079	0.286207119	0.28620708	0.286207085	0.286207079	0.301840355



1.0705	0.288370084	0.288370084	0.288370124	0.288370085	0.28837009	0.288370084	0.304780981
1.0805	0.290579638	0.290579638	0.290579678	0.290579639	0.290579644	0.290579638	0.30780789
1.0905	0.292836942	0.292836942	0.292836981	0.292836943	0.292836947	0.292836942	0.310924524
1.1005	0.295143241	0.295143241	0.295143281	0.295143242	0.295143247	0.295143241	0.314134518
1.1105	0.297499827	0.297499827	0.297499866	0.297499828	0.297499833	0.297499827	0.317441712
1.1205	0.29990804	0.29990804	0.299908079	0.29990804	0.299908045	0.29990804	0.320850163
1.1305	0.302369268	0.302369268	0.302369307	0.302369269	0.302369273	0.302369268	0.324364164
1.1405	0.304884954	0.304884954	0.304884993	0.304884955	0.304884959	0.304884954	0.327988259
1.1505	0.307456596	0.307456596	0.307456635	0.307456597	0.307456601	0.307456596	0.331727262
1.1605	0.310085748	0.310085748	0.310085787	0.310085749	0.310085753	0.310085748	0.335586278
1.1705	0.312774025	0.312774025	0.312774064	0.312774026	0.31277403	0.312774025	0.339570724
1.1805	0.315523106	0.315523106	0.315523145	0.315523107	0.315523111	0.315523106	0.343686355
1.1905	0.318334735	0.318334735	0.318334774	0.318334737	0.31833474	0.318334735	0.347939288
1.2005	0.321210727	0.321210727	0.321210766	0.321210728	0.321210731	0.321210727	0.352336034
1.2105	0.324152967	0.324152967	0.324153006	0.324152969	0.324152972	0.324152967	0.356883527
1.2205	0.327163421	0.327163421	0.32716346	0.327163422	0.327163426	0.327163421	0.361589161
1.2305	0.330244132	0.330244132	0.330244171	0.330244133	0.330244137	0.330244132	0.366460827
1.2405	0.333397228	0.333397228	0.333397268	0.33339723	0.333397233	0.333397229	0.371506958
1.2505	0.336624928	0.336624928	0.336624968	0.33662493	0.336624933	0.336624928	0.376736573
1.2605	0.339929543	0.339929543	0.339929583	0.339929544	0.339929547	0.339929543	0.382159331
1.2705	0.343313481	0.343313481	0.343313521	0.343313483	0.343313485	0.343313481	0.387785588
1.2805	0.346779256	0.346779256	0.346779297	0.346779258	0.346779261	0.346779256	0.393626459
1.2905	0.350329491	0.350329491	0.350329532	0.350329493	0.350329496	0.350329491	0.399693894
1.3005	0.353966924	0.353966924	0.353966965	0.353966926	0.353966928	0.353966924	0.406000752
1.3105	0.357694412	0.357694412	0.357694454	0.357694414	0.357694417	0.357694412	0.412560891
1.3205	0.361514945	0.361514945	0.361514987	0.361514947	0.361514949	0.361514945	0.419389268
1.3305	0.365431644	0.365431644	0.365431686	0.365431647	0.365431649	0.365431644	0.426502048
1.3405	0.369447776	0.369447776	0.369447819	0.369447779	0.369447781	0.369447777	0.433916733
1.3505	0.373566759	0.373566759	0.373566801	0.373566761	0.373566763	0.373566759	0.441652294
1.3605	0.377792169	0.377792169	0.377792212	0.377792171	0.377792173	0.377792169	0.449729339
1.3705	0.382127754	0.382127754	0.382127797	0.382127756	0.382127758	0.382127754	0.458170284
1.3805	0.38657744	0.38657744	0.386577484	0.386577443	0.386577445	0.38657744	0.466999563
1.3905	0.391145346	0.391145346	0.39114539	0.391145349	0.39114535	0.391145346	0.476243855
1.4005	0.39583579	0.39583579	0.395835834	0.395835793	0.395835795	0.39583579	0.48593235
1.4105	0.400653307	0.400653307	0.400653351	0.40065331	0.400653311	0.400653307	0.496097049
1.4205	0.405602658	0.405602658	0.405602703	0.405602661	0.405602663	0.405602659	0.506773118
1.4305	0.410688849	0.410688849	0.410688894	0.410688852	0.410688853	0.410688849	0.517999277
1.4405	0.415917141	0.415917141	0.415917186	0.415917144	0.415917145	0.415917141	0.529818272
1.4505	0.421293072	0.421293072	0.421293117	0.421293075	0.421293076	0.421293072	0.542277404
1.4605	0.426822471	0.426822471	0.426822517	0.426822475	0.426822476	0.426822472	0.555429157
1.4705	0.432511482	0.432511482	0.432511528	0.432511485	0.432511486	0.432511482	0.569331925
1.4805	0.438366579	0.438366579	0.438366625	0.438366582	0.438366583	0.438366579	0.58405087
1.4905	0.444394594	0.444394595	0.44439464	0.444394598	0.444394599	0.444394595	0.599658929
1.5005	0.450602741	0.450602741	0.450602787	0.450602745	0.450602746	0.450602742	0.61623801
1.5105	0.45699864	0.45699864	0.456998686	0.456998644	0.456998645	0.456998641	0.633880417
1.5205	0.463590349	0.463590349	0.463590394	0.463590353	0.463590353	0.463590349	0.65269055
1.5305	0.470386394	0.470386394	0.470386439	0.470386398	0.470386398	0.470386394	0.672786954
1.5405	0.477395803	0.477395803	0.477395848	0.477395807	0.477395807	0.477395804	0.6943048
1.5505	0.484628148	0.484628148	0.484628192	0.484628152	0.484628152	0.484628148	0.717398905
1.5605	0.492093579	0.492093579	0.492093622	0.492093583	0.492093583	0.49209358	0.742247434
1.5705	0.499802874	0.499802874	0.499802916	0.499802878	0.499802878	0.499802875	0.769056474
1.5805	0.507767486	0.507767486	0.507767527	0.50776749	0.50776749	0.507767487	0.798065728
1.5905	0.515999597	0.515999597	0.515999635	0.5159996	0.5159996	0.515999597	0.829555658
1.6005	0.524512174	0.524512174	0.524512211	0.524512178	0.524512178	0.524512175	0.863856534
1.6105	0.533319041	0.533319041	0.533319076	0.533319044	0.533319044	0.533319041	0.901360006
1.6205	0.54243494	0.54243494	0.542434973	0.542434944	0.542434943	0.54243494	0.942534052
1.6305	0.551875618	0.551875618	0.551875647	0.551875621	0.551875621	0.551875618	0.987942532

1.6405	0.561657908	0.561657908	0.561657933	0.56165791	0.56165791	0.561657908	1.038271061
1.6505	0.571799825	0.571799825	0.571799847	0.571799827	0.571799827	0.571799825	1.094361752
1.6605	0.582320674	0.582320674	0.582320692	0.582320676	0.582320676	0.582320675	1.157260573
1.6705	0.593241167	0.593241167	0.593241179	0.593241168	0.593241168	0.593241167	1.228282997
1.6805	0.604583548	0.604583548	0.604583554	0.604583549	0.604583549	0.604583548	1.309106785
1.6905	0.616371746	0.616371746	0.616371744	0.616371746	0.616371746	0.616371746	1.401905926
1.7005	0.628631529	0.628631529	0.628631519	0.628631528	0.628631528	0.628631529	1.509548745
1.7105	0.641390689	0.641390689	0.64139067	0.641390687	0.641390688	0.641390689	1.635899153
1.7205	0.654679244	0.654679244	0.654679214	0.654679241	0.654679242	0.654679244	1.786289646
1.7305	0.668529663	0.668529663	0.668529621	0.668529658	0.66852966	0.668529663	1.968292287
1.7405	0.682977123	0.682977123	0.682977067	0.682977116	0.682977119	0.682977123	2.193032352
1.7505	0.698059795	0.698059795	0.698059723	0.698059786	0.69805979	0.698059795	2.47754953
1.7605	0.713819173	0.713819173	0.713819083	0.713819162	0.713819167	0.713819173	2.849330603
1.7705	0.73030044	0.73030044	0.730300328	0.730300426	0.730300432	0.730300439	3.355765226
1.7805	0.747552887	0.747552887	0.747552751	0.74755287	0.747552877	0.747552886	4.086142003
1.7905	0.765630392	0.765630392	0.765630229	0.765630372	0.765630381	0.765630392	5.231093357
1.8005	0.784591967	0.784591967	0.784591772	0.784591942	0.784591953	0.784591966	7.283341087
1.8105	0.80450238	0.804502379	0.804502148	0.80450235	0.804502363	0.804502379	12.02868239
1.8205	0.825432876	0.825432876	0.825432603	0.82543284	0.825432857	0.825432875	34.88012138
1.8305	0.84746201	0.84746201	0.847461689	0.847461968	0.847461988	0.847462009	-38.32096684
1.8405	0.870676605	0.870676605	0.870676229	0.870676555	0.870676579	0.870676604	-12.32128363
1.8505	0.895172869	0.895172869	0.895172429	0.89517281	0.895172839	0.895172867	-7.324645693
1.8605	0.921057699	0.921057699	0.921057185	0.921057629	0.921057664	0.921057697	-5.203174196
1.8705	0.948450207	0.948450207	0.948449607	0.948450125	0.948450166	0.948450204	-4.029733388
1.8805	0.977483516	0.977483515	0.977482816	0.977483419	0.977483468	0.977483513	-3.28493124
1.8905	1.00830688	1.00830688	1.008306065	1.008306766	1.008306825	1.008306877	-2.77019533
1.9005	1.041088207	1.041088206	1.041087255	1.041088073	1.041088142	1.041088202	-2.393201155
1.9105	1.076017059	1.076017058	1.076015949	1.076016901	1.076016985	1.076017054	-2.105195016
1.9205	1.113308269	1.113308267	1.113306972	1.113308083	1.113308182	1.113308262	-1.878003485
1.9305	1.153206285	1.153206283	1.153204768	1.153206065	1.153206184	1.153206277	-1.694210649
1.9405	1.195990463	1.195990461	1.195988685	1.195990204	1.195990345	1.195990454	-1.542471073
1.9505	1.241981524	1.241981522	1.241979436	1.241981218	1.241981387	1.241981514	-1.415076901
1.9605	1.291549503	1.291549501	1.291547046	1.29154914	1.291549343	1.291549492	-1.306608187
1.9705	1.345123608	1.345123605	1.345120706	1.345123176	1.34512342	1.345123595	-1.213142641
1.9805	1.403204534	1.40320453	1.403201094	1.403204018	1.403204312	1.403204518	-1.131771762
1.9905	1.466379955	1.46637999	1.466375902	1.466379377	1.466379733	1.466379976	-1.060293174
2.0005	1.535344485	1.535344479	1.535339593	1.535343741	1.535344173	1.535344462	-0.9970086
2.0105	1.610924678	1.61092467	1.610918801	1.610923777	1.610924305	1.61092465	-0.940587442
2.0205	1.694112444	1.694112434	1.694105344	1.694111349	1.694111997	1.69411241	-0.889972381
2.0305	1.786108283	1.78610827	1.786099648	1.786106942	1.786107742	1.786108241	-0.844312652
2.0405	1.888379212	1.888379196	1.888368634	1.888377559	1.888378553	1.888379161	-0.80291595
2.0505	2.002737074	2.002737054	2.002724007	2.002735019	2.002736264	2.002737011	-0.765213179
2.0605	2.131446166	2.13144614	2.13142987	2.131443587	2.131445162	2.131446087	-0.730732213
2.0705	2.277373867	2.277373834	2.277353323	2.277370596	2.277372609	2.277373768	-0.699078082
2.0805	2.444205737	2.444205693	2.444179508	2.444201535	2.444204139	2.44420561	-0.669917834
2.0905	2.636759726	2.636759668	2.636725751	2.636754251	2.636757668	2.636759562	-0.642968819
2.1005	2.861457244	2.861457165	2.861412479	2.861449988	2.861454547	2.861457028	-0.617989536
2.1105	3.127050688	3.127050579	3.126990507	3.127040878	3.127047083	3.127050397	-0.594772411
2.1205	3.445786588	3.445786433	3.445703705	3.445773001	3.44578165	3.445786187	-0.573138038
2.1305	3.835342354	3.835342127	3.835224804	3.835322977	3.835335389	3.835341785	-0.552930556
2.1405	4.322211654	4.322211311	4.322038743	4.322182995	4.322201465	4.322210816	-0.534013916
2.1505	4.947982274	4.94798173	4.947715852	4.94793788	4.947966661	4.947980983	-0.516268825
2.1605	5.78186765	5.781866735	5.781431362	5.781794567	5.781842222	5.781865535	-0.499590242
2.1705	6.948203527	6.948201853	6.947426957	6.948072764	6.948158514	6.94819976	-0.483885318
2.1805	8.69492587	8.694922416	8.693366013	8.69466186	8.694835945	8.6949183	-0.469071671
2.1905	11.5977434	11.59773478	11.59395113	11.59709825	11.59752595	11.59772499	-0.455075954
2.2005	17.36734107	17.36731066	17.35429794	17.36511039	17.36659696	17.36727771	-0.441832649

2.2105	34.31530221	34.31505482	34.2119956	34.29751465	34.30942816	34.31479913	-0.42928305
2.2205	61.83798824	61.78727019	46.31277272	58.43763588	60.68400809	61.73680924	-0.417374399
2.2305	-35.55342368	-35.55312159	-35.4331079	-35.53250862	-35.54665648	-35.55283764	-0.406059154
2.2405	-17.80131176	-17.80127247	-17.78596929	-17.79863784	-17.80045557	-17.80123722	-0.395294357
2.2505	-11.87911478	-11.87910262	-11.87446653	-11.87830129	-11.87885692	-11.87909221	-0.385041096
2.2605	-8.922631837	-8.922626471	-8.920623458	-8.922278821	-8.922521056	-8.922622087	-0.375264039
2.2705	-7.151044679	-7.151041807	-7.149990896	-7.150858648	-7.150986878	-7.151039565	-0.365931034
2.2805	-5.971213842	-5.971212105	-5.970588801	-5.971103023	-5.971179749	-5.97121081	-0.357012755
2.2905	-5.129212881	-5.12921174	-5.128809477	-5.129141054	-5.129191	-5.129210925	-0.348482401
2.3005	-4.498199831	-4.498199033	-4.497922907	-4.498150316	-4.498184894	-4.498198488	-0.340315429
2.3105	-4.00776285	-4.007762267	-4.007563602	-4.007727076	-4.007752163	-4.007761885	-0.332489323
2.3205	-3.615682591	-3.615682148	-3.615533827	-3.615655772	-3.615674657	-3.61568187	-0.324983386
2.3305	-3.295106934	-3.295106589	-3.294992496	-3.29508622	-3.295100865	-3.29510638	-0.317778563
2.3405	-3.028142763	-3.028142487	-3.028052538	-3.028126367	-3.028138005	-3.028142327	-0.310857277
2.3505	-2.802407442	-2.802407217	-2.802334826	-2.802394194	-2.802403634	-2.802407091	-0.304203295
2.3605	-2.609059259	-2.609059073	-2.608999782	-2.609048366	-2.609056158	-2.609058972	-0.297801595
2.3705	-2.441616233	-2.441616076	-2.441566778	-2.441607141	-2.441613669	-2.441615994	-0.291638261
2.3805	-2.295218157	-2.295218024	-2.295176494	-2.295210469	-2.29521601	-2.295217956	-0.285700378
2.3905	-2.166149279	-2.166149165	-2.166113775	-2.166142703	-2.16614746	-2.166149108	-0.279975949
2.4005	-2.051520178	-2.05152008	-2.051489614	-2.051514496	-2.051518621	-2.051520031	-0.274453809
2.4105	-1.949050169	-1.949050084	-1.949023618	-1.949045215	-1.949048825	-1.949050041	-0.269123558
2.4205	-1.856915023	-1.856914948	-1.85689177	-1.856910669	-1.856913853	-1.856914911	-0.263975498
2.4305	-1.773638222	-1.773638156	-1.773617708	-1.773634367	-1.773637195	-1.773638123	-0.259000569
2.4405	-1.698011886	-1.698011828	-1.697993668	-1.698008451	-1.69801098	-1.698011799	-0.254190303
2.4505	-1.629038344	-1.629038292	-1.629022067	-1.629035265	-1.629037539	-1.629038266	-0.249536774
2.4605	-1.565886313	-1.565886267	-1.565871688	-1.565883537	-1.565885594	-1.565886243	-0.245032555
2.4705	-1.507857605	-1.507857564	-1.507844398	-1.50785509	-1.50785696	-1.507857542	-0.240670679
2.4805	-1.45436152	-1.454361483	-1.454349535	-1.454359229	-1.454360938	-1.454361462	-0.236444608
2.4905	-1.404894927	-1.404894894	-1.404884004	-1.404892833	-1.4048944	-1.404894875	-0.232348195
2.5005	-1.359026625	-1.359026595	-1.359016629	-1.359024702	-1.359026145	-1.359026577	-0.228375658
2.5105	-1.316384931	-1.316384905	-1.316375748	-1.316383159	-1.316384494	-1.316384888	-0.224521554
2.5205	-1.276647761	-1.276647737	-1.276639293	-1.276646122	-1.27664736	-1.27664772	-0.220780751
2.5305	-1.239534621	-1.2395346	-1.239526785	-1.2395331	-1.239534252	-1.239534583	-0.217148411
2.5405	-1.20480011	-1.204800092	-1.204792836	-1.204798694	-1.20479977	-1.204800076	-0.213619966
2.5505	-1.172228602	-1.172228586	-1.172221828	-1.172227279	-1.172228287	-1.17222857	-0.2101911
2.5605	-1.141629861	-1.141629847	-1.141623534	-1.141628622	-1.14162957	-1.141629832	-0.206857732
2.5705	-1.112835419	-1.112835407	-1.112829491	-1.112834255	-1.112835148	-1.112835391	-0.203616001
2.5805	-1.085695546	-1.085695536	-1.085689977	-1.085694449	-1.085695293	-1.08569552	-0.200462251
2.5905	-1.060076721	-1.060076712	-1.060071474	-1.060075685	-1.060076484	-1.060076696	-0.197393016
2.6005	-1.035859497	-1.03585949	-1.03585454	-1.035858515	-1.035859274	-1.035859474	-0.194405009
2.6105	-1.012936697	-1.012936691	-1.012932002	-1.012935764	-1.012936487	-1.012936675	-0.191495113
2.6205	-0.991211879	-0.991211875	-0.991207421	-0.991210992	-0.991211682	-0.991211859	-0.188660366
2.6305	-0.970598031	-0.970598028	-0.970593786	-0.970597183	-0.970597844	-0.970598011	-0.185897953
2.6405	-0.95101644	-0.951016438	-0.951012388	-0.951015629	-0.951016263	-0.951016421	-0.183205199
2.6505	-0.932395736	-0.932395735	-0.932391858	-0.932394958	-0.932395568	-0.932395718	-0.180579558
2.6605	-0.914671051	-0.914671052	-0.914667331	-0.914670303	-0.914670891	-0.914671034	-0.178018605
2.6705	-0.897783302	-0.897783304	-0.897779723	-0.897782581	-0.897783149	-0.897783286	-0.175520032
2.6805	-0.881678558	-0.881678561	-0.881675106	-0.881677861	-0.881678411	-0.881678542	-0.173081638
2.6905	-0.866307493	-0.866307497	-0.866304155	-0.866306817	-0.866307352	-0.866307477	-0.170701324
2.7005	-0.851624908	-0.851624913	-0.851621673	-0.851624252	-0.851624772	-0.851624893	-0.168377087
2.7105	-0.837589311	-0.837589317	-0.837586167	-0.837588672	-0.83758918	-0.837589297	-0.166107014
2.7205	-0.824162544	-0.824162551	-0.82415948	-0.82416192	-0.824162417	-0.82416253	-0.163889279
2.7305	-0.811309455	-0.811309463	-0.811306462	-0.811308844	-0.811309332	-0.811309442	-0.161722137
2.7405	-0.798997616	-0.798997625	-0.798994684	-0.798997016	-0.798997496	-0.798997603	-0.159603917
2.7505	-0.787197059	-0.787197069	-0.787194178	-0.787196469	-0.787196941	-0.787197046	-0.157533023
2.7605	-0.775880052	-0.775880062	-0.775877215	-0.77587947	-0.775879937	-0.775880039	-0.155507927
2.7705	-0.765020896	-0.765020908	-0.765018095	-0.76502032	-0.765020783	-0.765020883	-0.153527163

2.7805	-0.754595744	-0.754595756	-0.754592971	-0.754595173	-0.754595633	-0.754595732	-0.15158933
2.7905	-0.744582438	-0.744582451	-0.744579685	-0.74458187	-0.744582328	-0.744582425	-0.149693083
2.8005	-0.734960363	-0.734960377	-0.734957623	-0.734959797	-0.734960254	-0.734960351	-0.147837134
2.8105	-0.72571032	-0.725710334	-0.725707585	-0.725709754	-0.725710212	-0.725710307	-0.146020246
2.8205	-0.716814403	-0.716814419	-0.716811668	-0.716813837	-0.716814296	-0.716814391	-0.144241233
2.8305	-0.708255901	-0.708255917	-0.708253157	-0.708255332	-0.708255794	-0.708255889	-0.142498954
2.8405	-0.700019194	-0.70001921	-0.700016435	-0.70001862	-0.700019086	-0.700019181	-0.140792315
2.8505	-0.692089671	-0.692089688	-0.69208689	-0.692089092	-0.692089563	-0.692089659	-0.139120266
2.8605	-0.684453653	-0.68445367	-0.684450843	-0.684453067	-0.684453544	-0.68445364	-0.137481794
2.8705	-0.677098318	-0.677098336	-0.677095473	-0.677097724	-0.677098208	-0.677098305	-0.135875927
2.8805	-0.670011639	-0.670011657	-0.670008751	-0.670011035	-0.670011527	-0.670011626	-0.134301732
2.8905	-0.663182324	-0.663182343	-0.663179387	-0.66318171	-0.663182211	-0.663182311	-0.132758306
2.9005	-0.656599765	-0.656599784	-0.656596771	-0.656599138	-0.65659965	-0.656599752	-0.131244785
2.9105	-0.650253985	-0.650254004	-0.650250927	-0.650253344	-0.650253868	-0.650253972	-0.129760333
2.9205	-0.644135595	-0.644135614	-0.644132466	-0.644134938	-0.644135476	-0.644135581	-0.128304147
2.9305	-0.638235755	-0.638235774	-0.638232547	-0.63823508	-0.638235633	-0.638235741	-0.126875451
2.9405	-0.632546134	-0.632546153	-0.632542839	-0.63254544	-0.632546009	-0.63254612	-0.1254735
2.9505	-0.627058877	-0.627058895	-0.627055486	-0.627058162	-0.627058748	-0.627058862	-0.124097572
2.9605	-0.621766572	-0.621766589	-0.621763078	-0.621765834	-0.621766439	-0.621766556	-0.122746974
2.9705	-0.616662222	-0.61666224	-0.616658617	-0.616661461	-0.616662086	-0.616662207	-0.121421033
2.9805	-0.611739221	-0.611739237	-0.611735495	-0.611738432	-0.61173908	-0.611739205	-0.120119105
2.9905	-0.606991322	-0.606991338	-0.606987467	-0.606990505	-0.606991177	-0.606991306	-0.118840562

## VITA

Sany Izan Ihsan was born in Kuching, Sarawak, Malaysia on November 9, 1971.

His parents are Mr. Ihsan Hj. Awang and Mrs. Aisah Abdullah.

He attended primary and middle school in Kuala Lumpur, and high school in Shah Alam, under a special preparatory program. He obtained his Bachelor of Science degree in Mechanical Engineering from the University of Wisconsin at Madison on May 1995. In January 1997, he entered the University of Tennessee Space Institute, Tullahoma and in May 1999, received a Master of Science degree in Aerospace Engineering.

He is presently employed as an assistant lecturer at the International Islamic University of Malaysia and is currently under study leave.

He is married to Mrs. Suriza Ahmad Zabidi and they are blessed with 2 children – Muhammad (18 months) and Zubair (4 months).